THE JOURNAL OF THE INSTITUTION OF ENGINEERS, MALAYSIA KDN PP5476/10/2012 (030203) | ISSN 0126-513X

IEM JOURNAL

VOL. 83, NO. 2

DECEMBER 2022

IEM

The Institution of Engineers, Malaysia

Vol. 83, No. 2, December 2022
KDN PP5476/10/2012 (030203) ISSN 0126-513X

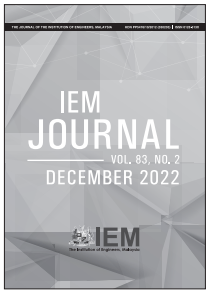

CONTENTS

THIS ISSUE WAS PUBLISHED IN OCTOBER 2023

THE INSTITUTION OF ENGINEERS, MALAYSIA
Bangunan Ingenieur, Lots 60 & 62, Jalan 52/4,
P.O.Box 223 (Jalan Sultan),
46720 Petaling Jaya, Selangor Darul Ehsan.
Tel: 03-7968 4001/4002
Fax: 03-7957 7678
E-mail: pub@iem.org.my **Homepage:** http://www.myiem.org.my

PRINT QUANTITY: *500 COPIES*

PERFORMANCE OF SANDWICHED KENAF FIBRE AND SUGARCANE HUSK IN TREATING PAVEMENT RUNOFF

(Date received: 12.01.2023/Date accepted: 28.08.2023)

Nor Azlina Alias[1*], Badronnisa Yusuf[2]

[1,2]Department of Civil Engineering, Faculty of Engineering
University Putra Malaysia, Selangor, Malaysia

[*]Corresponding author: a_norazlina@upm.edu.my

ABSTRACT

Rapid urbanisation appears to cause more paved parking areas being provided which contributed into a greater impermeable surface area. Pavement runoff from the impermeable surface area does indeed have a high concentration of contaminants and it has been identified as a major cause of deterioration of nearby recipient water bodies. The more develop the country is, the poorer the water quality they have (Ashantha, et. al 2005). It carries pollutants, sediments, nutrients and heavy metals. An intensifying development in areas with impervious surface leads rainwater with small particles runs rapidly into drainages and rivers that may cause blockage that eventually leads to flash flood problem. Changes in land use increased the degree of soil imperviousness led to the increased of stormwater volume (Kundzewicz, et al., 2007). This study used a potential block system that is equipped with inner storage and expected to give minimal impact to the environment in order to improve the water quality and prevent ponding in the paved and impermeable areas. Figure 1 illustrates the simulation of pavement runoff was conducted to evaluate the performance of kenaf fibre and sugarcane husk that sandwiched in a modular block at a model scale in the hydraulic laboratory. The collected pavement runoff stored lower tank were tested and parameters observed were chemical oxygen demand, biological oxygen demand, amounts of suspended solids and turbidity. Water quality before and after being treated with the filtration media were compared. The performance and effectiveness of the two bio-composite materials as filter media were also assessed in decelerating the rate of runoff. Results show that the two proposed bio-composite materials are capable in reducing surface runoff, storing water, and reducing pollutant concentrations. The kenaf fibre appears to perform better in treating the polluted pavement runoff while sugarcane husk has a better performance in storing runoff and reduce the peak flow of runoff.

Keywords: Bio-Composite, Integrated Storage, Pavement Runoff, Wastewater Treatment

1.0 INTRODUCTION

Earlier in 1997, Boller stated that the pollutants from streets and roofs carried by stormwater was the major contributor in surface water pollution. Nowadays, runoff from pavement is one of the main causes of urban water pollution and has become a major concern as it transports large quantities of contaminants to receiving waters in many countries including Malaysia (Lee, *et al.,* 2007). In rapid urban areas, the pavement runoff has proven to be a significant source of contamination that threatens the quality of urban water (Qian *et al.,* 2021) in which the parking areas are a common type of impervious surface that is directly proportionate to rapid urbanisation. The entire presence of contaminants, including heavy metals, organic matter, and petroleum hydrocarbon pollutants, is increasing tremendously due to the growing number of cars, factories, and people (Markiewicz *et al*., 2017). The roadways serve as depositories for a vehicular where road-deposited sediments (RDS) such as sand, loose gravel, mud or tar from vehicles typically attach to fine-grained particles accumulated on roadway systems between the periods of precipitation. These pavement runoff with particles will be washed out and directly enters the water bodies.

Figure 1: Lab Scale Simulation of Pavement Runoff using Rainfall Simulator System (RSS)

Pavement runoff contains a mass of pollutants and known to be a significant contributor to the deterioration of receiving water bodies (Park *et al*., 2015, Qin *et al*., 2016, Risch *et al*., 2018). According to Ma *et al*. (2018), 69.24 percent of the particle pollution is caused by runoff from road surfaces. However, the types and sources of road surface pollutants diverse depends on regional characteristics; thus the quality of pavement runoff varies by regions. Table 1 tabulates the typical pollutant in pavement

runoff in the US and Asian. Studies reported that different rainfall events also result to varies greatly (Xue *et al*. 2020).

Capturing and treating urban runoff before it enters the receiving water courses is one of available methods in solving this issue. Hence, the aim of this study is to propose a sustainable media in treating pavement runoff before it enters the drainage system. Thus, the specific objective is to evaluate the performance and the effectiveness of sandwiched bio-composite materials that are kenaf fibre and sugarcane husk as filter media. This study is to also promote sustainability in treating the contaminated water.

Table 1: Typical Concentration of Pollutants in Pavement Runoff (Kang et, al. 2019)

Parameter	Locations			
	United States of America	Australia	China	Korea
Total Suspended Solid (mg/l)	12-129	60-1350	439	536
COD (mg/l)	37-130		373	468

2.0 FILTRATION USING BIO-COMPOSITE MEDIA

A variety of filtration systems have been developed and proved to be useful for alleviating the pavement runoff pollution. These systems mainly include filtration facilities such as filtration trenches, gutter systems and basins storage systems such as constructed eco-wetlands/lagoons, vegetated retention ponds (Eriksson *et al*., 2007) which requires large areas and restrict the application. As Fuerhacker *et al*., 2011 in his studies mentioned that filtration systems for parking areas have been developed and showed effective results for treating the polluted urban road runoff. Thus, a modular integrated storage brick for urban drainage system is proposed.

It is widely known that the kenaf fibre is mostly used as reinforcement in concrete and less studies on the performance of kenaf fibre and sugarcane husk in treating contaminated water were discussed. Researchers discussed more on the potential of Kenaf as reinforcement (Kumar and Velmurugan, 2022). Shirvani *et.al*, (2019) concluded that reinforcement of structural elements and construction materials this natural fiber has gained popularity among researchers and industries due to environmental concerns. Thus, this paper focused on the performance on these two bio-composite raw materials in treating the polluted water. Since the primary goal of employing biological wastes is to filter tiny particles in pavement runoff, both were washed with tap water, rinsed thoroughly and dried. No chemical treatment was done to the bio-composite materials used. Both fibres were then compacted and sandwiched in the brick opening. For sustainability, the bio-composite wastes are selected to promote greeneries in parking areas besides minimizing the impervious areas. Figure 2 shows the types of bio-composite materials used in this study.

Kenaf fiber *Sugarcane husk*

Figure 2: Bio-Composite Materials as Filter Media

Since a system that equipped with layered filter media can reduce the pollution by adsorption, absorption, ion exchange, or complexation reactions (Pitcher *et al*., 2004; Fuerhacker *et al*., 2011), therefore, selecting and configuring the filter media are essential issues for a runoff treatment system.

3.0 FILTRATION TEST EQUIPMENT

A modular mortar brick with an inner opening is designed to store and elongate the surface runoff time. The opening section in the centre of brick is the area where bio-composite materials are to be placed at the same time to reduce individual's brick weight. The brick was casted in halved for easy handling with average weight of 1.85 kg. The contaminated pavement runoff will be filtrated by the sandwiched bio-composite materials before entering the water bodies. A single brick is design to have 200 m x 75 mm x 80 mm (length x width x thick) with 30 mm x 30 mm x 80mm (length x width x thick) opening in the middle.

A 2.0 m long and 1.0 m wide Rainfall Simulator System (RSS) that is equipped with storage tank was used to simulate rainfall. The storage tank was filled up with 100L pavement runoff that was collected at parking area nearby UPM Hydraulic Laboratory prior to the experiment. While columns of modular brick were placed inside the catchment area. Figure 3 illustrates the arrangement of modular brick and its opening where kenaf and sugarcane husk were placed.

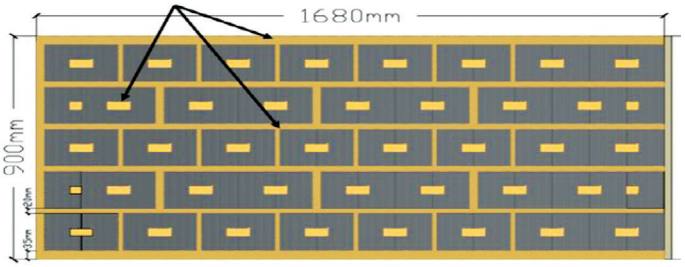

Figure 3: Plan View of Modular Brick in RSS Catchment Area

Altogether, about 82 bricks were placed in the RSS catchment area. As mentioned earlier, the opening sections were filled with the bio-composite materials; kenaf fibre and sugarcane husk as shown in Figure 4. Half of the bricks' height was filled with the bio-composite. Based on the density of kenaf fiber and sugarcane husk (Hazrol *et al*., 2023 and Sharzad *et al*., 2022), each brick carries about 50 gram and 43 gram of kenaf and sugar cane husk respectively.

The gaps between bricks were also filled with a bio-composite medium. This is to ensure that all contaminated pavement runoff is filtered. The pavement runoff was collected during the monsoon season between November to January. The amount of runoff collected from each rainfall event was tested three times for its quality once been filtrated by Kenaf fibre.

Kenaf fiber *Sugarcane husk*

Figure 4: Openings and Gaps were filled up with Bio-Composite Materials

Pump and a flow meter attached to the RSS to control the discharge at 2.5L/m imitating the moderate rainfall intensity at 26.5 mm/hr. The test was run immediately after the runoff was stored into the storage tank to ensure the pavement runoff properties remain unchanged. The duration for each rain simulation was about 40 minutes until the storage tank is emptied. Those procedures were repeated for Sugarcane husk. Once the pavement runoff run and infiltrated through the media, it was then collected at the outlet and tested for its quality. The treated pavement runoff filtrated by kenaf and sugarcane husk were compared with untreated pavement runoff.

4.0 COMPARATIVE STUDY: PERFORMANCE OF BIO-COMPOSITE MEDIA

Following Li, H *et. al.,* (2017), a column experiment to study pollutants form urban storm-runoff was conducted and the concentrations of total suspended solids (TSS) and chemical oxygen demand (COD) were among the parameter observed in the influent and effluent thus, in order to evaluate the performance of bio-composite media used in treating the contaminated pavement runoff, the effluent were tested for its turbidity, bio-chemical oxygen demand (BOD), chemical oxygen demand (COD) and total suspended solid (TSS).

The average readings on pavement runoff quality before and after treated by bio-composite materials are as in Table 2. The results obtained after the pavement runoff being treated (effluent) by both bio-composite materials were compared with the untreated pavement runoff referred as influent. Figure 5 summarized the results obtained.

From Table 2 above, pavement runoff that has been filtered through both materials were improved. Most of the parameters tested on the effluent gave better readings compared to the influent. The ability of kenaf fibre and sugarcane husk to lowered COD level may lead to positive environmental where both bio-composites were found effective in treating the chemical oxygen demand (COD). Kenaf fibre and sugarcane husk record 75% and 58% COD reduction respectively. Comparing the results with the Department of Environment quality index, the COD value treated by kenaf fibre had improved from Class V to Class IV but the one treated by sugarcane husk remained in Class V.

It is well known that lower BOD value indicates less polluted or cleaner water. The BOD of untreated pavement runoff was less than 20 mg/L which can be considered nearly contaminated. Introducing the bio-composite materials to reduce the BOD seems like a good approach. From analysis, the percentage of BOD removal rate by kenaf fibre and sugarcane husk were around 20%. The filtered runoff was about 80% lesser before being classified as contaminated and nearly to fall in Class IV.

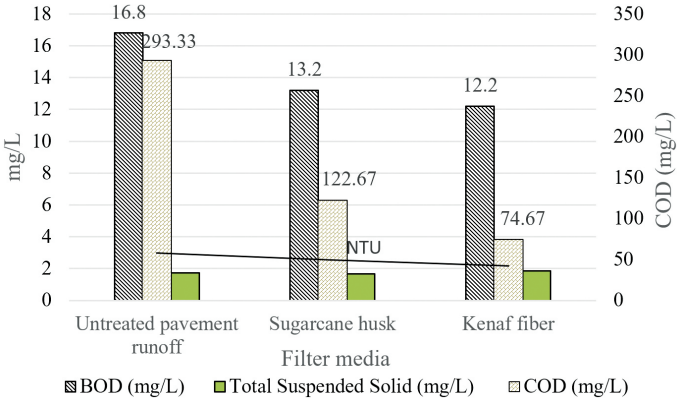

Figure 5: Comparison between Treated and Untreated Pavement Runoff

Referring to Figure 5, it clearly shows that the readings of COD, BOD and turbidity improved except for TSS. It is known that TSS often related to turbidity. If the TSS is high, turbidity is expected to increase proportionately. This is approved by tests conducted where the turbidity increased when TSS increased as in Table 2. The ratio between turbidity to TSS of untreated pavement runoff was 1.73 while 1.17 and 1.52 were the ratio obtained for the pavement runoff filtered by kenaf and sugarcane husk respectively. From the turbidity test conducted, kenaf and sugarcane filtered and reduced the percentage of turbidity. Around 28% and 14% turbidity in pavement runoff were reduced by kenaf fibre and sugarcane husk respectively.

Table 2: Pavement Runoff Quality

Parameter	Untreated Pavement Runoff	Treated with Bio-Composite Materials Sandwiched in Modular Block System		DOE Water Index Class IV
		Kenaf Fibre	Sugarcane Husk	
COD (mg/L)	293.33	74.67	122.67	50-100
BOD (mg/L)	16.8	12.2	13.2	6-12
Total Suspended Solid (mg/L)	1.72	1.84	1.68	150-300
Turbidity (NTU)	2.98	2.16	2.55	

A significance improvement in water quality between 20% to 75% were observed. Overall, the turbidity improved from 2.98 NTU to 2.16 NTU and 2.55NTU, turbidity compared to TSS in pavement runoff that was filtered by kenaf was better. Higher turbidity at minimum TSS observed in sugarcane husk could be due to its texture that dusty. Hence, it is agreed that the bio-composite materials used were able to treat the turbidity.

Referring to Figure 6, both bio-composite materials were capable and performing well in filtering and improving the quality of pavement runoff except for the total suspended solid. The only parameter seems unable to be directly improved the pavement runoff was total suspended solid (TSS). Sugarcane husk recorded 2% improvement of TSS however the kenaf fibre found to be downgrading the quality on pavement runoff in the beginning. Although TSS is worsened, the turbidity improved much. In detail comparison between two types of bio-composite materials used in this study, kenaf fibre was found better in treating the pavement runoff where three out of four parameters tested improved the water quality immediately. The percentage of removal in Figure 6 is supported by several studies on the performance of additive materials particularly the kenaf and coconut husk in treating the polluted water. (S. Nimesha *et. al.,* 2021, U.O. Benjamin, at. al., 2021, Dilaeliyana *et. al.,* 2022). Studies revealed the percentage of removal efficiencies using kenaf and coconut husk ranges from 43 to 90% and 66-69% respectively.

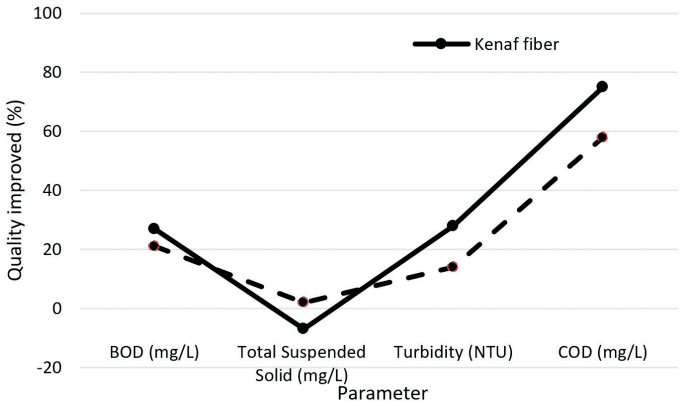

Figure 6: Percentage of Improvement

5.0 CONCLUSION

Results and analysis conducted show that the kenaf fibre and sugarcane husk that sandwiched in the brick opening area were efficient and can be used in preliminary stage of in treating the pavement runoff. From laboratory work conducted, the quality of contaminated pavement runoff filtrated by the sandwiched bio-composite materials were improved before released into the water bodies. It can be concluded that the research objectives have been achieved where the proposed bio-composite material sandwiched in the designed brick were able to enhance the pavement runoff quality. A better brick and bio-composite arrangement are expected to improve the pavement runoff quality which can escalate the water quality from Class V to IV. Between two types of bio-composite materials proposed, kenaf fibre performed better in all aspects and has potential in treating pavement runoff.

Since the pollutants in pavement runoff are closely related to rainfall volume, rainfall intensity, traffic condition and other factors (Dos Santos *et al*. 2019; Du *et al*. 2019) thus, there is still room for improvement. It is suggested that this research to be extended with the used of different types of brick surfaces as the pavement runoff quality also influenced by the chemical reaction between brick surfaces and contaminant transported.

6.0 ACKNOWLEDGEMENTS

The authors thank the Universiti Putra Malaysia (UPM), for providing financial support under the Putra Research Grant (GP-IPM9661700). The authors also acknowledge the support from Civil Engineering Department for assistance with field data collections and laboratory works. ■

REFERENCES

[1] Ashantha, G., Gilbert, D, Ginn, S., and Thomas, E. 2005. Understand the Role of Land Use in Urban Stormwater Quality Management. Journal of Environmental Management. 74: 1-2.

[2] Benjamin U. Okoro, Soroosh Sharifi, Mike Jesson, John Bridgeman, and Rodrigo Moruzzi. 2021. Characterisation and Performance of Three Kenaf Coagulation Products under Different Operating Conditions. Journal of Water Research. 188: 1-14.

[3] Boller, M. 1997. Tracking Heavy Metals Reveals Sustainability Deficits of Urban Drainage Systems. Journal of Water, Science and Technology. 35: 77-87.

[4] Dilaeleyana, A.B.S., Angel, L.N., Vyranath, K.M., Pavithra, K., Aida, M., Nurul, I.M.I., and Nur, H.H.H. (2022). Performance of Coconut Husk Activated Carbon (CHAC) for Polluted River Water Treatment. Multidisciplinary Applied Research and Innovation MARI. 3(1), 15-21

[5] Dos Santos, P. R. S., Fernandes, G. J. T., Moraes, E. P. and Moreira, L. F. F. 2019. Tropical Climate Effect on the Toxic Heavy Metal Pollutant Course of Road-Deposited Sediments. Environmental Pollution. 251, 766–772.

[6] Du, X., Zhu, Y., Han, Q. and Yu, Z. 2019. The Influence of Traffic Density on Heavy Metals Distribution in Urban Road Runoff in Beijing, China. Environmental Science and Pollution Research. 26 (1), 886–895.

[7] Fuerhackera, M., Tadele, M. H., Bernhard, M., and Mentler, A. 2011. Performance of a Filtration System Equipped with Filter Media for Parking Lot Runoff Treatment. Desalination. 275. 118-125.

[8] Hazrol, M.D., Sapuan, S.M., Ilyas, R.A., Zainudin, E.S., Zuhri, M.Y.M. and Abdul, N.I. 2023. Effect of Corn Husk Fibre Loading on Thermal and Biodegradable Properties of Kenaf/Cornhusk Fibre Reinforced Corn Starch-Based Hybrid Composites. Heliyon. 9(4).

[9] Kumar, L. V. R., and Velmurugan, V., 2022 Mechanical Characterization and Experimental Testing of Kenaf Natural Fiber Composites with Cellulose Reinforcement. Materials Today: Proceeding, 51(2022)1172-1178.

[10] Kundzewicz, Z.W., Mata, L.J., Arnell, N., Döll, P., Kabat, P., Jiménez, B., Miller, K., Oki, T., Şen, Z. and Shiklomanov, I. 2007. Freshwater Resources and Their Management. Climate Change 2007: Impacts, Adaptation and Vulnerability. The Fourth Assessment Report of the Intergovernmental Panel on Climate Change

[11] Latimer, J. S., Mills, G. L., Hoffman, E. J., and Quinn, J. G. 1986. Treatment of Solids and Petroleum Hydrocarbons in Storm Runoff with an On-Site Detention Basin. Bulletin of Environmental Contamination and Toxicology, 36(1), 548–555.

[12] Lee, H., Swamikannub, X., Radulescub, D., Kimc, S., and Stenstrom, M.K., 2007. Design of Stormwater Monitoring Programs. Water Research 41 (18), 4186-4196.

[13] Li, H., Li, Z., and Zhang, X. 2017. The Effect of Different Surface Materials on Runoff Quality in Permeable Pavement Systems. Environmental Science and Pollution Research 24, 21103–21110.

[14] Ma, Y., Hao, S., Zhao, H., Fang, J., Zhao, J., and Li, X. 2018. Pollutant Transport Analysis and Source Apportionment of the Entire Non-Point Source Pollution Process in Separate Sewer Systems. Chemosphere, 211, 557–565.

[15] Markiewicz, A., Björklund, K., Eriksson, E., Kalmykova, Y., Strömvall, A. M., and Siopi, A. (2017). Emissions of Organic Pollutants from Traffic and Roads: Priority Pollutants Selection and Substance Flow Analysis. Science of the Total Environment, 580, 1162– 1174.

[16] Park, D., Kang, H., Jung, S.H., and Roesner, L.A., 2015. Reliability Analysis for Evaluation of Factors Affecting Pollutant Load Reduction in Urban Stormwater BMP Systems. Environmental Modelling and Software 74, 130-139

[17] Pitcher, S.K., Slade, R.C.T., and Ward, N. I., 2004. Heavy Metal Removal from Motorway Stormwater Using Zeolites. Sci. Total Environ. 334-335, 161-166.

[18] Qin, H. Peng, H. K. and Mao, Fu. G., 2016. Modeling Middle And Final Flush Effects Of Urban Runoff Pollution in an Urbanizing Catchment. J. Hydrology. 534, 638-647

[19] Qian, G., Zhang, J., Li, X., Yu, H., Gong, X., and Chen, J. 2021. Study on Pollution Characteristics of Urban Pavement Runoff. Water Science and Technology, 84(7), 1745–1756.

[20] Risch, E., Gasperi, J., Gromaire, M.C., Chebbo, G., Azimi, S., Rocher, V., Roux, P., Rosenbaum, R.K., and Sinfort, C., 2018. Impacts from Urban Water Systems on Receiving Waters. How To Account For Severe Wet-Weather Events In LCA? Water Res. 128, 412-423

[21] Shahrzad, M., Ebrahim, T., Parham, Soltani., Seyed, E.S., and Ali, K. 2022. Sugarcane Bagasse Waste Fibers as Novel Thermal Insulation and Sound-Absorbing Materials for Application in Sustainable Buildings. Journal of Building and Environment. 211, 108753.

[22] Shirvani, N., E., Ghalesari, A., T., Tabari. M., K., and Choobbasti, A., J. 2019. Improvement of the Engineering Behavior of Sand-Clay Mixtures Using Kenaf Fiber Reinforcement. Journal of Transportation Geotechnics. (19), 1-8

[23] Xue, H., Zhao, L. and Liu, X. 2020. Characteristics of Heavy Metal Pollution in Road Runoff in the Nanjing Urban Area, East China. Water Science and Technology. 81 (9), 1961–1971.

[24] Wang, J., Huang, J. J., and Li, J. 2020. Characterization of the Pollutant Build-Up Processes and Concentration/Mass Load in Road Deposited Sediments over a Long Dry Period. Science of the Total Environment, 718, 137282.

PROFILES

TS. DR NOR AZLINA BINTI ALIAS is a senior lecturer at Civil Engineering Department, Ts. Dr Nor Azlina binti Alias has joined Universiti Putra Malaysia in 2018. She had previously served at the Faculty of Civil Engineering and Earth Resources, Universiti Malaysia Pahang, for 12 years. Her doctorate thesis discussed on the development of hydrodynamic flow model; thus her research interest includes water resources engineering and is not limited to hydraulics and hydrodynamics, flood forecasting, numerical modelling and grey water treatment. Her recent works related to grey water treatment using waste materials, floating treatment wetland, integrated handwash facility with sustainable treatment system. Her interest in extensive waste materials drags her to explore on the diverse uses of waste materials that can lead to improvement in the quality of the environment.
Email address: a_norazlina@upm.edu.my

ASSOC. PROF. DR BADRONNISA BINTI YUSUF has over 25 years of experience teaching and research. First joined as a lecturer in 1997, Dr Badronnisa is now appointed an Associate Professor at Civil Engineering Department, Faculty of Engineering UPM. Experienced in supervising more than 30 local and international students at both Master and PhD levels, Dr Badronnisa expertise in multiple areas related to Water Resources. She is currently fully enthusiastic in her research on hydraulic structures modelling and is deeply interested in research related to phytoremediation, sedimentation, flow modelling and many more.
Email address: nisa@upm.edu.my

INVESTIGATION OF CAUSES AND CHARACTERISTICS OF MONSOON EXTREMES IN PAKISTAN: A CASE STUDY FOR SUMMER MONSOON 2022

(Date received: 08.05.2023/Date accepted: 01.09.2023)

Haris U. Qureshi[1], Syed Muzzamil H. Shah[2*], Mohamed A. Yassin[3], Sani I. Abba[4], Zahiraniza Mustaffa[5]

[1]Associated Consulting Engineers Limited, Karachi, Pakistan

[2, 3, 4] Interdisciplinary Research Centre for Membranes and Water Security, King Fahd University of Petroleum and Minerals, Dhahran, 31261, Saudi Arabia

[5]Department of Civil and Environmental Engineering, Universiti Teknologi PETRONAS, Perak, Malaysia

[*]Corresponding author: syed.shah@kfupm.edu.sa

ABSTRACT

Apart from the long-term changes in the climate patterns, the extreme weather conditions (heat waves, heavy precipitation, and droughts) have also emerged as a prominent consequence of the global climate change. Pakistan being listed among the most susceptible nations to the changing climate patterns has witnessed an increasing trend of extreme precipitation (particularly during monsoon). Therefore, this study was conducted to probe the major meteorological causes of extreme monsoon precipitation in Pakistan, with a special focus on the monsoon 2022, that lead to severe flooding and devastation of infrastructure, agriculture, and loss of lives. The methodology included an in-depth analysis of unusual atmospheric conditions that triggered exceptionally high precipitation. For this purpose, a number of 25 stations across the country lying in the southwest monsoon zone were selected.

The analysis revealed that in April 2022, about 1.2 to 6.0 °C above normal temperature was observed in Balochistan, 2.0 to 4.5 °C in Sindh, and 3.0 to 5.8 °C in Punjab and KPK. Similarly, in May, about 1.0 to 3.5 °C above normal temperature was observed in Sindh and Balochistan, and 1.0 to 3.0 °C in Punjab and KPK. Due to this exceptional warming, an intense trough developed over the area. In April, about 0.5 to 2.5 mb below normal air pressure was observed in Sindh and Balochistan, and 1.5 to 2.2 mb in Punjab. In May, about 1.0 to 3.0 mb below normal air pressure was observed over the study area. For precipitation, the analysis unearthed that in July 2022, about 100 to 300 mm above normal monthly rainfall was received in Sindh, 50 to 200 mm in Punjab and Balochistan, and 5 to 30 mm in KPK. In August, about 100 to 500 mm above normal rainfall was received in Sindh, and 50 to 250 mm in KPK and Balochistan. However, in September, about 15 to 75 mm above normal rainfall was received in Punjab, while the remaining stations showed a negative departure. Conclusively, the unusual pre-monsoon heating resulted in an intense depression over the plains that facilitated the excess moisture penetration from the Indian Ocean, and consequentially extreme precipitation in Pakistan in 2022. The study outcomes are expected to help in devising an effective climate change adaptation and mitigation strategy for the country and to conduct further research on the prediction and analysis of extreme weather conditions under the changing climate patterns.

Keywords: Climate Change, Extreme Precipitation, SDG13, Southwest Monsoon, Temperature

1.0 INTRODUCTION

The occurrence of extreme precipitation events has gained much momentum around the world during the past decades as a consequence of the changing global climate patterns. Climate change generally refers to the long-term changes in the normal weather patterns of an area [1, 2]. These long-term changes are mainly caused due to the anthropogenic activities including land cover alterations and sprawling urbanization, declining forest cover, and emission of toxic greenhouse gases into the air which destabilizes the global heat balance (a balance between the incoming shortwave and the outgoing longwave solar radiation) by trapping the outgoing solar radiation [3]. This trapping of the outgoing heat leads to the warming earth temperature, which consequently results in the changing atmospheric and land surface conditions [4, 5]. Among all weather parameters, air temperature is generally considered to be the most influential on the overall climate pattern of an area, as it significantly impacts (accelerates) the hydrological cycle by expediting the movement of water vapors from land to atmosphere (via increased evapotranspiration), and also influences the other components of weather system including the air pressure gradient and wind circulation, evaporating potential of atmosphere, air moisture availability, cloud cover, and the precipitation characteristics [6]. During the last century, the mean global air temperature has increased by about 0.74 °C [7, 8], whereas regionally, the mean

temperature over South Asia rose by about 0.75 °C [9]. Due to the rising earth temperature and changing wind circulation and other atmospheric variables, the precipitation patterns have undergone significant variations around the world. For instance, during the last century, the mean global land surface precipitation increased at the rate of about 0.04 inch/decade [10, 11]. However, due to the highly variable nature of precipitation, and due to its high sensitivity towards the spatial features of an area, some regions of the world also witnessed a declining precipitation. For example, Alahacoon *et al*. (2020) used the Mann-Kendall test to investigate the rainfall trends in the African continent, and found a declining precipitation pattern in Mozambique, sub-tropical northern desert, west coast river basin of South Africa, and the northern African region, at the rate of about 0.437, 0.80, 0.360, and 1.07 mm/year respectively [12]. Merabtene *et al*. (2016) studied the rainfall patterns in Sharjah (UAE), and found a negative trend of annual rainfall at the rate of about 3 to 9.4 mm per decade [13]. A similar nature of trend was found in a study conducted by Almazroui (2020) in the Kingdom of Saudi Arabia (KSA), according to which the annual mean rainfall declined at the rate of about 5.89 mm/decade during the last four decades over the country [14].

Apart from the long-term changes in the precipitation patterns (form, amount, seasonality, and its spatial coverage), climate change has also impacted the intensity and extremity of precipitation around the globe. A high intensity precipitation generally refers to the large amount of precipitation received over an area in a short period of time [15]. During the past decades, the frequency of occurrence of high intensity extreme rainfall events has increased globally, mainly due to the warming air temperatures, as the warm air can hold more water vapors in it as compared to the cold air, and the availability of water vapors serves as the key ingredient for heavy rainfall [16]. According to the Center for Climate and Energy Solution, for each degree centigrade rise in air temperature, the air water holding capacity can increase by about 7% on average globally [17]. Thus, the warm areas are more prone to the intense storm events as compared to the cold areas [18]. Another atmospheric parameter which significantly influences the wind circulation and the precipitation characteristics is the air pressure, which strongly depends on the air and land surface temperatures and the geographical location of an area. Due to the differential solar heating of the earth surface, a noticeable latitudinal variation in the air pressure exists around the globe known as the Pressure belts, which facilitate the global wind circulation [19]. In general, winds follow a pressure gradient, and are blown from a high pressure area to a low pressure area, with greater the pressure gradient, the more will be the wind velocity [20]. These High and Low Pressure Systems (HPS and LPS respectively) are mainly characterized on the basis of air temperature and wind circulation. Warm areas generally result in the formation of LPS (also known as Depression or Cyclone), characterized by high wind convergence towards its center, higher cloud cover due to the rising moist air and condensation, and heavy precipitation due to sufficient availability of moisture and convergence of air masses [21]. Moreover, in warm areas, winds blow spirally in the counter-clockwise direction in the Northern Hemisphere and clockwise in the Southern Hemisphere due to the Coriolis Effect [22]. On the other hand, cold areas generally result in HPS (also known as Anticyclones), characterized by fair weather and moderate winds blowing spirally outward in a clockwise direction (Northern Hemisphere), low cloud cover, and less precipitation [23]. A weather condition which is formed due to the intense heating of land surface is known as the Thermal low, Heat low or the Trough. Around the world, the strongest thermal lows are developed over the Sahara, Australian Great Western Deserts, Arabian Kalahari, and Sonoran Deserts due to the intense surface heating [23]. It is important to note that lower the air pressure, the higher the warm air containing moisture will rise into the atmosphere and form clouds after condensation of water vapors in air, with the greater probability of intense storm events [24, 25].

During the recent past decades, a number of intense rainfall events have been observed over the different parts of world, as a consequence of warming temperatures and changing global air circulation patterns. For example, in summer 2020, the Baixada Santista metropolitan region in the Sao Paulo state of Brazil received about 320 mm of rainfall in a single day, breaking the country's previous highest 24-hr rainfall record [23]. Similarly, in 2022, Taiwan received the third highest winter rainfall in the country's history during January to February. As per Huang *et al*. (2022), Taiwan normally receive its winter rainfall from the precipitation system originating in the northern South China Sea without frontal structure. However, in the year 2022, contrary to the normal rainfall pattern, the winter monsoon induced orographic rainfall penetrated the country along with the frontal rainfall, thereby bringing about 130% higher rainfall than the normal. The occurrence of this extreme storm event was also linked to the enhanced winter background circulation, which included an enhancement of the regional northeasterly wind at 925 hPa in conjunction with the enhancement of the southwesterly wind conveying moisture at 700 hPa, due to which a vigorous convection zone extending from the southeastern Bay of Bengal to Taiwan was censured for the extreme rainfall in January to February 2022 [26]. A similar 24-hour extreme rainfall event was witnessed in Auckland (New Zealand) on 14th January 2023, when the city received about 258 mm of rainfall, making it the wettest day in the city on record with the total rainfall of about 539 mm was received in January over the city [27].

The word "Monsoon" generally refers to the seasonal change in the prevailing wind pattern due to the temporal latitudinal shifting of the Intertropical Convergence Zone (ITCZ) between its extreme limits as the Tropic of Cancer (23.5 °N) and Tropic of Capricorn (23.5 °S) in the northern and southern hemispheres respectively [28]. Globally, the major monsoon systems include the African monsoon, Asian monsoon, North American monsoon, Australian monsoon, and the European monsoon [29]. The Asian monsoon has two branches as the South Asian monsoon and the East Asian monsoon [30]. The South Asian monsoon covers the Indian sub-continent and the surrounding regions including Nepal, Myanmar, and Bangladesh, whereas the East Asian monsoon covers southern China, Korea, Taiwan, and Japan [31]. Based on the seasonal wind pattern, the South Asian monsoon is further divided into two categories as the Southwest Summer monsoon (advancing monsoon) and the Northeast Winter monsoon (retreating monsoon) [32]. Pakistan receive its summer precipitation from the southwest summer monsoon during July to September, which contributes about 60% to the country's annual total precipitation, and holds a significant importance in terms of the replenishment of

streamflows and groundwater resources, and favoring the Kharif crop production [33].

The major factors which govern the mechanism of the southwest summer monsoon system include the differential heating of the land mass in the Indian sub-continent and the Indian Ocean, development of a high pressure system over the Indian Ocean, seasonal latitudinal shifting of ITCZ at the Tropic of Cancer, formation of Tibetan trough, Sub-Tropical Westerly Jet Streams (STWJ) and the Tropical Easterly Jet streams (TEJ), and El-Nino Southern Oscillation (ENSO) [33, 34]. In South Asia, the southwest summer monsoon system generally initiates with the differential heating and the development of air pressure gradient between the Indian Ocean and the land masses in India and Pakistan. With the onset of summer season in the northern hemisphere, the Thar desert and the nearby warm arid and hyper arid plains in India and Pakistan warms up more quickly as compared to the Indian Ocean, due to the fact that the rate of heat absorbance of soil surface is higher than that of water. Due to this differential heating, a high pressure system called as the Mascarene high is developed over the Indian Ocean (between the latitudes 30 to 35 °S and between the longitudes 40 to 90 °E) along the eastern coast of Madagascar, while a low pressure system is developed over the landmasses due to the higher surface heating. This air pressure gradient created between the plains and Indian Ocean results in a strong moist wind system originating from the Indian Ocean (Madagascar region), that starts to march towards the equator in the northwest direction, and after crossing the equator, the wind system is diverted, and it blows from the southwest direction towards the southern Indian peninsula, where due to its topography, the southwest monsoon system is divided into its two branches as the Arabian sea and Bay of Bengal in the Indian Ocean [35, 36].

Due to the seasonal latitudinal shifting of ITCZ at the Tropic of Cancer during summers in the northern hemisphere, an intense heating takes place over the Tibetan plateau, which results in the formation of LPS over the area, known as the Tibetan trough. This LPS also plays an important role in pulling the moist monsoon winds from the Arabian Sea and Bay of Bengal towards the land areas of India and Pakistan. In addition, the latitudinal shifting of ITCZ and heating of Tibetan plateau also impacts the pattern of jet streams in the region. For instance, the sub-tropical westerly jet streams normally travel in the upper troposphere from west to east, closer to 30 °N along the southern edge of Himalayan range all over the year. However, with the onset of summer season and shifting of ITCZ in the northern hemisphere, STWJ is displaced towards the northern Himalaya. The Himalayan belt also impacts the incoming moist monsoon winds from the Bay of Bengal by acting as a physical barrier and preventing the monsoon incursion into the Central Asia. Due to the seasonal heating of Tibetan plateau and formation of Tibetan trough, the warm air over the area rises up and cools as it reaches the upper troposphere, resulting in the formation of a high pressure system (approximately 200 hpa) over the altitude, which weakens the blowing STWJ over the northern Himalaya and results in the formation of Tropical Easterly Jet streams (TEJ) on the southern side of the high pressure system. This TEJ then moves westward over the Indian Ocean towards the eastern Africa and descends into the Mascarene high, thereby strengthening the high pressure cells of the Madagascar high pressure system. It is important to note that the intensity and location of Mascarene high significantly impact the strength of monsoon rainfall system in India and Pakistan [37, 38]. The monsoon precipitation typically begins from 1st June in India, and then the rainy system enters Pakistan on the first week of July. In Pakistan, the southwest monsoon system penetrates the country via its two branches, i.e. the Arabian Sea and the Bay of Bengal. The monsoon rainfalls in Pakistan generally starts with the moisture carrying wind system coming from the Bay of Bengal, which enters the country from the eastern and northeastern side, and results in generous rainfall over the northern areas, northern and central Punjab, and Kashmir. The other branch of southwest Monsoon i.e. the southwesterly moist winds from the Arabian sea then enters Pakistan, and brings good amount of rainfall over the southeastern parts of country including Sindh and Balochistan [39].

As discussed earlier, the El-Nino Southern Oscillation (ENSO) also influences the South Asian Monsoon [40]. For instance, the El-Nino which is the warmer phase of the El-Nino Southern Oscillation (ENSO) and generally takes place due to the unusual warming of sea surface temperature of the eastern Pacific Ocean along the South American coast, adversely affects the monsoon precipitation in Pakistan and India by causing drought conditions. This is due to the fact that during El-Nino, the air moisture from the Mascarene high is diverted towards the eastern Pacific Ocean due to the formation of an intense low air pressure condition over the eastern pacific along the coast of South America [41]. In Pakistan, the history's worst drought during 1998 to 2001 was mainly attributed to El-Nino. In contrast to El-Nino, La-Nina, which is the cooler phase of ENSO, brings above normal Monsoon precipitation. For example, the 2010 extreme Monsoon rainfalls in Pakistan was mainly linked to the occurrence of La-Nina [42, 43].

1.1 Literature Review

Synchronously to the changing global climate patterns, the weather patterns in Pakistan have also undergone significant variations over the years. For instance, the mean annual temperature of Pakistan increased by about 0.64 °C during the period 1900-2009, at the rate of about 0.064 °C per decade [44]. Interestingly, the rate of warming was higher during the latter part of century as compared to the earlier years over the country, which was reported in a study conducted by the Asian Development Bank, according to which the mean annual temperature of Pakistan increased at the rate of about 0.07 °C per decade during 1960-2021, with the magnitude of change as 0.47 °C during the period. Seasonally, the warming trends in Pakistan have been found to be more inclined towards the spring, post-monsoon, and the winter months, as compared to the summer season [45, 46]. Due to the warming air temperatures, and the consequential changes in the air moisture conditions and wind patterns, the frequency of short duration extreme rainfall events has significantly increased in the country during the past decades, as shown in the Figure 1. For example, on 23rd July 2001, about 621 mm of rainfall was received in Islamabad in 10 hours, thereby causing severe urban flooding in the city. Similarly, on 18th July 2009, about 207 mm of rainfall was received in Karachi, making it one of the highest one-day rainfall recorded in the city [47]. On 19th August 2022, Padidan received the record breaking 355 mm of rainfall due to the formation of intense low air pressure conditions over the northern belt of Sindh province (*PMD Annual Climate Report,*

2022). The details of some of the 24-hour extreme rainfall events that took place over the country during the past 30 years are shown in Table 1.

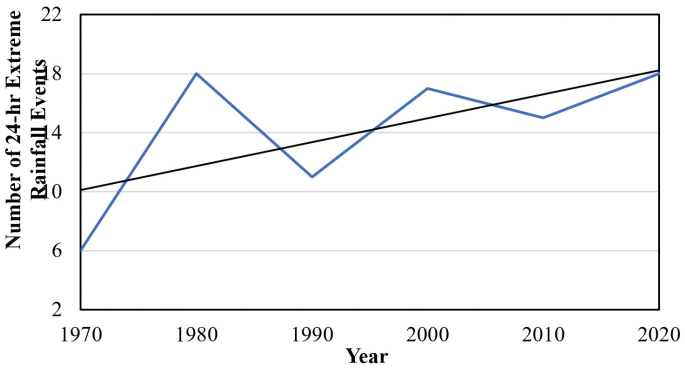

Figure 1: Frequency of Occurrence of Extreme Rainfall Events in Pakistan with Rainfall Above 200mm Received in 24 Hours

Source: Pakistan Meteorological Department (PMD)

The above statistics clearly indicate that the occurrence of extreme rainfall events has significantly increased in Pakistan, especially during the monsoon season. For instance, in 2003, Sindh received above normal monsoon precipitation, which resulted in severe flooding in the province. During the two-day rainfall spell, 284.5 mm of rainfall was received in Karachi, and 404 mm in Thatta. In 2007, Khyber Pakhtunkhwa (KPK), Sindh, and the coastal belt of Balochistan was severely affected due to the extreme monsoon rainfall. In 2009, Karachi received 147 mm of rainfall during 17th to 19th July, which resulted in severe urban flooding in the city. In 2010, Pakistan faced the worst flood in its history due to the occurrence of extreme monsoon precipitation (80% above normal) over the country that inundated about 20% of its land area [43]. The post event analysis by PMD revealed that the above normal rainfall was mainly caused due to La-Nina. The other contributing factors included the unusual change in the position of monsoon depression formed over the Bay of Bengal, that moved towards the northeastern side in Balochistan and caused a large amount of moisture incursion from the Bay of Bengal and Arabian sea, and then its convergence over Khyber Pakhtunkhwa due to the orographic effect, thereby causing extreme precipitation over the area. The spatial features of the flood-hit areas also played a significant role in the convergence and lifting of water vapors. In this context, near to the middle troposphere, the cold air advection from 500 mb occurred over the Pakistan's latitudes, and the lower elevated warm and moist air was overtaken by the cold air mass which created an intense cellular vertical circulation. This resulted in a continuous incursion of moisture from both branches of southwest monsoon. Moreover, the presence and stagnancy of STWJ over the northern Pakistan was another factor which played a significant role in the incursion and movement of water vapors over the higher latitudes of country, which resulted in extreme precipitation. As per PMD, during 27th July 2010 to 30th July 2010, 415 mm of rainfall was received in Risalpur, 394 mm in Islamabad, 373 mm in Murree, 372 mm in Cherat, 333 mm in Peshawar, 292 mm in Muzaffarabad, 256 mm in Balakot, 222 mm in Gujranwala, 220 mm in Dera Ismail Khan, and 219 mm was received in Rawalpindi. Comparatively, the monthly rainfall in July 2010 was 80% above normal, while in August, 102% above normal rainfall was received in the country. The intense rainfall induced floods caused approximately $43 billion loss to the national economy, 1700 loss of lives, and damage to about $500 million worth of crops [48].

Table 1: Details of 24-Hour Extreme Rainfall Events in Pakistan During the Last 30 Years

Source: Pakistan Meteorological Department (PMD)

Date	Station	Rainfall (mm)
10th September 1992	Muzaffarabad	208
27th August 1997	Islamabad	200
27th August 1997	Murree	233.8
24th July 2001	Islamabad	200
23rd July 2001	Rawalpindi	335
7th July 2003	Larkana	209
29th July 2007	Sargodha	205
13th August 2008	Lahore	221
18th July 2009	Karachi	205
29th July 2010	Risalpur	280
29th July 2010	Peshawar	274
30th July 2010	Islamabad	257
29th July 2010	Cherat	257
29th July 2010	Kohat	233
30th July 2010	Murree	231
6th June 2010	Gwadar	227
4th August 2010	Dera Ismail Khan	202
11th August 2011	Tando Ghulam Ali	350
7th September 2011	Diplo	312
10th August 2011	Mithi	291
26th August 2011	Kohat	240
31st August 2011	Padidan	238
7th September 2011	Mithi	225
11th August 2011	Tando Muhammad Khan	200
11th August 2011	Tando Ghulam Haider	200
10th September 2012	Jacobabad	305
5th September 2014	Lahore	300
5th September 2014	Jhelum	296
5th September 2014	Islamabad	297
5th September 2014	Mangla	251
5th September 2014	Sialkot	251
2nd September 2020	Bahawalnagar	240
28th August 2020	Karachi	231
19th August 2022	Padidan	355
25th August 2022	Shaheed Benazirabad	123
22nd August 2022	Larkana	157.3
6th July 2022	Gwadar	58
27th July 2022	Ormara	62
22nd July 2022	Rahim Yar Khan	58

In 2011, the situation was different as the extreme monsoon precipitation was mainly concentrated in Sindh, unlike in 2010 that affected KPK and Punjab. In July 2011, Pakistan as a whole received below normal rainfall. However, in August and September, the country received more than average rainfall [49].

As per PMD, a strong weather system was formed over Uttar Pradesh in India on 6th August 2011, which then moved in the westward direction. The first healthy spell of summer monsoon began lately in the country from 9th August as a result of deviation of monsoon depression from its usual route. Normally, the southwest monsoon system enters Pakistan from the northeast, and rainfall begins with the generous showers in central and northern Punjab with till mid of August, with most parts of country are covered by the monsoon precipitation. In 2011, contrarily to the normal pattern, the location of monsoon depression remained southwest in India and a high pressure system was developed over the Bay of Bengal that moved in the southwest direction, instead of its usual northwestern route, thereby entering Pakistan from Rajasthan to Sindh. As discussed earlier, a high pressure system is characterized as having light winds and air subsidence. The Tibetan high (generally located above 30°N during monsoon) restricts the incursion of monsoon winds, and the monsoon activities normally take place below its ridge. However, in 2011, the Tibetan high moved unusually downward at about 26 °N due to which the air moisture could not traveled in the upper parts of country and was therefore restricted only to the lower parts. Secondly, the intense surface heating in Balochistan during the summer season results in seasonal LPS over the area with the normal pressure of about 1000 hpa prevails in the province during the season. However, on 9th August, the air pressure was 4 hpa less than its normal value due to the exceptionally high air temperatures recorded over the province, thereby pulling excess moisture from the monsoon system present at the eastern boundary of Sindh. On 10th August, the trough formed over the arid plains in Sindh facilitated the incursion of excess moisture from the Arabian Sea and resulted in monsoon extreme precipitation [50]. As per PMD, during the first two weeks of September, about 760 mm of rainfall was received in Mithi, 603 mm in Mirpur Khas, 353 mm in Nawabshah, 348 mm in Dadu, 268 mm in Dadu, 244 mm in Hyderabad, and 212 mm was received in Karachi (*PMD Annual Climate Report, 2011*).

In 2012, due to the unusual heating of the Indian Ocean, a depression was formed over the Bay of Bengal in the last week of August that moved towards Sindh and resulted in extreme monsoon precipitation over the province. As per PMD, during the intense rainfall spell from 5th to 11th September, 481 mm was received in Jacobabad, 216 mm in Larkana, 206 mm in Sukkur, and 205 mm in Rohri (*PMD Annual Climate Report, 2012*). In 2013, normal to slightly above normal monsoon precipitation was received in Pakistan as a whole, except the Sindh province (21% below normal). In July, 31% below normal rainfall was received in Pakistan, with the highest withdrawal in Sindh (-84%), followed by Balochistan (-57%), KPK (-11%), Punjab (-9%), and Azad Jammu & Kashmir (-7%). However, in August, Pakistan as a whole received 59% above average rainfall, with Balochistan (+144%), Gilgit-Baltistan (+108%), Sindh (+50%), KPK (+40%), and Azad Jammu & Kashmir (+24%). In September, the monsoon system was weak, and the country received 24% less rainfall than usual (*PMD Annual Climate Report, 2013*).

In 2014, unusual drought conditions prevailed during the first two months of monsoon in Pakistan, where in July, Pakistan received 39% below normal rainfall, with the highest deficit was found in Sindh (-97%), followed by Balochistan (-42%), and Azad Jammu & Kashmir (-24%). Similarly, in August, the drought conditions sustained, and the country received 49% below normal rainfall. However, in September, due to the unusual heating over the northern areas, a trough was formed over Kashmir, which then moved eastward towards the northern Pakistan. This depression played a key role in pulling the moisture from Indian Ocean towards the northern areas, that resulted in torrential rainfalls over Azad Kashmir (+181%), Gilgit-Baltistan (+531%), and Punjab (+225%), while below average rainfall was observed in Sindh (-12%) and Balochistan (-12%). As per PMD, during the four-day rainfall spell from 1st to 5th September, 557 mm of rainfall was received in Lahore, 523 mm in Sialkot, 345 mm in Rawalpindi, 345 mm in Mangla, 298 mm in Islamabad, 228 mm in Faisalabad, and 220 mm of rainfall was received in Jhelum (*PMD Annual Climate Report, 2014*).

In 2015, Pakistan as a whole received 27% above normal monsoon rainfall, with the highest departure was observed in Gilgit-Baltistan (+116%). In July, Pakistan as a whole received 40% above normal rainfall, with Gilgit-Baltistan (+95%), KPK (+19%), Punjab (+69%), and Sindh (+78%), while a deficit (-22%) was observed in Balochistan. Contrarily, in August, Pakistan received 8% below normal rainfall, with the highest withdrawal was found in Sindh (-96%), followed by Balochistan (-62%), and Azad Jammu and Kashmir (-37%), while Punjab and KPK received 20 % and 54 % above normal rainfall respectively. In September, Pakistan as a whole received 41% above average rainfall, with the highest departure in Gilgit-Baltistan (+316%), followed by Punjab (+71%), Sindh (+29%), and Azad Jammu & Kashmir (+28%), while below normal rainfall was observed in Balochistan (-30%) (*PMD Annual Climate Report, 2015*). In 2016, Pakistan as a whole received 25% above normal monsoon rainfall, with the highest departure was observed in Punjab (+55%). In July, Pakistan received slightly less than normal rainfall (-14%), with the highest withdrawal was found in Balochistan (-41%), followed by Azad Jammu and Kashmir (-15%). However, in August, 76% above normal rainfall was received in Pakistan, with the highest departure in Sindh (+149%), followed by Punjab (+107%), KPK (+56%), Gilgit-Baltistan (+23%), and Balochistan (+6%). In September, slightly above normal rainfall was received in Pakistan as a whole (+7%), with Gilgit-Baltistan (+44%), KPK (+32.4%), Punjab (+39%), while in Sindh, 92% below normal rainfall was received (*PMD Annual Climate Report, 2016*). In 2017, drought conditions prevailed during the monsoon, where Pakistan as a whole received 22% below normal rainfall. In July, Pakistan received 20% below normal rainfall, except Sindh, where close to normal rainfall was received. In August and September, the similar pattern was sustained, and the country received 28% and 19% below normal rainfall respectively (*PMD Annual Climate Report, 2017*). In 2018, similar drought conditions were noticed during monsoon, where Pakistan as a whole recorded 31% below normal rainfall, with the highest deficit was observed in Sindh and Balochistan. In July, Pakistan as a whole received 12% below average rainfall, while provincially, above normal rainfall was received in Punjab, KPK, and Gilgit-Baltistan. In August and September, the similar pattern prevailed, and the country received 51% and 35% below average rainfall respectively (*PMD Annual Climate Report, 2018*).

In 2019, Pakistan as a whole received near to normal monsoon rainfall, with the above normal monsoon precipitation was mainly focused on the Sindh province (+46%). In July, Pakistan as a whole received 8% below normal rainfall, with the highest deficit was observed in Gilgit-Baltistan (-59%), followed by Azad Jammu & Kashmir (-24%), Balochistan (-19%), KPK (-11%), and Punjab (-9%), while Sindh received 24% above normal rainfall. In August, 52% above average rainfall was received in Sindh and 35% above normal in Gilgit-Baltistan, while the remaining parts of country recorded below normal rainfall. In September, Pakistan as a whole received 15% above normal rainfall, with Sindh (+99%), Balochistan (+48%), and Punjab (+28%), while a negative departure was found in Gilgit-Baltistan (-75%), KPK (-49%), and Azad Jammu & Kashmir (-23%) (*PMD Annual Climate Report, 2019*). In 2020, Pakistan received 41% above normal monsoon rainfall, making it the 4th wettest year since 1960, with the extreme precipitation was mainly centered in Sindh and Balochistan during the early monsoon. Apart from precipitation, the temperature patterns were also extreme during the year. In 2020, Pakistan recorded 0.22 °C higher mean annual temperature than normal. In August, the country observed 0.76 °C above normal temperature, with Sindh observed 1.1 to 2.2 °C, and Balochistan observed 0.1 to 1.9 °C above normal temperature. Similarly, in September, Pakistan recorded 0.29 °C above normal temperature, with Sindh observed 0.8 to 2.3 °C, and Balochistan observed 0.7 to 1.9 °C above average temperatures. These unusual high temperatures resulted in intense depression over the arid plains of Sindh and Balochistan, thereby maintaining an active intrusion of moisture from the Indian Ocean, which resulted in extreme precipitation over the country. In July, Pakistan as a whole received 34% below normal rainfall. However, in August, the monsoon gained strength, and the country as a whole received 108% above normal rainfall, with Sindh (+363%), Balochistan (+271%), Punjab (+14%), KPK (+9%), and Gilgit-Baltistan (+20%). In September, the rainy season shifted northwards, with the highest departure was observed in Punjab (+139%), followed by KPK (+120%), Gilgit-Baltistan (+113%), Sindh (+87%), Azad Jammu & Kashmir (+24%), while a significant deficit was noted in Balochistan (-96%) (*PMD Annual Climate Report, 2020*).

In 2021, the intrusion of monsoon system in Pakistan was delayed by 5 days from its usual date (30th June), with 19% above average monsoon rainfall was received in Gilgit-Baltistan, while Pakistan as a whole received 9% below normal rainfall. In July, Pakistan received 4% above normal rainfall, with the highest departure in Gilgit-Baltistan (+86%), followed by KPK (+28%), and Balochistan (+22%), while a significant deficit was observed in Sindh (-47%). In August, Pakistan as a whole received 89% below normal rainfall, with the highest deficit was observed in Sindh (-89%), followed by Punjab (-67%), Azad Jammu & Kashmir (-63%), Balochistan (-54%), and KPK (-39%). Contrarily, in September, Pakistan as a whole received 60% above normal rainfall, with the highest departure in Sindh (+234%), followed by Balochistan (+64%), Punjab (+44%), and Azad Jammu & Kashmir (+18%), while below normal rainfall was observed in Gilgit-Baltistan (-19%) and KPK (-1%) (*PMD Annual Climate Report, 2021*).

In 2022, Pakistan witnessed one of the worst floods in its history due to the exceptionally high monsoon rainfall, and the expeditious melting of glaciers and snow mass over its northern areas due to the unusual high temperatures. On the annual scale, Pakistan observed 0.84 °C above normal temperature, with the mean maximum temperature was 0.95 °C, and the mean minimum temperature was 1.29 °C above normal. Spatially, the mean annual temperature anomaly was highest over KPK (+1.14 °C), followed by Azad Jammu and Kashmir (1.04 °C), and Gilgit-Baltistan (+0.14 °C). As per PMD, 16 Glacier Lake Outburst Flood (GLOF) events took place in KPK and Gilgit-Baltistan in 2022, as compared to the usual 5 to 6 GLOF events every year. Due to the warm temperatures and intense tough over the plains, rainfall amount and intensity also deviated significantly from its normal pattern. In 2022, Pakistan received 175% above normal monsoon precipitation, with the rainy system was most intense in Balochistan (+450%) and Sindh (+426%), as shown in the Figure 2. In July, Pakistan as a whole received 181% above normal rainfall with the highest departure in Balochistan (+450%), followed by Sindh (+307%), Punjab (+116%), KPK (+30%), and Gilgit-Baltistan (+32%), as shown in the Figure 3. In August, the situation was more severe with 243% above average rainfall was received in the country. Spatially, the departure was highest in Sindh (+726%), followed by Balochistan (+590%), Gilgit-Baltistan (+233%), KPK (+58%) and Punjab (+52%), as shown in the Figure 4. During the heavy rainfall spell from 1st July to 26th August, the Padidan station in Sindh received the record high 1764 mm of rainfall due to the consistent trough over Sindh. In September, due to the beginning of monsoon retreating from the country, Pakistan received 21% below normal rainfall, with the highest deficit in Balochistan (-59%), followed by Punjab (-21%), Gilgit-Baltistan (-19%), and KPK (-16%) as shown in the Figure 5 (*PMD Annual Climate Report, 2022*).

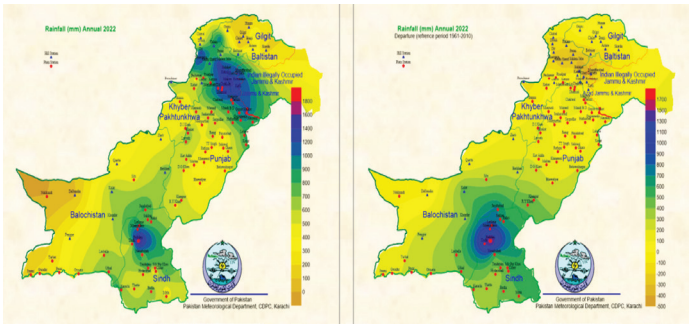

Figure 2: Pakistan Spatial Distribution of 2022 Annual Precipitation and Departure from Normal

Source: PMD Annual Climate Report, 2022

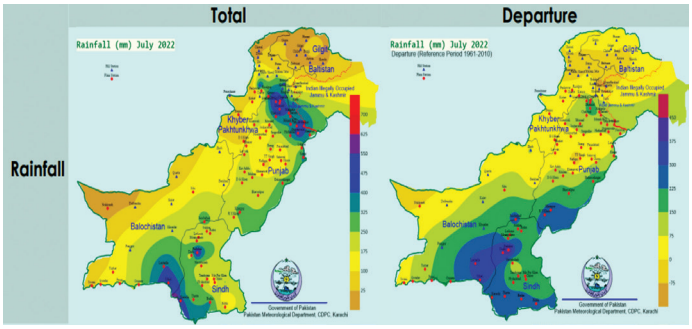

Figure 3: Pakistan Spatial Distribution of July 2022 Precipitation and Departure from Normal

Source: PMD Annual Climate Report, 2022

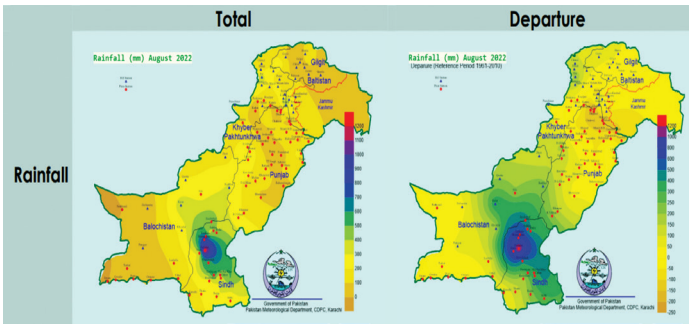

Figure 4: Pakistan Spatial Distribution of August 2022 Precipitation and Departure from Normal

Source: PMD Annual Climate Report, 2022

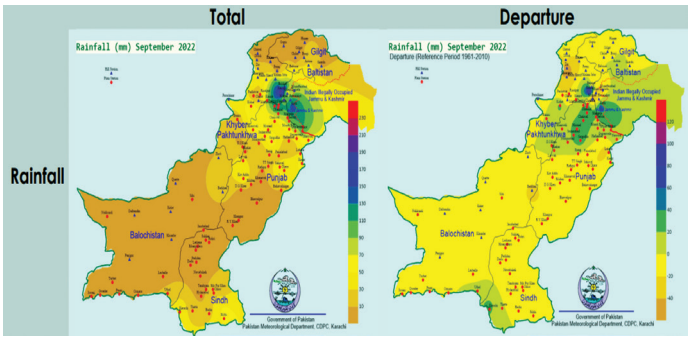

Figure 5: Pakistan Spatial Distribution of September 2022 Precipitation and Departure from Normal

Source: PMD Annual Climate Report, 2022

The above literature review clearly showed that the extremity in monsoon precipitation in Pakistan is gaining momentum as a consequence of the changing climate patterns, which necessitates to investigate the major atmospheric factors behind the occurrence of severe storm events in the country. Therefore, this study was conducted to probe the major meteorological causes behind the extreme monsoon precipitation in Pakistan in 2022. The methodology adopted to achieve the study outcomes is shown in the Figure 6. The outcomes of this study are expected to deeply understand the major factors that played a key role in the occurrence of extreme monsoon precipitation in 2022, and to devise an effective climate change adaptation and mitigation strategy for the country.

2.0 DATA AND METHODOLOGY

2.1 Study Area

Pakistan spatially lies in the Temperate zone and partially in the Sub-Tropics, between the latitudes 23 to 35 °N and between the longitudes 60 to77 °E with a total area of about 796,096 km^2, with the political map of country shown in the Figure 7. Geographically, Pakistan is divided into three main zones including the northern highlands, the Indus river plain, and the Balochistan plateau [51]. The northern highlands consist of the Hindukush, Karakoram, and the Pamir mountain ranges. The Balochistan plateau is located in the west and the vast Thar Desert in the eastern part of country. The 1609 km length of Indus River and its tributaries flow through the country from Kashmir to the Arabian Sea, with an expanse of alluvial plains along the river basin in Punjab and Sindh [52].

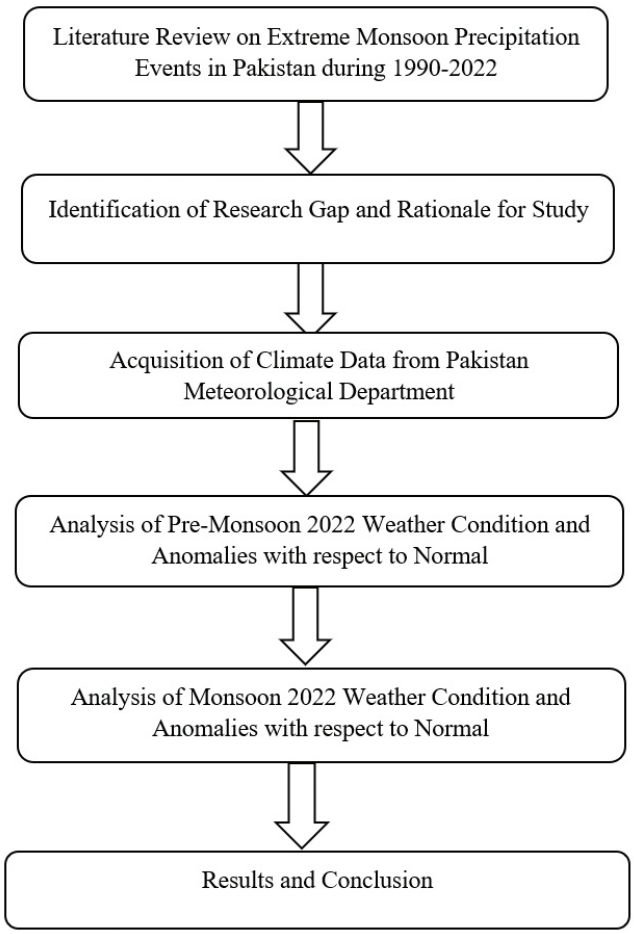

Figure 6: Flow Chart Describing the Methodology Adopted to Achieve the Study Objectives

Climatologically, Pakistan has a continental type of climate with high climate variations over the year. The mean annual precipitation of Pakistan is about 300 mm, with 141 mm comes from the southwest summer monsoon, and 74 mm from the winter precipitation. Seasonally, the weather patterns vary as cool, dry winter from December to February, a hot spring from March to May, followed by a rainy summer season due to the intrusion of southwest monsoon moist winds into the country, and the retreating monsoon period from October to November. Depending on the location and season, Pakistan receives all three kinds of precipitation including the convective, frontal, and orographic precipitation [53]. During the pre-monsoon period, localized convective rainfall is received occasionally which normally contributes about 12% to the annual total rainfall of country. During summer, Pakistan receives the major share of its annual precipitation from the southwest monsoon during July to September. The post-monsoon period in the country is relatively dry, and acts as a transition period between the summer and winter season. The scarce rainfall in autumn contributes about 4% to the annual precipitation of Pakistan. During the winter season, Pakistan receives generous snowfall over the northern and northwestern highlands, and liquid precipitation over the northern and central Punjab, KPK, and Kashmir [47]. In this study, a number of 25 climate stations across Pakistan lying in the southwest monsoon zone were selected (as shown in Figure 8). The geographical and climate details of the selected stations are shown in the Table 2.

Figure 7: Political Map of Pakistan

Source: Survey of Pakistan

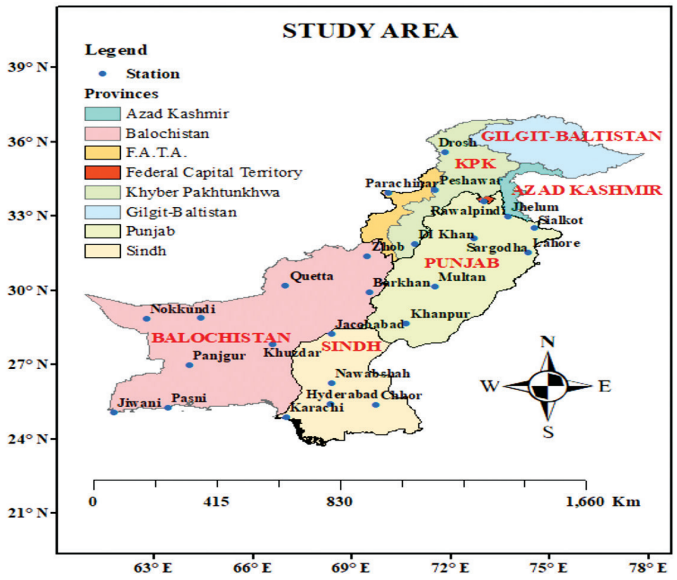

Figure 8: Description of Study Area Showing the Selected Climate Stations

The climate data required for the study was acquired from PMD for the period 1990-2022. The acquired data consisted of monthly maximum and minimum air temperature (°C), air pressure and vapor pressure at station level (mb), and rainfall (mm), along with the monthly climate normal for the period 1961-2010 for all selected stations.

2.2 Methodology

2.2.1 Analysis of Pre-Monsoon 2022 Weather Condition and Anomalies

As discussed earlier, the pre-monsoon weather conditions in Pakistan strongly influence the monsoon precipitation characteristics in the country. Therefore, in this study, in order to investigate the prime atmospheric factors that lead to the extreme monsoon precipitation in Pakistan in 2022, the monthly air temperature and pressure data for the pre-monsoon months (April to June) for the year 2022 was comprehensively analyzed, and the magnitude of anomaly with respect to normal (1961-2010) was computed for all stations, so as to understand the extent of variation from the normal pattern that resulted in the unusual weather conditions in the country.

Table 2: Geographic and Climate Details of the Selected Stations

Source: Pakistan Meteorological Department (PMD)

Station	Latitude (°N)	Longitude (°E)	Mean Annual Temperature (°C)	Mean Annual Precipitation (mm)
Khyber Pakhtunkhwa				
Drosh	35.56	71.8	17.60	588
Peshawar	34.01	71.52	22.70	404
Parachinar	33.90	70.08	15.30	782
DI Khan	31.86	70.90	24.20	318
Punjab				
Rawalpindi	33.56	73.01	21.30	1200
Sargodha	32.07	72.68	24.70	501
Jhelum	32.94	73.72	23	875
Sialkot	32.49	74.52	22.6	972
Lahore	31.52	74.35	24.30	636
Multan	30.15	71.52	25.65	254
Khanpur	28.63	70.65	25.10	97.3
Balochistan				
Zhob	31.34	69.46	19.10	285
Quetta	30.17	66.97	15.70	261
Barkhan	29.89	69.52	21.60	418.6
Nokkundi	28.82	62.75	24.50	35.30
Dalbandin	28.88	64.39	22.40	80.70
Panjgur	26.97	64.08	22.10	109
Khuzdar	27.81	66.60	21.50	252
Jiwani	25.05	61.77	25.60	114
Pasni	25.25	63.41	26.28	115
Sindh				
Jacobabad	28.24	68.38	27.10	223
Nawabshah	26.24	68.39	26.70	161
Hyderabad	25.39	68.35	26.80	156
Chhor	25.35	69.73	26.50	245.50
Karachi	24.86	67	26.60	175

2.2.2 Analysis of Summer Monsoon 2022 Weather Condition and Anomalies

In this study, after the comprehensive analysis of unusual pre-monsoon weather conditions, the monthly precipitation and vapor pressure data for the monsoon months (July to September) for the year 2022 was analyzed for all stations, and the magnitude of anomaly with respect to normal was estimated.

3.0 RESULTS AND DISCUSSION

3.1 Analysis of Pre-Monsoon 2022 Weather Condition and Anomalies:

The results obtained from the pre-monsoon air temperature and pressure analysis for the year 2022 are shown in the Figures 9 to 14 as under:

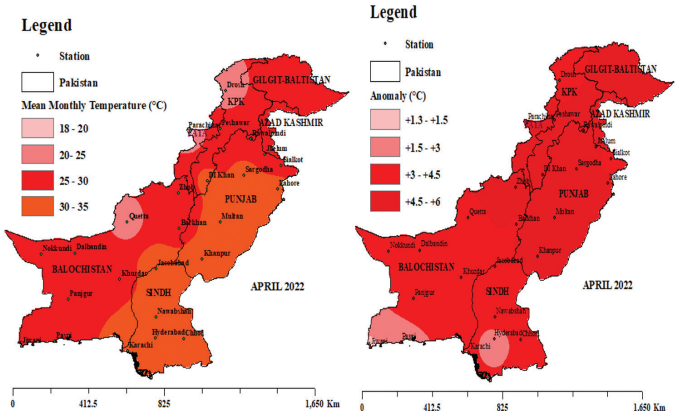

Figure 9: Mean Monthly Temperature (°C) in April 2022 (on left) and the Magnitude of Anomaly (°C) (on right)

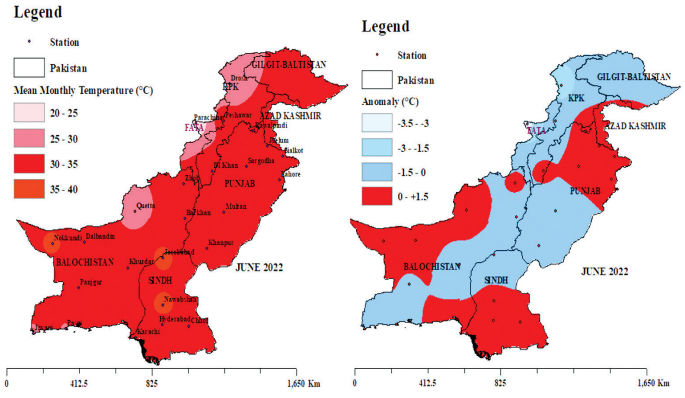

Figure 11: Mean Monthly Air Temperature (°C) in June 2022 (on left) and the Magnitude of Anomaly (°C) (on right)

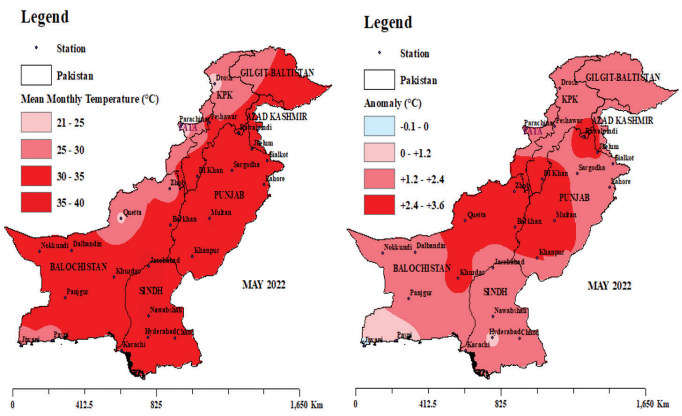

Figure 10: Mean Monthly Air Temperature (°C) in May 2022 (on left) and the Magnitude of Anomaly (°C) (on right)

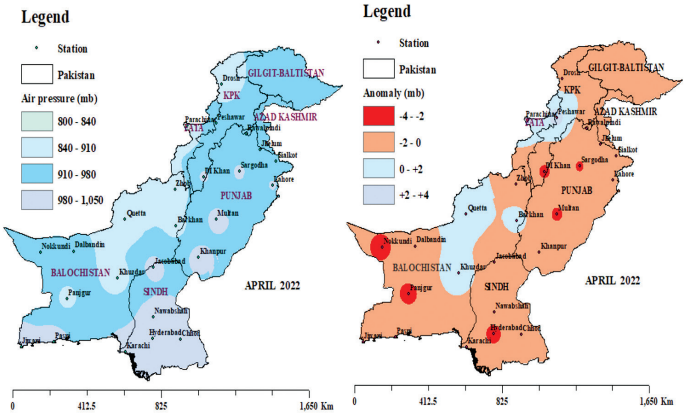

Figure 12: Mean Monthly Air Pressure (mb) in April 2022 (on left) and the Magnitude of Anomaly (mb) (on right)

Table 3: Summary of Mean Monthly Temperature Analysis and Anomalies in °C for the Pre-Monsoon Period 2020-2022, Sindh

2022									
Station	**April**	**Normal**	**Anomaly**	**May**	**Normal**	**Anomal**	**June**	**Normal**	**Anomaly**
Karachi	31.5	28.5	+3	32.4	30.8	+1.6	32.2	31.7	+0.5
Chhor	32.9	29.9	+3	34.5	33.2	+1.3	34.1	33.6	+0.5
Hyderabad	33.2	31	+2.2	34.4	33.4	+1.0	34.2	34.1	+0.1
Nawabshah	33.7	29.5	+4.2	36.3	34.1	+2.2	35.9	35.6	+0.3
Jacobabad	34.1	30.2	+3.9	37.3	35.2	+2.1	36.1	37	-0.9
2021									
Karachi	30.9	28.5	+2.4	32.6	30.8	+1.8	32.2	31.7	+1.1
Chhor	32.2	29.9	+2.3	34.2	33.2	+1.0	33.9	33.6	+0.6
Hyderabad	31.6	31	+0.6	33.3	33.4	-0.1	33	34.1	-0.3
Nawabshah	31.7	29.5	+2.2	34.6	34.1	+0.5	35.1	35.6	-0.3
Jacobabad	31	30.2	+0.8	35.7	35.2	+0.5	36.6	37	-0.4
2020									
Karachi	28	28.5	-0.5	31	30.8	+0.2	31.9	31.7	+0.2
Chhor	31.3	29.9	+1.4	33.4	33.2	+0.2	33.9	33.6	+0.3
Hyderabad	31.2	31	+0.2	33.9	33.4	+0.5	33.9	34.1	-0.2
Nawabshah	29.9	29.5	+0.4	34.5	34.1	+0.4	36	35.6	+0.4
Jacobabad	30.8	30.2	+0.6	35.9	35.2	+0.7	37.9	37	+0.9

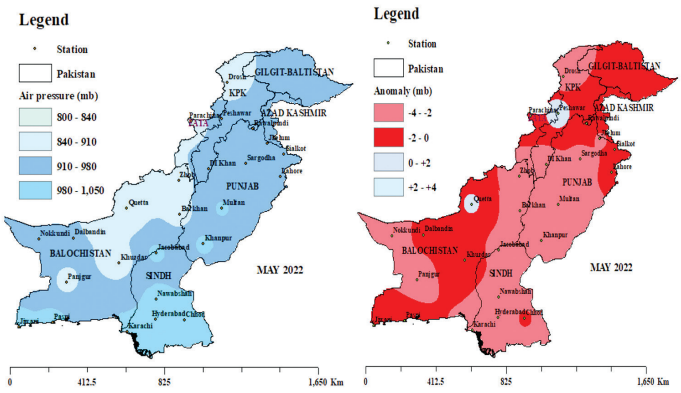

Figure 13: Mean Monthly Air Pressure (mb) in May 2022 (on left) and the Magnitude of Anomaly (mb) (on right)

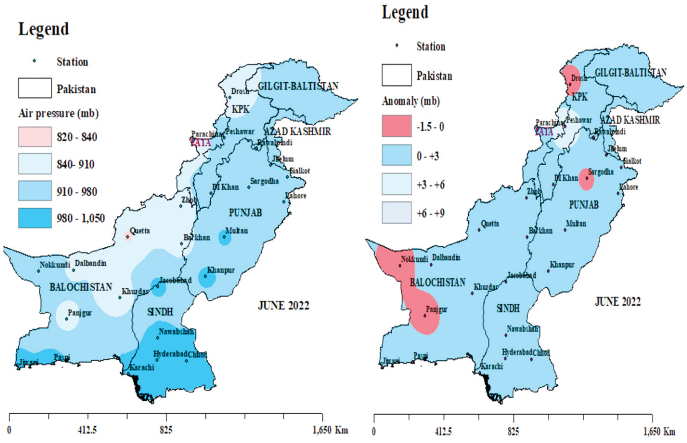

Figure 14: Mean Monthly Air Pressure (mb) in June 2022 (on left) and the Magnitude of Anomaly (mb) (on right)

The results obtained from the analysis showed that the pre-monsoon temperatures were exceptionally high across the country in 2022. As mentioned earlier, the pre-monsoon heating over the landmasses in Pakistan plays a vital role in the formation of seasonal trough that sets an adequate ground for the incursion of moisture-laden winds from the Arabian Sea and Bay of Bengal into the country. In this study, the pre-monsoon air temperature analysis showed that the magnitude of temperature anomaly was highest in Balochistan throughout the pre-monsoon season. In April 2022, Balochistan recorded about 1.2 to 6.0 °C above normal monthly temperature as shown in the Figure 9, with the magnitude of anomaly was found to be highest at the Zhob station (+5.9 °C), followed by Panjgur (+4.4 °C), Khuzdar (+4.3 °C), Nokkundi (+4.1 °C), Dalbandin (+3.4 °C), and Pasni (+1.6 °C). In Sindh, about 2.0 to 4.5 °C above normal temperature was found, with Nawabshah (+4.2 °C), Jacobabad (+3.9 °C), Karachi (+3 °C), and Hyderabad and Chhor (+2.2 °C) as shown in the Table 3. In Punjab, about 4.0 to 5.8 °C above normal temperature was found with the highest anomaly at the Rawalpindi station (+5.8 °C), followed by Sargodha (+5.4 °C), Multan (+4.6 °C), Jhelum (+4.5 °C), and Sialkot (+4.1 °C). In KPK, about 3.5 to 5.5 °C above normal temperature was found, with the maximum anomaly in Dera Ismail Khan (+5.5 °C), followed by Peshawar (+4.6 °C), Parachinar (+4.4 °C), and Drosh (+3.7 °C). In May, the monthly temperature anomaly was found to be +1.0 to +3.5 °C in Balochistan as shown in the Figure 10, with the highest anomaly detected in Zhob (+3.2 °C), followed by Barkhan (+2.7 °C), Khuzdar (+2.5 °C), Dalbandin (+2.3 °C), and Panjgur (+1.9 °C). In Sindh, about 1.0 to 2.5 °C above normal temperature was noticed, with Nawabshah (+2.2 °C), Jacobabad (+2.1 °C), and Karachi (+1.6 °C). In Punjab, about 1.2 to 3 °C above normal temperature was found, with Rawalpindi (+2.9 °C), Multan (+2.5 °C), Sargodha (+2.4 °C), and Lahore (+1.8 °C). Similarly, in KPK, about 1.0 to 3 °C above normal temperature was found during the analysis, with the highest anomaly in Dera Ismail Khan (+3 °C). In June, 0.1 to 0.5 °C above normal temperature was found in Sindh, 0.2 to 1.2 °C in Punjab, while below normal temperature was observed at majority of stations in KPK and Balochistan, as shown in the Figure 11.

Due to the profound relation between the air temperature and pressure, the pre-monsoon air pressure conditions in 2022 also deviated from its normal pattern due to the unusual high air temperatures. In this study, the analysis revealed that in April 2022, majority of the stations in Sindh, Punjab, and Balochistan observed significant below normal mean monthly air pressure, with the air pressure anomaly ranging from about -0.5 to -2.5 mb (millibar) in Balochistan, -1.0 to -2.5 mb in Sindh, and about -1.5 to -2.2 mb in Punjab, as shown in the Figure 12. Similarly, in May, Sindh recorded about 2.0 to 3.0 mb below normal air pressure, and Balochistan and Punjab observed 1.0 to 3.0 mb below average air pressure, as shown in the Figure 13. However, in June, majority of the selected stations showed a positive anomaly as shown in the Figure 14.

Based on the above analysis, it was concluded that the unusual pre-monsoon heating during April and May over the plains in Sindh, Punjab and Balochistan played a key role in the development of intense low air pressure system, that paved the way for the excess moisture intrusion from the Arabian sea and Bay of Bengal into the country. This excess moisture penetration consequently lead to high air moisture conditions, and ultimately extreme precipitation in Pakistan.

3.2 Analysis of Monsoon 2022 Weather Condition and Anomalies:

In this study, after the investigation of unusual pre-monsoon weather conditions in Pakistan in 2022, the monsoon seasonal air moisture conditions (evaluated in terms of vapor pressure) and rainfall were investigated for the year 2022. The results obtained from the analysis are shown in the Figures 15 to 20 as under:

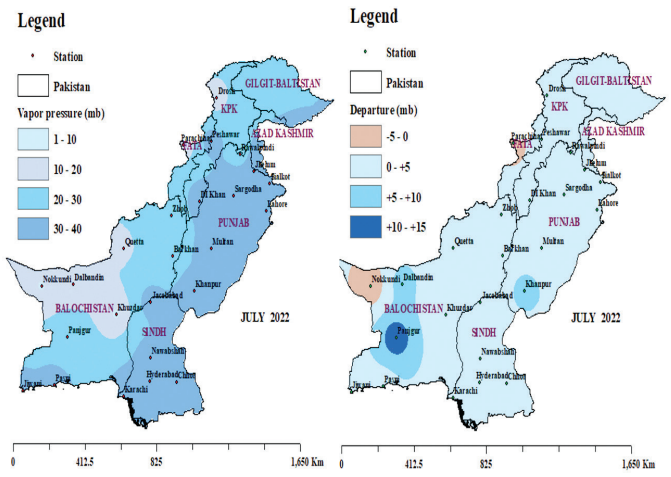

Figure 15: Mean Monthly Vapor Pressure (mb) in July 2022 (on left) and the Magnitude of Anomaly (mb) (on right)

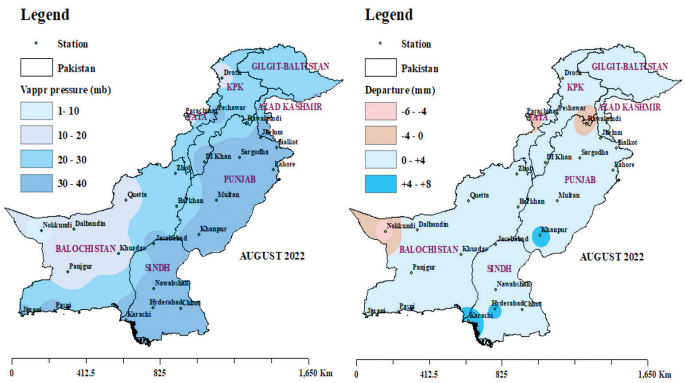

Figure 16: Mean Monthly Vapor Pressure (mb) in August 2022 (on left) and the Magnitude of Anomaly (mb) (on right)

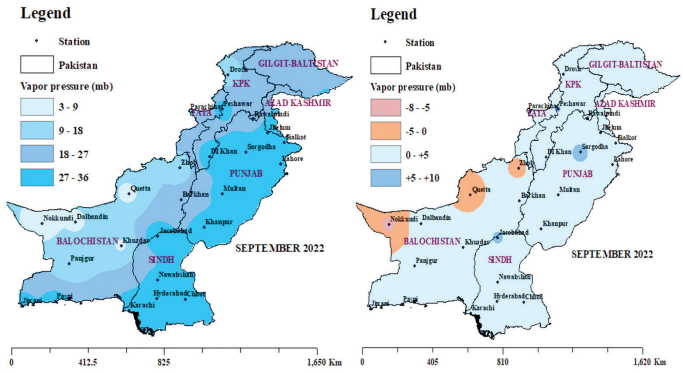

Figure 17: Mean Monthly Vapor Pressure (mb) in September 2022 (on left) and the Magnitude of Anomaly (mb) (on right)

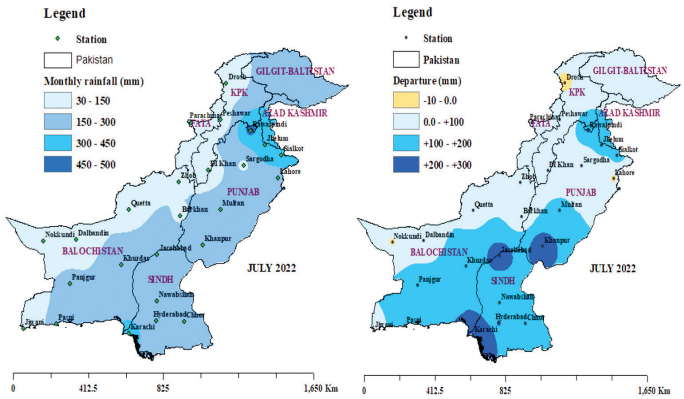

Figure 18: Monthly Rainfall (mm) in July 2022 (on left) and the Magnitude of Departure (mm) (on right)

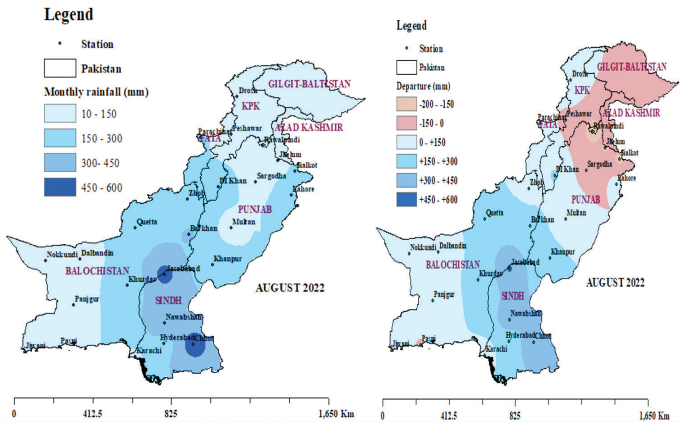

Figure 19: Monthly Rainfall (mm) in August 2022 (on left) and the Magnitude of Departure (mm) (on right)

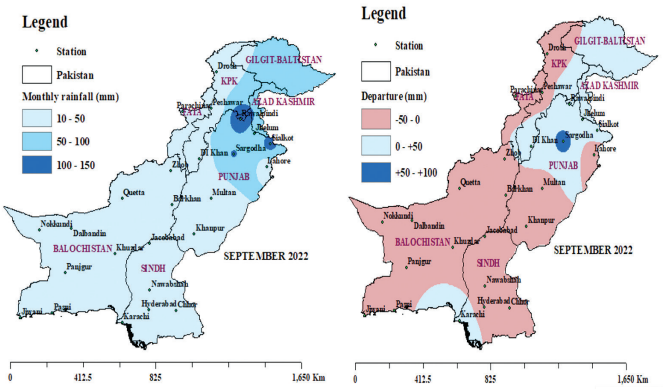

Figure 20: Monthly Rainfall (mm) in September 2022 (on left) and the Magnitude of Departure (mm) (on right)

As discussed earlier, vapor pressure generally indicates the availability of water vapors in air and strongly governs the intensity and the amount of precipitation. In this study, the analysis showed that in July 2022, about 0.4 to 4.0 mb above normal mean monthly vapor pressure was observed in Balochistan, 0.2 to 4.0 mb in Sindh, and 1.0 to 5.0 mb in Punjab and KPK, as shown in the Figure 15. In August, the analysis showed about 1.0 to 4.0 mb above normal mean monthly vapor pressure in Balochistan, and 1.5 to 5.0 mb in Sindh and Punjab, as shown in the Figure 16. In September, about 3.0 to 6.0 mb above normal vapor pressure was found in Sindh and Balochistan during the analysis, as shown in the Figure 17. As discussed earlier, the availability of high amount of water vapors in air serve as a key cause of heavy precipitation. In this study, the rainfall analysis revealed that the extreme monsoon system was more active in Sindh and Balochistan, as compared to the other parts of country in 2022. In July 2022, Sindh received about 100 to 300 mm above normal monthly rainfall as shown in the Figure 18, where Karachi and Jacobabad stations received 282 and 247 mm above normal precipitation respectively. In Balochistan, about 50 to 200 mm above normal rainfall was received, with 177 mm above normal rainfall in Khuzdar, followed by Panjgur (+165 mm), Pasni (+162 mm), and Zhob (+78 mm). Similarly, in Punjab, about 50 to 180 mm above normal rainfall was received, with 176 mm above normal rainfall in Rawalpindi, followed by Jhelum (+120.5 mm), and Sialkot (+119 mm). In KPK, about 5 to 30 mm above normal rainfall was received, where Peshawar received 22 mm above average rainfall. In August, precipitation over the country was found to be more vigorous than July during the analysis, where Sindh received about 100 to 500 mm above normal rainfall (as shown in the Figure 19), with the highest departure was found in Jacobabad (+457 mm), followed by Chhor (+435 mm), Nawabshah (+402 mm), Hyderabad (+180 mm), and Karachi (+67 mm). In Balochistan, about 50 to 250 mm above average rainfall was received, with 224 mm above normal rainfall in Barkhan, followed by Quetta (+194 mm), Khuzdar (+170 mm), Zhob (+111 mm), and Panjgur (+62 mm). However, in Punjab, all selected stations received below normal rainfall. In KPK, 161 mm above normal rainfall was received in Dera Ismail Khan, followed by Drosh (+122 mm), and Parachinar (+68 mm). In September, the intense monsoon system was found to be retreated from the country with less extremity in rainfall as compared to July and August. In Sindh, Karachi recorded 33 mm above normal rainfall, while the remaining stations received below average precipitation. In Punjab, about 15 to 75 mm above

normal rainfall was received, with 75 mm above normal rainfall in Sargodha, followed by Rawalpindi (+28 mm), and Sialkot (+20 mm), as shown in the Figure 20.

Based on the above analysis, it was concluded that the unusual heating and the formation of intense low air pressure condition during April to May over Sindh, Punjab, and Balochistan resulted in the excess penetration of moisture from the Arabian sea and Bay of Bengal, that lead to air moisture levels, and consequently extreme precipitation in the country. The series of heavy monsoon rainfall events severely affected the human lives, livestock and agriculture, and infrastructure in Pakistan. As per the Pakistan Agricultural Research Council (PARC), about 1.9 million tons of rice, 3.1 million bales of cotton, and 10.5 million tons of sugarcane worth of $543, 485, and 273 million respectively was destroyed in Sindh as a consequence of extreme monsoon precipitation.

4.0 SIGNIFICANCE AND RESEARCH CONTRIBUTION

This study comprehensively highlighted the causes and extremity of extreme monsoon precipitation in Pakistan during the past 30 years. In addition, it also unearthed the occurrence of unusual weather conditions that lead to the exceptionally high monsoon precipitation in 2022. The outcomes of study are expected to provide a way forward for the national and international research community in investigating the causes and impacts of extreme weather patterns, and to suggest effective climate change adaptation and mitigation measures.

5.0 RESEARCH SCOPE AND LIMITATIONS

This study included an in-depth literature review on the past extreme monsoon rainfall events in Pakistan, and also probed the meteorological factors behind the extreme monsoon rainfall in 2022. Additionally, to devise a more holistic and effective climate change adaptation and mitigation strategy, the Global or the Regional Climate Models can also be employed to capture the future possible trend and extremity of southwest monsoon in the region.

6.0 CONCLUSION AND RECOMMENDATIONS

This study was conducted to probe the major meteorological causes behind the extreme monsoon precipitation in Pakistan in 2022. Based on the analysis, the following conclusions were reached:

- The detailed literature review on the past monsoon precipitation pattern in Pakistan revealed that the extreme monsoon rainfall events have significantly increased in the country as a consequence of shifting climate patterns.
- The temperature analysis revealed that in April 2022, unusual high air temperatures were recorded across the country, with Sindh observed 2.0 to 4.5 °C, Balochistan observed 1.5 to 6.0 °C, Punjab observed 4 to 5.8 °C, and KPK observed 3.5 to 5.5 °C above normal temperature. Similarly, in May, about 1.0 to 2.5 °C above normal temperature was found in Sindh, 1.0 to 3.5 °C in Balochistan, Punjab, and KPK.
- Due to the exceptionally high air temperature, an intense low pressure system was developed over the country's landmasses. In April 2022, about 0.5 to 2.5 mb below normal air pressure was observed in Sindh and Balochistan, and 1.5 to 2.5 mb in Punjab. In May, 2.0 to 3.0 mb below normal air pressure was found in Sindh and 1.0 to 3.0 mb in Balochistan and Punjab.
- In July 2022, about 0.5 to 4.0 mb above normal vapor pressure was found in Sindh and Balochistan, while Punjab observed 1.0 to 5.0 mb above normal vapor pressure. In August, about 1.5 to 5.0 mb above normal vapor pressure was found in Sindh, Punjab, and Balochistan, while in September, about 3.0 to 6.0 mb above normal vapor pressure was found in Sindh and Balochistan during the analysis.
- Due to the high moisture availability, about 100 to 300 mm above normal monthly rainfall was received in Sindh in July, with 50 to 200 mm in Balochistan and Punjab, and about 30 mm in KPK. In August 2022, about 100 to 500 mm above normal rainfall was received in Sindh, and 50 to 250 mm in Balochistan. In Punjab, majority of the stations received below normal rainfall, while in KPK, about 50 to 180 mm above average rainfall was received. In September, the monsoon system weakened in the country, with Sindh, Balochistan, and KPK received below average rainfall, while Punjab received 15 to 75 mm above normal rainfall.
- Conclusively, it was found that the unusual heating during April to May in Sindh, Punjab, and Balochistan resulted in the formation of intense trough that facilitated the continuous moisture penetration from the Bay of Bengal and Arabian sea into the country. This uninterrupted incursion of water vapors lead to increased vapor pressures (high air moisture conditions) and consequently extreme precipitation in the country.
- The study outcomes briefly explained the causes of extreme monsoon precipitation in Pakistan in 2022, which may help to devise an effective climate change adaptation and mitigation strategy, so as to reduce the risks of extreme climate patterns on the water and food security in Pakistan.
- In the authors opinion, in order to reduce the risk and consequences of severe hydrological and climate events (floods, extreme rainfall and heat waves) in Pakistan, a continuous real time monitoring of hydro-climatological patterns, along with the implementation of a well-integrated climate change mitigation policy is essential so as to ensure the state of water, food, and economic security in the country.

7.0 ACKNOWLEDGEMENT

The authors would like to extend gratitude to the Pakistan Meteorological Department (PMD) for supplying the required climate data for the study. ■

REFERENCES

[1] [1] Setzer, J. and C. Higham, Global Trends in Climate Change Litigation: 2022 Snapshot. 2022.

[2] Talpur, M.A.H., et al., Computing Travel Impendences Using Trip Generation Regression Model: A Phenomenon of Travel Decision- Making Process of Rural Households. Environment, Development and Sustainability, 2023. 25(7): P. 5973-5996.

[3] Rivera-Collazo, I., Environment, Climate and People: Exploring Human Responses to Climate Change. Journal of Anthropological Archaeology, 2022. 68: P. 101460.

[4] Bazrafshan, O., et al., Predicting Crop Yields Using a New Robust Bayesian Averaging Model Based on Multiple Hybrid ANFIS and MLP Models. Ain Shams Engineering Journal, 2022. 13(5): P. 101724.

[5] Bhatti, L., et al., The Challenges Faced in the Collection and Disposal Of Municipal Solid Waste (MSW) Management: A Case Study Of Sanghar City. Sukkur IBA Journal of Computing and Mathematical Sciences, 2021. 5(1): P. 59-72.

[6] Fung, K.F., et al., Evaluation of Spatial Interpolation Methods and Spatiotemporal Modeling of Rainfall Distribution in Peninsular Malaysia. Ain Shams Engineering Journal, 2022. 13(2): P. 101571.

[7] Shah, M.I., et al., Predicting Hydrologic Responses to Climate Changes in Highly Glacierized and Mountainous Region Upper Indus Basin. Royal Society Open Science, 2020. 7(8): P. 191957.

[8] Lv, X., et al., Random Walk Method for Modeling Water Exchange: An Application to Coastal Zone Environmental Management. Journal of Hydro-Environment Research, 2016. 13: P. 66-75.

[9] Hamed, M.M., et al., Inconsistency in Historical Simulations and Future Projections of Temperature and Rainfall: A Comparison of CMIP5 and CMIP6 Models Over Southeast Asia. Atmospheric Research, 2022. 265: P. 105927.

[10] Panagos, P., et al., Global Rainfall Erosivity Projections for 2050 and 2070. Journal of Hydrology, 2022. 610: P. 127865.

[11] Chandio, I.A., K.A. Rang, and M.A.H. Talpur, Research Article Impact of the Pedestrian System on Environment and Individual Safety in MUET, Pakistan. 2020.

[12] Alahacoon, N., et al., Rainfall Variability and Trends Over the African Continent Using TAMSAT Data (1983–2020): Towards Climate Change Resilience and Adaptation. Remote Sensing, 2021. 14(1): P. 96.

[13] Merabtene, T., M. Siddique, and A. Shanableh, Assessment of Seasonal and Annual Rainfall Trends and Variability in Sharjah City, UAE. Advances in Meteorology, 2016. 2016: P. 1-13.

[14] Almazroui, M., Rainfall Trends and Extremes in Saudi Arabia in Recent Decades. Atmosphere, 2020. 11(9): P. 964.

[15] Utsumi, N. and H. Kim, Observed Influence of Anthropogenic Climate Change on Tropical Cyclone Heavy Rainfall. Nature Climate Change, 2022. 12(5): P. 436-440.

[16] Liang, X.Z., Extreme Rainfall Slows the Global Economy. 2022, Nature Publishing Group UK London.

[17] Song, F., et al., Trends in Surface Equivalent Potential Temperature: A More Comprehensive Metric for Global Warming and Weather Extremes. Proceedings of the National Academy of Sciences, 2022. 119(6): P. E2117832119.

[18] Doan, Q.V., et al., Increased Risk of Extreme Precipitation Over an Urban Agglomeration With Future Global Warming. Earth's Future, 2022. 10(6): P. E2021ef002563.

[19] Wang, J., et al., Prediction of the Typhoon Wind Field in Hong Kong: Integrating the Effects of Climate Change Using the Shared Socioeconomic Pathways. Climate Dynamics, 2022. 59(7-8): P. 2311-2329.

[20] Luber, G. and M. Mcgeehin, Climate Change and Extreme Heat Events. American Journal of Preventive Medicine, 2008. 35(5):P.429-435.

[21] Scherer, C.M., et al., Changes in Prevailing Surface-Palaeowinds of Western Gondwana during Early Cretaceous. Cretaceous Research, 2020. 116: P. 104598.

[22] Kamae, Y., et al., Atmospheric Rivers Bring More Frequent and Intense Extreme Rainfall Events Over East Asia under Global Warming. Geophysical Research Letters, 2021. 48(24): P. E2021gl096030.

[23] Palharini, R., et al., Analysis of Extreme Rainfall and Natural Disasters Events Using Satellite Precipitation Products in Different Regions of Brazil. Atmosphere, 2022. 13(10): P. 1680.

[24] Talpur, M.A.H., et al., Transportation Planning Studies for Socio-Economic Development of Depressed Sub-Regions: A Review. Mehran University Research Journal of Engineering & Technology, 2018. 37(3): P. 603-614.

[25] Shi, X., et al., Impacts and Socioeconomic Exposures of Global Extreme Precipitation Events in 1.5 And 2.0 C Warmer Climates. Science of the Total Environment, 2021. 766: P. 142665.

[26] Huang, S.-C., et al., Characteristics and Causes of Taiwan's Extreme Rainfall in 2022 January and February. Weather and Climate Extremes, 2022. 38: P. 100532.

[27] Pohl, B., et al., Precipitation and Temperature Anomalies Over Aotearoa New Zealand Analysed By Weather Types and Descriptors of Atmospheric Centres of Action. International Journal of Climatology, 2023. 43(1): P. 331-353.

[28] Jouberton, A., et al., Warming-Induced Monsoon Precipitation Phase Change Intensifies Glacier Mass Loss in the Southeastern Tibetan Plateau. Proceedings of the National Academy of Sciences, 2022. 119(37): P. E2109796119.

[29] Forbes, J.M., M. Ern, And X. Zhang, The Global Monsoon Convective System as Reflected In Upper Atmosphere Gravity Waves. Journal of Geophysical Research: Space Physics, 2022. 127(9): P. E2022ja030572.

[30] Han, J., et al., Annual Paddy Rice Planting Area and Cropping Intensity Datasets and Their Dynamics in the Asian Monsoon Region from 2000 to 2020. Agricultural Systems, 2022. 200: P. 103437.

[31] Nie, J., et al., Late Miocene Tarim Desert Wetting Linked With Eccentricity Minimum and East Asian Monsoon Weakening. Nature Communications, 2022. 13(1): P. 3977.

[32] Khadka, D., et al., An Evaluation Of CMIP5 and CMIP6 Climate Models in Simulating Summer Rainfall in the Southeast Asian Monsoon Domain. International Journal of Climatology, 2022. 42(2): P. 1181-1202.

[33] Safdar, F., et al., Climate Change Indicators and Spatiotemporal Shift in Monsoon Patterns in Pakistan. Advances in Meteorology, 2019. 2019: P. 1-14.

[34] Sun, H., et al., Subannual-To-Biannual-Resolved Travertine Record of Asian Summer Monsoon Dynamics in the Early Holocene at the Eastern Margin of Tibetan Plateau. Applied Geochemistry, 2022. 141: P. 105305.

[35] Gadgil, S., The Indian Monsoon and Its Variability. Annual Review of Earth and Planetary Sciences, 2003. 31(1): P. 429-467.

[36] Dong, W., Y. Ming, And V. Ramaswamy, Projected Changes in South Asian Monsoon Low Pressure Systems. Journal of Climate, 2020. 33(17): P. 7275-7287.

[37] Huang, X., Et Al., South Asian Summer Monsoon Projections Constrained by the Interdecadal Pacific Oscillation. Science Advances, 2020. 6(11): P. Eaay6546.

[38] Ashfaq, M., Topographic Controls on the Distribution of Summer Monsoon Precipitation Over South Asia. Earth Systems and Environment, 2020. 4(4): P. 667-683.

[39] Wang, Z., et al., Tibetan Plateau Heating As a Driver of Monsoon Rainfall Variability in Pakistan. Climate Dynamics, 2019. 52: P. 6121-6130.

[40] Kripalani, R. and A. Kulkarni, Climatic Impact of El Nino/La Nina on the Indian Monsoon: A New Perspective. Weather, 1997. 52(2): P. 39-46.

[41] Rashid, A., Impact of El-Nino on Summer Monsoon Rainfall of Pakistan. Pakistan Journal of Meteorology, 2004. 1(2).

[42] Iqbal, A. And S.A. Hassan, ENSO and IOD Analysis on the Occurrence of Floods in Pakistan. Natural Hazards, 2018. 91: P. 879-890.

[43] Hashmi, H.N.,et al., A Critical Analysis of 2010 Floods in Pakistan. African Journal of Agricultural Research, 2012. 7(7): P.1054-1067.

[44] Khan, M.A., et al., The Challenge Of Climate Change and Policy Response in Pakistan. Environmental Earth Sciences, 2016. 75: P. 1-16.

[45] Ahmad, D., S.Z.A. Shah, and M. Afzal, Flood Hazards Vulnerability and Risk of Food Security in Bait Community Flood- Prone Areas of Punjab Pakistan: In Sdgs Achievement Threat. Environmental Science and Pollution Research, 2022. 29(59): P. 88663-88680.

[46] Soomro, M., H. Marvi, and R. Khaskheli, A Comprehensive Traffic Volume Study of Qasim Chowk Hyderabad, Sindh, Pakistan. Global Regional Review, VI, 2021. 6: P. 352-359.

[47] Salma, S., S. Rehman, and M. Shah, Rainfall Trends in Different Climate Zones of Pakistan. Pakistan Journal of Meteorology, 2012. 9(17).

[48] Wang, S.Y.S., et al., Changes in Monsoon Extremes Affecting Climate Prediction—Example of the 2010 Pakistan Floods. 2012.

[49] Jamshed, A., et al., How Do Rural-Urban Linkages Change After an Extreme Flood Event? Empirical Evidence from Rural Communities in Pakistan. Science of the Total Environment, 2021. 750: P. 141462.

[50] Khan, M., Z. Hussain, and I. Ahmad, Regional Flood Frequency Analysis, Using L-Moments, Artificial Neural Networks and OLS Regression, of Various Sites of Khyber-Pakhtunkhwa, Pakistan. Appl. Ecol. Environ. Res, 2021. 19: P. 471-489.

[51] Talpur, M.A.H., et al., Transportation Planning Survey Methodologies for the Proposed Study of Physical and Socio-Economic Development. Modern Applied Science, 2012. 6(7).

[52] Talpur, M.A.H., et al., A Brief Review on the Role of Regional Transport Accessibility in the Development Process of Distant Sub-Regions. Indian Journal of Science and Technology, 2016. 9(13): P. 1-9.

[53] Talpur, M.A.H., et al., Development of a Regional Transport Policy Support System for Rural Planning Agencies in Developing World. Procedia Engineering, 2014. 77: P. 2-10.

PROFILES

MR. HARIS UDDIN QURESHI is a Civil Engineer with specialization in Water Resources Engineering. He is having an experience of 04 years in academics, research and consultancy. His area of research is focused on the hydrological modelling of watersheds, hydrological assessment of reservoirs, climate change and extreme weather analysis, agricultural meteorology, bias correction of climate models, modelling of agricultural water demand, smart agriculture, and groundwater hydrology. As a professional engineer, he has worked on multiple projects related to water resources management funded by the national government and international donor agencies.
Email address: harisqureshi39@yahoo.com

DR SYED MUZZAMIL HUSSAIN SHAH is serving as a postdoctoral research fellow at the Interdisciplinary Research Center for Membranes and Water Security, King Fahd University of Petroleum and Minerals, Dhahran – Kingdom of Saudia Arabia. Previously, he has served in the academics as a senior faculty personnel. His area of research includes, ground water security, ground water remediation, water quality, pollutants control, sustainable development, groundwater monitoring, hydrodynamics, etc.
Email address: syed.shah@kfupm.edu.sa

DR MOHAMED YASSIN is serving as Research Scientist-III at King Fahd University of Petroleum and Minerals, Dhahran – Kingdom of Saudia Arabia. Dr Yassin is a Geoscientist with almost 15 years of petroleum industry and research experience. His research focuses on: Structural geology, basin analysis, Seismic Interpretation, Quantitative Seismic Interpretation, Reservoir characterization and Modeling.
Email address: mohamedgadir@kfupm.edu.sa

DR SANI ISAH ABBA currently works as a postdoctoral research fellow at the Interdisciplinary Research Center for Membranes and Water Security, King Fahd University of Petroleum and Minerals, Dhahran – Kingdom of Saudia Arabia. Dr. Abba does research in Artificial Intelligence, Machine Learning, Remote Sensing, GIS, Water Security, Membrane and Destination, Wastewater, Water Quality, Water Resources, Hydro-Environmental Modeling, and Simulation, Public health, and Pollution Control, Climate Change, Sustainable Development. He is currently a reviewer in more than 50 ISI/SCI journals in different publishers including Springer, Elsevier, IEEE, MDPI, Taylor, Hindawi.
Email address: sani.abba@kfupm.edu.sa

DR ZAHIRANIZA MUSTAFFA works as an Associate Professor at the Department of Civil and Environmental Engineering, Universiti Teknologi PETRONAS, Malaysia with a vast experience in Academics. Her research expertise includes, Pipeline Engineering, Hydrology, Probabilistic Design, Offshore Engineering, Water Resources Engineering, Hydraulic Structures, Urban Hydraulics, etc.
Email address: zahiraniza@utp.edu.my

A REVIEW ON CONCRETE HOLLOW BLOCK WALLS: MATERIALS AND MECHANICAL PROPERTIES

(Date received: 27.06.2023/Date accepted: 22.09.2023)

Kabiru A. Musa[1*], Badorul H. Abu Bakar[2], Teh S. Abd Manan[3]

[1,2,3] School of Civil Engineering, Engineering Campus, Universiti Sains Malaysia, 14300 Nibong Tebal, Pulau Pinang, Malaysia

[*]Corresponding author: ayagikabirumusa@gmail.com

ABSTRACT

Concrete hollow blocks are commonly used in building construction, particularly for multi-story buildings, factories, and residential structures. Hollow blocks are more practical because of their lightweight, and the most significant feature is the ease with which they can be ventilated. Mortar is the glue that holds the blocks together in a masonry assembly. Mortar must be long-lasting and capable of holding the masonry together while also helping to form a water-resistant barrier. Typically, cement and sand are used to make mortar, with lime or a plasticiser added to increase workability. This paper provides an overview of modern masonry hollow block wall construction, starting with an overview of its applications and benefits, and offers an experimental work of concrete hollow block and mortar units, such as water absorption, 5-hour boiling test, compressive strength, density, flexural strength test, and compressive strength, and consistency test for mortar. The findings revealed that the compressive strength for a masonry hollow block is 8.39 MPa at 28 days which does not pass the specifications for it to be a load-bearing unit and the compressive strength of mortar is approximately 21.34 MPa at 28day. To improve economy and productivity, compressive strength, density, masonry hollow block properties, and masonry wall behaviour with the factors to consider for load-bearing and non-load-bearing wall construction were summarised and described, and key reference lists were included. A review of the Concrete Hollow Block material and mechanical properties.

Keywords: Construction, Experiment, Hollow Blocks, Masonry, Materials

1.0 INTRODUCTION

The concrete hollow block allows for thinner walls, resulting in more floor space because the air space in the block accounts for 25% of the total area of the block, moreover, it is still among the earliest building materials in use today (Yang *et al*., 2019, Umair *et al*., 2022, Edri *et al*., 2020). Cement concrete blocks are more popular than traditional building materials like bricks and stones. To use blocks in construction, the overall length and height of the wall must be fixed to allow for the use of a single or half-length block. Due to their low cost, these concrete hollow blocks are commonly used in compound walls and because of their lightweight, concrete hollow blocks are more useful, and the most important feature is their ease of ventilation. Cement, sand, and stone chips are used to make concrete hollow blocks. It lowers construction costs by reducing the use of cement in masonry work (Varshney, 2016). For thousands of years, masonry was the dominant building material until the nineteenth century, when modern materials like concrete, steel, and wood appeared (Maldonado *et al*., 2019). Masonry is the only traditional in-fill material used in reinforced concrete frames. Due to variables including resource availability, societal limitations, cultural affinity, and economic feasibility, structured masonry has gained popularity in the construction of monumental, administrative, and residential buildings (Parajuli *et al*., 2020, Parsekian *et al*., 2018). In previous studies, to form masonry walls, beds, and head joints were used to connect concrete hollow blocks (Hasan *et al*., 2021, Ma *et al*., 2016, Gabor *et al*., 2019, Reboul *et al*., 2018, Al-Shugaa *et al*., 2019, Chi *et al*., 2019, Calderón *et al*., 2020, Materials & 2018) this implies that skilled workers are required in the construction process. For thousands of years, using mortar to bond block units on top of each other has proven to be a successful technique, primarily justified by its simplicity and durability during construction (Popescu *et al*., 2015). The masonry has good sound, heat, and moisture insulation properties because of the hollow space between the blocks, the air space in the block accounts for 25% of the total area of the block, and hollow blocks enable thinner walls and more floor space. Cement concrete blocks have surpassed traditional building materials such as bricks and stones in popularity. To use blocks in construction, the wall's overall length and height must be fixed, allowing for the use of a single or half-length block. The hollow concrete blocks were discovered for a variety of reasons:

- Sound management,
- Dead load is low,
- Resistance to fire,
- Sufficient strength,
- Outstanding thermal insulation,
- Economy,
- Exceptionally long-lasting,
- Environmentally Sound,

- Reduced mortar consumption,
- Quick and Easy Building System,
- Improved architectural features.

Disadvantages are:

- The load-bearing capability of hollow blocks is decreased by the combined mass of wall decoration materials.
- Hanging heavy objects on such walls is extremely dangerous.

Applications are:

- In load-bearing structures, hollow blocks are used.
- It's used to build frame structures like high-rise residential apartments and other similar structures.
- It is used on the ground, such as roadside walkways.
- It is also used in unusual applications such as roadside and backyard plantation tree guard blocks.

Concrete hollow block is most effective in load-bearing structures, where it can provide load support, space division, fire and weather protection, and thermal and acoustic insulation, all of which must be separately accounted for in a framed building. According to the allowable stress design, under a working load, the stresses developed in a member must be less than the allowable stresses (Varzaneh *et al*., 2020, Muthukumar & Kumar, 2015). Clay bricks, both unfired and fired, concrete bricks, and hollow concrete blocks are just a few of the masonry materials available (A. L. Murmu and A. Patel, 2018). Concrete blocks hollow have the potential to reduce energy consumption, consume fewer raw materials, and have a lower environmental impact, as a result, concrete hollow blocks have become increasingly important in the construction industry (N. Sathiparan, M. K. N. Anusari, 2014).

1.1 Literature Review

The compressive strength of masonry was reported by Udi *et al*., (2020) where it is affected by several factors, such as the aspect ratio of the units, the mortar strength, the unit strength, and the relative values of the units and mortar (ratio of height to least horizontal dimension). Unit orientation with reference to the applied load direction and bed joint thickness. The criteria stated highlight how difficult it is to determine the strength of the brickwork with accuracy. (Kuddus & Fabregat, (2017) discovered that the compressive strength of blockwork would also be affected by the change in mortar designations. The strength of block wall panels could be significantly increased by using high-strength mortar instead of low-strength masonry units while building blockwork, and vice versa. Bakhteri *et al*., (2012), shown empirically that for a brick of a certain height, the strength of a brick falls as the junction thickness grows, and it was demonstrated by Bakhteri *et al*., (2004) using the aid of finite element modelling. Additionally, it was discovered that eccentricity of loading also has an impact on the brickwork's strength. When force is applied farther from the centre of a wall panel that is uniformly loaded, there is sometimes an apparent increase in compressive strength. Sureshchandra *et al*., (2014) find out the compressive strength of hollow blocks with partial and full replacement of sand by quarry dust. After replacement he found that 50% replacement of sand gave high strength, and 100% replacement of sand gave low strength. Fortes *et al*., (2015) studied the compressive strength of un-grouted, grouted masonry and masonry units. This research work indicates an increase in the compressive strength of the masonry with increasing compressive strength of the units.

2.0 MATERIALS

2.1 Standard Sizes of Concrete Hollow Block

A concrete hollow block is one with at least one large hole or cavity running through it and solid material accounting for 50 to 75% of the total volume calculated from the block's overall dimensions (Varzaneh *et al*., 2020). Concrete hollow block units come in a wide range of sizes and shapes to accommodate a wide range of construction needs, examples include stretchers, corners, double corners, piers, jambs, headers, bullnoses, partition blocks, and concrete floor units. The concrete hollow blocks' nominal dimensions must be used, whether hollow (open or closed cavity) or solid, and the concrete blocks' nominal sizes are as follows:

Length: 400, 500, or 600 mm,
Height: 200 or 100 mm,
Width: 50, 75, 100, 150, 200, 250, or 300 mm.

Along with the previously mentioned blocks, half lengths of 200, 250, and 300 mm are required to match the full lengths. Table 1 shows the sizes and weights of different concrete hollow blocks. The length tolerance of the units must not exceed +/- 5 mm, and the maximum height and width variation must not exceed +/- 3mm (Nalon *et al*., 2022).

Table 1: Different sizes and weights of hollow blocks (Varshney, 2016)

S/No	Description	Size in (cm)	Approximate mass in Kgs
1	Entire hollow	39 x09 x 19	10.0
2	Hollow in half	19 x 09 x 19	5.1
3	Half a lintel	19 x 14 x19	7.5
4	Hollow lintel	19 x19 x 19	9.3
5	Floor slab	50 x 20 x 12.5	18.0

2.2 The Geometry of the Concrete Hollow Block

Concrete hollow block units for masonry construction are available in different shapes and sizes, and strengths, the standard block is the most common type, which comes in two shapes, open-end units, double-open-end units, lintel units, and knock-out units are popular styles. To improve the thermal reduction of vertical partitions, openings in concrete hollow blocks are used and the lightening/simplification of block handling lowers the structural load of the building (Nalon *et al*., 2022). Compared to solid blocks, although using hollow elements saves material costs, internal acoustic resonances within the blocks can be increased by the core holes in the blocks, which are associated because of their lower surface weight, resulting in a significant reduction in the system's sound reduction. The sound reduction index is influenced by the geometry of the holes, which is determined by the blocks' net and gross area ratios, with their weight ratios, resulting in various sound transmission reduction curves (Oliveira *et al*., 2021). When producing high-strength concrete blocks, some plants used a variety of concrete block geometries. Because the net area increases and the desired

Table 2: Concrete Hollow Blocks Classification Based on Compressive Strength and Density (ASTM C140/C140M-14, 2014)

Type	Grade	The block density is kg/mm^3	Minimum Compressive Strength Unit Average N/mm^2	Individual Unit Minimum Strength N/mm^2
Hollow block (open & closed cavity) loadbearing unit	A (3.5)	Not less than 1500	3.5	2.8
	A (4.5)		4.5	3.6
	A (5.5)	Not less than 150 but not less than 1,000	5.5	4.4
	A (7.0)		7.0	5.6
	B (2.0)		2.0	1.6
	B (3.0)		3.0	2.4
	B (5.0)		5.0	4.0
Hollow block (open & closed cavity) non-loadbearing unit	C (1.5)	Less than 1500 but not less than 1,000	1.5	1.2
Solid load	D (5.0)		5.0	4.0
Bearing unit	D (4.0)	Not less than 1800	4.0	3.2

compressive strength is easier to achieve, 32mm thick face-shell concrete hollow blocks will be produced if the plant lacks a strong compressive block moulding machine. This is an option, however, has some drawbacks: the mass of concrete hollow blocks rises (by about 15%), putting building lower ends under stress the productivity of laying the units falls; and transportation costs increase. Another advantage of using this type of concrete hollow block is that involuntary changes in the high-strength of concrete are avoided due to the thinner face-shell thickness of these blocks (Gauthier & Hawley, 2007, Abd Manan *et al*., 2019, Abd Manan *et al*., 2021, Beddu *et al*., 2020) lower-strength concrete hollow blocks are less likely. This choice is significant because it avoids the need for the plant to halt production when the compressive strength of the block varies, like other large-scale companies that typically produce concrete hollow blocks with a 25 mm face-shell thickness, plants frequently alter the proportions of the mixture as well as the settings of the equipment (Cintya3 *et al*., 2012).

2.3 Concrete Hollow Block Classification Based on Compressive Strength and Density

These types of masonry units are categorised as concrete hollow blocks load-bearing and non-load-bearing units (open and closed cavity) and shall conform to the following grades as can be seen from Table 2. The minimum block density for Grade A concrete block unit is 1,500 kg/m^3 as load bearing is designed at 28 days to have low average compressive strengths of 3.5, 4.5, 5.5, 7.0, 8.5, 10.0, 12.5, and 15.0 N/mm^2. Group B concrete hollow block units are also used as load-bearing units, and their block density must be between 1,100 kg/ m^3 and 1,500 kg/ m^3, and at 28 days should have average compressive strengths of at least 3.5 and 5.0 N/mm^2 (Amalkar *et al*., 2020). Grade C units are non-load bearing and must have a minimum block density of 1,500 kg/ m3 but not less than 1,000 kg/m3, and they are designed to have average compressive strengths of at least 1.5 and 1.2 N/mm^2 at 28 days (ASTM C140/C140M-14, 2014).

2.4 Physical Properties of Concrete Hollow Block

The basic requirement for any concrete hollow block is to provide Moisture Movement, absorption of water, drying Shrinkage, compressive strength, density, and durability (Varshney, 2016). Hollow concrete blocks, apart from providing the above-listed benefits, possess adequate strength and structural stability, are highly durable, fire resistant, economical, and provide a fast and easier construction system. In addition to this, they provide aesthetic beauty by providing better architectural features (Hendry, 2001). The physical characteristics of masonry hollow concrete blocks are shown in Table 3:

Table 3: Physical Properties of Concrete Hollow Block

S/N	Type	Grade
1	Moisture Movement	A maximum of 0.09%
2	Absorption of Water	A maximum of 10%
3	Drying Shrinkage	A maximum of 0.06%
4	Compressive Strength	For Grade A: 3.5 to 15.0 N/mm^2 For Grade B: 3.5 and 5.0 N/mm^2
5	Density	For Grade A: 1500 kg/m^3 For Grade B: 1100 kg/m^3 to 1500 kg/m^3

3.0 EXPERIMENT

3.1 Concrete Hollow Block

The Malaysian city of Penang provided the masonry hollow block units for this investigation, the prepared block is shown in Figure 1. The concrete hollow block units used have identical dimensions and configurations and are manufactured in a single production batch (190 mm × 140 mm × 390 mm).

Figure 1: Masonry Hollow Block

Figure 2: Boiling Machine Test

3.2 Mortar

The type of mortar used in this study was grade 30 (1:3), this type of mortar is described by (BSI 5628: British standards institution (BSI). BSI-5628, 1992, G. Mohamad *et al.,* 2007). The volume ratio of cement and sand used was that suggested by Wheeler, (2005). The water-to-cement ratio used for mortar was 0.5, and the mortar was batched immediately before mixing. The mortar was mixed with water until a homogenous mixture was obtained. A pan-type mixer was used, with each batch receiving a minimum mixing time of 5 minutes. Throughout the test procedure, consistent sources of material were used, and all ingredients were rigorously batch-mixed by volume to ensure consistency of mortar qualities.

3.3 Water Absorption

The amount of water that a unit can hold when saturated is referred to as its water absorption. Absorption can reveal a concrete mix's degree of compaction, or the volume of voids present in a block. Variations in absorption may be a sign of hazardous substances in the combination, inadequate mixing, and/or compaction of the concrete mix, as well as variations in compressive strength, tensile strength, and durability, issues with laboratory procedures, or other causes for a specific mix design, manufacturing, and curing process (ASTM C140/C140M-14, 2014, BS 1881-122:2011+A1, 2020).

3.4 5-Hour Boiling Test

The concrete hollow block used in this study is not suitable to be tested using the vacuum method due to its size; the boiling test method shown in Figure 2 was adopted. The first step of the process is to dry the concrete block samples for 72 hours (temperature 110ºC) in the oven. They were then cooled at room temperature and weighed. The concrete hollow blocks were transferred into a water tank for one-hour heating and subsequently boiled for 5 hours. The cooling process was done again at room temperature for 16 to 19 hours for the blocks to naturally lose heat. After that, the samples were removed from the water, wiped down with a damp cloth, and weighed. The following equation is used to calculate water absorption. This test complied with (MS 76, 1972).

Water absorption, % =

$$\% = \frac{100(w_d - w_s)}{w_d} \quad (1)$$

Where: w_d = dry weight of the specimen
w_s = saturated weight of the specimen

3.5 Compressive Strength Test

Concrete hollow block units are subjected to compressive strength testing to make sure they adhere to the applicable unit specifications' minimum strength criteria *(EVALUATING THE COMPRESSIVE STRENGTH OF CONCRETE MASONRY - 2012 IBC/2011 MSJC - NCMA*, n.d.), according to Figure 3. This test is performed on a concrete block with a dimension of 140mm x 190mm x 390mm to find the failure and breakage point of the concrete block as well as the strength. It is applicable for production control, performance, and compliance testing. The compressive strength is calculated using the following formulae:

$$f = \frac{W}{A} \quad (2)$$

Where: f = compressive strength of the specimen (N/mm^2)
W = maximum load (N)
A = average of the gross area surfaces of the specimen (mm^2)

Figure 3: Compressive Strength Machine

3.6 Density Test

The density test determines the density of the concrete block, and the test is conducted with conformity to (BS EN 12390-7, 2009). At 100ºC, the concrete block samples are dried to a constant mass. Each block's dimensions are given in centimeters (to the nearest millimeter), and the total volume, V, in cubic centimeters must be calculated after the blocks have been cooled to room

temperature. After that, the blocks are weighed in kilograms (to the nearest 10 g) m_{dry}. The average for the three blocks is taken as the average density. The formula for the density of the concrete block is as shown in the Equation below:

$$D = \left(\frac{w_d}{w_s - w_i}\right) \times 1000 \quad (3)$$

where: D = density (kg/m^3)
w_d = oven dry weight (kg)
w_s = saturated weight (kg)
w_i = immersed weight (kg)

3.7 Flexural Strength

An object's modulus of rupture (or flexural strength) is the maximum amount of force that it can withstand before breaking or becoming permanently deformed. Flexural strength can be measured in two very similar ways. The ends of a long rectangular sample of the material are supported, leaving no support in the center, yet the ends are solid. The material is then loaded or pressed until the central section is broken. An increasing load is delivered to the center of the sample during a three-point bending strength test until the material permanently breaks or bends. Increased forces can be applied while the force at the failure point is carefully recorded using flexural test equipment.

Figure 4: Flexural Strength Test

The only difference between a four-point bending test and a two-point bending test is that the load is applied simultaneously at both points, once further toward the center of the sample. The flexural strength is easier to calculate when one load or force is applied halfway between the supports and another part is applied halfway between them. Figure 4 demonstrates how the test was conducted.

The three-point bending strength test was employed in this study, and since length, width, and depth are all measured in meters in SI units, the force is measured in newtons, resulting in pascals (Pa), or newtons per square meter. Lengths, widths, and depths will be measured in imperial inches, and force in pounds-force resulting in pounds per square inch. The results were calculated using the following formulae:

$$S = \frac{3W\left(H/2 - x\right)}{bd^2} \quad (4)$$

Where: S = flexural strength (N/mm^2)
W = maximum applied load (N)
H = distance between support (mm)
b = width of the specimen (mm)
d = depth of the specimen (mm)
x = distance from the plane of failure to the midspan (mm)

3.8 Compressive Strength of Mortar

The mortars were cast in 50 mm × 50 mm × 50 mm molds as per (ASTM C 270-07, 2007, Khalaf, 2015) compressive strength of mortar standard test method. The mortar was cured for 28 days and 1.5 hours after mixing, the initial setting was removed. For the first 24 hours, the cubes were stored and covered with a polythene sheet before being removed from the mold and cured in water at 20°C for 27 days. To determine the relative density of the mortar, the cubes were weighed in both air and water. They were then loaded at 0.1N/mm^2/sec to ascertain the mortar's compressive strength. The mortar cube during the compressive strength test is shown in Figure 5.

Figure 5: Mortar Compressive Strength

Figure 6: Dropping Ball Test Apparatus

The dropping ball apparatus, as shown in Figure 6, was used to perform the mortar consistency test and under (British Standards Institution BSI, 1980). A consistency of approximately ± 1mm was used for the 1:3 designation mortars. The calculation of the result is using the formula as follows:

Compressive strength of mortar = max load carried by specimen/top surface area of the specimen Eq. 5

4.0 RESULTS AND DISCUSSION

The outcomes of tests conducted on the concrete hollow block's density, water absorption, and workability as well as its strength (concrete hollow block and mortar) as shown in Table 4. In the dropping ball test, the mortar type (¡¡) with the designation 1:3 had a consistency of about 10 ± 1mm. The mortar was used 1.5 hours after mixing before the initial setting was discarded. The amount of water that a unit can hold when saturated is defined as absorption. Absorption can indicate a concrete mix's level of compaction or the volume of voids within a block. The water absorption for the concrete hollow block used was approximately 7.362%. The density for a concrete hollow block is approximately 1,203 kg/m^3.

The hollow concrete block unit is subjected to an axial compressive load until it fails. Compressive strength tests are performed on concrete masonry units to ensure that they meet the minimum strength requirements of the applicable unit specification. The concrete hollow block used has a compressive strength of approximately 8.39 N/mm^2. The compressive and tensile strengths of the mortar are approximately 21.34 MPa and 33.23 kN, respectively. An object's modulus of rupture (or

flexural strength) is the amount of force it can withstand before breaking or becoming permanently deformed. The flexural strength of the concrete hollow block used was approximately 3.91 N/m^2.

Table 4: Engineering Properties of Masonry Concrete Hollow Block

Engineering Properties	Values (Unit)
Workability (dropping ball apparatus)	10 ± 1mm
Water Absorption	7.362%
Density	1,203 kg/m^3
Compressive Strength (hollow concrete block unit)	8.39 N/mm^2
Compressive Strength (mortar)	21.34 MPa
Tensile Strength (mortar)	33.23 MPa
Flexural Strength (hollow concrete block unit)	3.91/mm^2

4.1 Construction of Concrete Hollow Block

Until recently, traditional masonry methods of wall construction mostly remained the same, drawing criticism that masonry buildings take too long to construct and are hard to locate competent labor, in part due to unpleasant on-site working conditions (Hendry, 2001). The utilisation of innovative site practices, pre-fabrication, and new sorts of units have been the main areas of attention in efforts to ameliorate the situation (Hendry, 2001). Masonry structures are defined by their shape and certain material characteristics, such as those of the mortar and masonry units. As a result, the material properties must be established before thinking about the structural behaviour of the structural element. When designing masonry structures, compressive strength and deformations are important mechanical features to consider. Masonry mechanical properties are significantly influenced by the composition of masonry units (Maroliya *et al*., 2012, Mohamad *et al*., 2007, Khalaf, 2015), hollowness, material type, and mortar bed joints are all factors to consider (Köksal *et al*., 2005 Hendry, 2001). Increased lateral strain due to nonlinearity in the stress-strain relationship is associated with concrete microcracking (G. Mohamad *et al*., 2011, Drysdale & Hamid, 1979, Shrive & El-Rahman, 1985). Understanding the mechanisms of deformation and failure is essential for determining a wall's carrying capacity and improving understanding of its compressive strength.

Masonry works best in load-bearing structures because it can sustain loads, offer thermal and acoustic insulation, separate spaces, and protect against weather and fire, all of which must be accounted for, separately in a framed building. According to the allowed stress design, the stresses generated in a member while it is supporting a working load must be fewer than the allowable stresses. It is assumed that unreinforced masonry can withstand tensile stresses within allowable limits; however, the tensile strength of the masonry is ignored in reinforced masonry. The ACI code uses this design strategy for both unreinforced and reinforced masonry, whereas the IS code only applies to unreinforced masonry (Muthukumar & Kumar, 2015). The masonry nominal strength members must be multiplied by a strength reduction factor to achieve the design strength, which must be equal to or greater than the required strength. The necessary strength must be determined using a legally adopted building code's strength design load combination (Muthukumar & Kumar, 2015).

4.2 Modelling of Concrete Hollow Block

Masonry is a versatile building material comprised of several types of blocks, stones, ashlars, adobes, irregular stones, and other materials, and other units are examples of units and joints. Other materials, such as clay, bitumen, chalk lime/cement-based mortar, glue, and others, can be used as mortar. The term "masonry" is called into doubt by the large variety of combinations that can be made by unit geometry, nature, and arrangement as well as mortar qualities (R.E. Klingner, 2010). High specific weight with low tensile and shear strengths and ductility are some of the mechanical properties of various types of masonry (brittle behaviour). For numerical analysis of masonry structures, the Finite Element Method is commonly used (FEM). Creating a finite element model of a structural element or the entire structure is the first step in the analysis process. Columns, arches, domes, and vaults can be represented in the geometrical model using trusses, beams, solid, membrane, plate, and/or shell elements. Various modeling strategies are available to represent the heterogeneous and anisotropy of masonry construction, depending on the desired level of simplicity and accuracy.

The most significant issue encountered when modeling such structures is the difference in the mechanical properties of the masonry unit and mortar used to construct the masonry structure. A variety of modeling techniques can be used to examine masonry structures and computer software. In some of these studies, various modeling techniques are used to compare the results of the experimental study to the analysis results, ANSYS software is used for research on numerical simulations of masonry buildings (Eslami *et al*., 2012, Kouris & Kappos, 2012). There are two types of masonry numerical modeling in general: macro modeling and micro modeling. The accuracy and precision of the simulation determine the modeling technique used in the analysis (Doran *et al*., 2022). Micro modeling is divided into two types: detailed micro and simplified micro and the strategies shown in Figure 7 are described in greater detail (P.B. Lourenc¸o, 1996).

a) Detailed micro-modeling: this is the most precise method of simulation of the behaviour of masonry bricks; running analyses, however, takes time and is only useful for tiny masonry walls (Liu & Crewe, 2020). Both mortar and masonry are discrete inelastic continuum components and discontinuous elements also represent the interface between the mortar and the units. This analysis necessitates familiarity with each masonry constituent (unit and mortar), all masonry failure mechanisms, such as joint cracking, unit cracking, masonry crushing, and sliding over one head or bed joint, must be considered, as well as the interface (L. Macorini, 2013). In applications, finite elements, discrete elements, and limit analysis can all be used (A. Ordun˜a, 2005). Micro-modeling: more computational effort is required for the studies, but the results provide a better understanding of masonry structural local behaviour. This method is ideal for research as well as small models for localised analysis (A. Giordano, 2002, P.B. Lourenc¸o, 1996).

b) Simplify micro-modeling: the behaviour of an expanded unit is the behaviour of a mortar joint, or a unit-mortar interface is represented by discontinuous elements known as interface elements, whereas the behaviour of a unit-mortar interface is represented by discontinuous elements known as interface

elements. Masonry can thus be thought of as a series of elastic blocks joined together at joints by potential fracture/slip lines (G. Giambanco, 2001).

c) Macro-modeling (homogenisation theory): is the most fundamental strategy: masonry units, mortar, and mortar-unit interfaces are smudged in a homogeneous continuum material. Masonry is thus represented as an anisotropic homogeneous continuum, with masonry's macro constitutive behaviour obtained through a mathematical procedure that includes masonry components' geometry and constitutive behaviour (S.Y. Chen, 2008, G. Milani, 2006). When a structure has large dimensions and the stresses are distributed uniformly along the macro length, macro models are more useful (P.B. Lourenc¸o, 1996, S.Y. Chen, 2008). Large-scale structures can be efficiently modelled using the macro modelling approach. however, it is incapable of accurately capturing the detailed failure mechanisms (P.B. Lourenc¸o, 1996, Liu & Crewe, 2020, Lourenço, 1994).

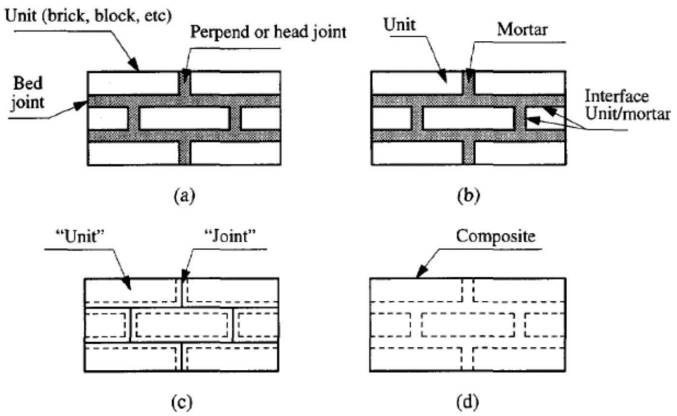

Figure 7: Methods for Modeling Block Masonry (a) An Example of Masonry; (b) Detailed Micro Modeling; (c) Simplified Micro Modeling; and (d) Macro Modelling (A. B. A. E. Mohamad & Chen, 2016)

4.3 Concrete Hollow Block Wall

A concrete hollow block wall is a heterogeneous structural composite material with mechanical properties determined by the composite components' properties and interactions (block and mortar), volume ratio, bond properties. Many researchers have conducted experiments to characterize the properties of masonry units for various masonry building systems Costigan *et al.,* 2015, Jafari *et al.,* 2017, Parajuli & Kiyono, 2015). The mechanical properties of masonry are influenced by the amount of stress in the joints, the direction of the bed joints, the shear modulus value, and the stiffness of the masonry structural parts (Kaushik *et al.,* 2007). The masonry's shear modulus was determined through compression tests and the diagonal test determined effective stiffness, which agreed well with the lateral tests that determined effective stiffness. Mathematical modeling of masonry, which is a composite material and, in general, refers to the material properties and constitutive elements relationship between masonry and its constituents, required for the combination of two different property materials, such as block and mortar. Masonry is an anisotropic, brittle composite material with distinct directional properties caused by brittle mortar joints, when subjected to extremely low levels of stress, masonry exhibits linear elastic behaviour, and after crack formation, high non-linearity is observed, causing stress redistribution through uncracked materials (Bui *et al.,* 2021). Increasing masonry bond tensile strength has a significant impact on transverse strength, as well as compressive and shearing strengths. Tensile splitting of the materials due to axial loading, rather than crushing or shear, is the most common type of compression failure (Kuddus & Fabregat, 2017). Out-of-plane failure mechanisms are prevented when the walls are not too thin and the connections between the floors and walls are appropriate. Masonry with sufficient strength at the corners and tension-resistant horizontal ties or bands are used to make the connections, and the masonry wall's in-plane shear capacity can then be utilized. The stiffness of walls degrades continuously under in-plane mechanisms after significant stiffness and strength loss, and the wall's gravity load-carrying capacity is eventually compromised, resulting in the structure's complete collapse due to the following reason:

- Mortar joint failure: this is common in masonry when the average compression is low.
- Shear tension failure of the unit: this occurs in masonry for intermediate average compression values.
- When the masonry's average compression is close to its uniaxial compressive strength, crushing failure occurs (Rai, 2017).

4.4 Compressive Strength of Masonry Block Wall

The compressive strength of the mortar influences masonry strength, significant variation in mortar strength causes variation in masonry strength (Nalon *et al.,* 2022). Mortar is made up of fine aggregate and binders that, when mixed with a small amount of water, form a workable and adhesive mixture (Nalon *et al.,* 2022). When calculating masonry compressive strength, several variables must be considered, including the thickness of the mortar joints, the height of the unit and its smaller horizontal dimension, the orientation of the unit concerning the direction of load application, and the strengths of the mortar and units. Many factors, both individually and in combination, indicate the difficulty of determining the masonry strength precisely. Masonry structural design necessitates a thorough understanding of the behaviour of the mortar and units assembled to withstand a variety of load conditions. The use of various types of blocks and mortar influences the behaviour of structural masonry elements significantly (Parsekian *et al.,* 2012). Masonry compressive strength is heavily influenced by block type, to a lesser extent by labor, and even less so by mortar type. The masonry's typical resistance to compressive loads is influenced by the unit's characteristic strength, the specified mortar used if the masonry is mortared, the shape of the unit, the thickness of the mortar joints, and the craftsmanship (Rai, 2017).

Masonry is constructed of two very distinct materials with extremely different mechanical properties: the stiffer block and the relatively malleable mortar, to which grout and reinforcement are added as necessary. Masonry has a very low tensile strength due to the regular distribution of various elements and the brittle connection between them. As a result, widely used unreinforced masonry should be expected to withstand compression loads. Under compression, masonry has three major modes of rupture depending on the relationship between the mortar's and the block's compressive strength:

a) When the mortar is very weak in comparison to the block, the masonry capacity is limited by the strength of the mortar, which usually fails by crushing.

b) When the mortar is moderately strong, the masonry capacity is determined by a combination of the compression and tension strength of the block, which typically fails due to lateral tension.
c) When the mortar is stronger than the block, the block's compressive strength limits masonry capacity.

Consider compressive strength as important property when designing masonry walls in a variety of loading scenarios. Several previous research studies on concrete hollow block masonry compressive behaviour have been conducted (Barbosa *et al*., 2010, Fortes *et al*., 2015), Thamboo & Dhanasekar, 2016, Zahra *et al*., 2021). Several provisions in masonry design standards are also described to predict the axial compression strength of concrete block masonry (Zahra *et al*., 2021, AS 3700, 2001). When it comes to predicting masonry compressive strength, however, there are differences between the standards. According to Rai, (2017) construction practices, geometry, the bond between the grout and the block, and other elements, all have an impact on how effectively grouted masonry works. Additionally, grouted masonry may be less effective than ungrouted masonry because the compressive strengths of ungrouted and grouted masonry varied depending on the materials employed (Atamturktur *et al*., 2017). Dry-stacked concrete masonry unit compressive strength and interface roughness with varying strengths were investigated. They concluded that interface roughness has a substantial impact on load-displacement behaviour and ultimate dry-stacked assembly capacity.

Concrete hollow block compressive strength is significant for two reasons: first and foremost, the greater the resistance, the longer the durability; second, the strength of the block is critical in structural masonry for compressive strength of the structural element, together with the appropriate mortar and grout specifications in terms of net area, with international standards requiring a minimum compressive strength of 10 MPa. Masonry structural design necessitates a thorough understanding of mortar and unit assembly behaviour to withstand a range of load conditions. The use of various types of blocks and mortar influences the behaviour of structural masonry elements. The compressive strength of masonry is the governing mechanical property in structures that contain these elements. Mortar strength, unit strength, mortar-to-unit strength ratio, the relationship between unit height and smaller horizontal dimension, unit orientation relative to load application direction, and mortar joint thickness all have an impact on masonry compressive strength (Rai, 2017). Even though masonry compressive strength is primarily influenced by masonry unit properties and the interfacial bond between masonry units and mortar, as well as the joint mortar, masonry unit moisture content at lazing, mortar thickness, masonry prism slenderness, workmanship, and other factors all play a role (Sajanthan *et al*., 2019). Bennett *et al*., (1997) was suggested to use a straightforward equation to compare the compressive strengths of bricks with masonry, with masonry compressive strength being equal to 0.3 times brick compressive strength. However, most of the other empirical expressions also consider mortar strength.

4.5 Tensile Strength of Concrete Hollow Block Wall

The tensile strength of the block is frequently the weak point of masonry under vertical loads, it is critical to avoid cracking. The tensile strength of a concrete block should be 10% to 15% of its compressive strength; this method yields approximately 120% direct tensile strength (Tennant *et al*., 2016). Concrete block masonry will shrink over time, just like any cement product if shrinkage is not managed, cracks can form, particularly in long walls. Extreme wall shrinkage can have an impact on the performance of other elements in the building, the amount of cement used, the type of aggregate used, and the environmental relative humidity all influence shrinkage deformation (Parsikian *et al*. 2019). Most of the shrinkage occurs during the steam curing process in the factory and shrinkage occurs more frequently in blocks that have only been moist cured. Units that have not been steam-cured for at least 28 days are therefore not recommended. Lightweight blocks shrink more than regular-weight blocks (from 0.04 to 0.08 percent) (from 0.02 percent to 0.05 percent). When wet blocks are used to build a wall, they expand and contract significantly after drying. The likelihood of shrinkage and pathologies increases when walls are laid wet, therefore, before installation, the concrete hollow block should not be wet (Inst., 1985). Masonry unit properties, mortar strength properties, loading eccentricity, all boundary conditions at the top and bottom of the wall, with the wall slenderness ratio (the ratio of effective height divided by effective thickness or effective length divided by effective thickness, whichever is greater) are considered (Amalkar *et al*., 2020). These are the elements that contribute to a masonry block wall's strength, in addition to the previously mentioned factors, workmanship has a significant impact on masonry strength (Udi *et al*., 2020). All the variables mentioned above changed during the construction and testing of full-scale wall panels, and a more realistic understanding of load-bearing masonry structural design was obtained, masonry's load-carrying capacity is typically measured in three ways:

- Tests on masonry components,
- Tests on masonry prism, and
- Full-scale wall specimens were subjected to tests.

Full-scale wall testing may provide a more realistic understanding of masonry performance because it considers all the preceding factors, plus the effect of masonry numerable joints (both vertical and horizontal). It is always best to create a full-scale masonry model that can be tested in real life when modeling any structure or element.

4.6 Flexural Bond Strength

Hardened mortar's most significant physical property is its flexural bond strength. The mortar's bond strength to brick units allows lateral loads to be transferred to veneer anchors in veneer applications. The bond influences the overall strength of the wall's ability to withstand lateral and flexural loads in load-bearing applications. Bond strength is influenced by block texture, suction, air content, water retention, the pressure used to form the joint, mortar proportions, and curing methods (Notes, 2020). Bond strength, also known as flexural strength, is a significant property that influences the structural performance of masonry walls, particularly when subjected to lateral loads such as winds and earthquakes. The penetration of cement hydration into the surface bond strength between the mortars determines masonry and the masonry units. Hamid & Drysdale, (1988) reported that, filling the hollow block cores with grout resulted in very significant increases in the bed joints' normal flexural tensile strength. These strengths were significantly greater than the 100% solid units built in block work.

In a study by M. Martinez and S. Atamturktur, (2018) and Martínez & Atamturktur, (2019) on masonry walls under flexural with various parameters; grout strength, reinforcement masonry unit, and grout place, according to them, converting partially grouted walls to fully grouted walls increased the ultimate load capacity. The grout's compressive strength was increased, which increased the prism's ultimate lateral load capacity. Tennant *et al.,* (2016) conducted research, they tested flexural with cement-stablisation soil blocks specimens, parallel to the bed's joints failed when the flexural strength test exceeded the bond strength with the masonry.

4.7 Suction Rate of Masonry Unit

When compared to clay and calcium silicate units, concrete hollow blocks have the highest suction rate. In practice, the initial suction rate is used to measure the surface porosity of the unit, capillary action is used to transport water from the mortar to the unit, affecting the unit-mortar bond (Inst., 1985). When mortar bonds are laid, they have an initial absorption rate of 30 g/min/30 inc^2 (30 g/min/194 cm^2) or less. If the initial rate of absorption of the brick is greater than this value, it should be wetted for 3 to 24 hours before lying down. The surface should be dry when laying a wetted block in a mortar (Borcheltl & Melande, 1999, Walker, 1996).

4.8 Unit Concrete Hollow Block and Mortar Interaction

Concrete hollow block mortar must be sufficiently durable to withstand relevant micro exposure conditions for the duration of the building's intended life, and it must not contain constituents that can impair the mortar's or abutting material's properties or durability. The mechanical and geometrical properties of the units, with the bond strength between the units and the mortar, all influence masonry behaviour (Venkatarama Reddy & Uday Vyas, 2008). Mortar joints between block units are critical in determining masonry behaviour, but they are frequently regarded as weak points (Dhanasekar, 2010). Hydrated lime and/or Ordinary Portland cement (OPC) are two common binder elements in mortar formulations. Water is required to achieve the desired workability, the most important intrinsic factor affecting the characteristics of fresh mortar, along with those of hardened mortar and the combination is the removal or migration of water. The parameters of the masonry unit-mortar interface are influenced by the removal or movement of water from the mortar bed. Changes in moisture cause the mortar and masonry components to shrink and swell, and the temperature has an impact on joint quality. Several factors related to both the unit and the mortar influence the variation in suction caused by the collision of a masonry unit and new mortar. The mortar may hold little or no water in some cases, while in others, the masonry unit absorbs all the water. Suction affects the mortar bond's strength and porosity, as well as its water tightness and other properties, the water present after suction, rather than the initial water content of the mortar determines its strength.

5.0 MORTAR

5.1 The Role of Mortar

Mortar is typically specified to meet ASTM C270 (Gheni *et al.,* 2017) and in a masonry assembly, mortar is the glue that holds the bricks together. Mortar must be strong enough to hold the masonry together while also aiding in the formation of a water-resistant barrier. Furthermore, when mortar is applied, it accounts for both dimensional variations and blocks physical properties. The mortar ingredient composition, proportions, and properties all have an impact on these requirements (Hendry, 2001). The shape of the mortar and grout has a large influence on the wall's tightness. Low-strength, easy-to-apply mortars will form a more weatherproof seal at the mortar/block interface. It is worth noting that the compressive and tensile strengths of the mortar must be less than those of the block (Rai, 2017). Masonry failure is caused primarily by the masonry units; therefore, strain compatibility for the physical interface is required (Chourasia *et al.,* 2019). Tensile cracking in the joint causes the masonry to fail if the block is more powerful than the mortar, the masonry will develop a vertical crack. Shear failure of the bond at the block mortar interface, resulting in tensile splitting. The block would crumble rather than split if it were tougher than the mortar (Sajanthan *et al.,* 2019). The strength grade of mortar is the most common way to identify it; an M12 mortar after 28 days should have a minimum compressive strength of 12 N/mm^2.

According to Euro code 6 (Kuddus & Fabregat, 2017), masonry mortar is classified into three types: general-purpose, thin-layer, and lightweight mortars, all of which can be designed or prescribed. Factory-made pre-batched masonry mortars and factory-made semi-finished masonry mortars (*Types of Mortar - Masonry Structures Eurocode - Euro Guide*, n.d.). Hardened mortar quality in designed mortars should be determined by its compressive strength, prescription mortars, on the other hand, use predetermined proportions for the intended use; in prescribed mortars, adequate adhesion depends on the type of mortar used, and the units to which it is applied determine the result. Masonry mortar composition varies depending on wall thickness and construction technique. For 220 mm thick masonry walls, a richer mix of 1: 6 is used, while for 115 mm thick non-load bearing (partition) walls, a richer mix of 1: 4 is used, and masonry mortar thickness ranges between 10 and 15 mm (Chourasia *et al.,* 2019). According to Bolhassani *et al.,* (2016), Portland cement lime mortar type 'S' after 28 days has an average compressive strength of 13 MPa and is used in constructing concrete masonry walls. The coarse grout meets ATSM C476 (*ASTM C476: Standard Specification for Grout for Masonry : American Society for Testing and Materials : Free Download, Borrow, and Streaming : Internet Archive*, n.d.) specifications, with a slump test of 250 mm and an average net of 23 MPa compressive strength.

5.2 Joint Thickness

Due to its inherent properties that meet the various requirements of both exterior and interior walls, concrete hollow block is a popular building material. While these are the most important reasons for the popularity of concrete hollow block, performance should not be overlooked. Like any other construction system, the field performance of a concrete hollow block wall system is heavily influenced by design decisions. When crack control measures, such as control joints, are used correctly, they can help ensure that the concrete hollow block performs satisfactorily. Control joints are one method of alleviating horizontal tensile stresses caused by shrinkage of concrete hollow block units, mortar, and grout; they are vertical planes of weakness with high stress built into the wall to allow for shrinkage-induced

longitudinal movement. A bond break is formed by using a backer rod and sealant to replace all or part of a vertical mortar joint, these seals the joint while allowing for slight movement. Joint reinforcement and other horizontal reinforcement at control joints should be avoided unless structurally necessary, as they limit horizontal movement (Scutaru, 2018).

General purpose and lightweight mortar beds and perpendicular joints should be not less than 6 mm thick and not more than 15mm thick, whereas thin-layer mortars should be not less than 0.5 mm thick and not more than 3mm thick (Zahra *et al*., 2021). The failure mode or mechanical properties of prisms built with strong mortars were unaffected by variations in joint thickness ranging from 5 to 20mm (Nalon *et al*., 2022). Vertical control joints in concrete hollow bock wall are only required when control joints are required. When using materials with different movement properties, such as concrete and clay masonry, the movement difference must be accounted for in the design.

5.3 Water Retentivity

Water retentivity refers to a mortar's ability to retain water against suction and evaporation, in general, it is an indirect measure of mortar workability (Notes, 2020). Unless an absorptive concrete hollow block unit is used, mortar should be able to withstand the rapid loss of mixing water to the atmosphere on a dry day (this prevents loss of plasticity). Because water loss stiffens the mortar, weather-tight joints are impossible to achieve. A water-retentive mortar long enough to remain soft and plastic to allow concrete hollow block, units must be precisely aligned, leveled, plumbed, and adjusted to the proper line without breaking the mortar's intimate contact or bond with the unit (Bindiganavile *et al*., 2016). Split blocks, for example, are low absorption units, and may float when they meet a mortar with a high water retentivity. As a result, a mortar's water retentivity should be within acceptable limits. Water improves mortar workability; entrained air, extremely fine aggregate, or cementitious materials improve not only the mortar's workability or plasticity but also its water retentivity.

5.4 Workability

Due to similarities between mortar and concrete materials, the most misunderstood aspect of concrete hollow block mortar is its water content. Many designers make mistake of assuming that mortar specifications are the same as concrete specifications, especially in terms of the water/cement ratio (Bindiganavile *et al*., 2016). Numerous specifications specify that the mortar should be mixed with as little water as possible while remaining workable, and they prohibit retempering the mortar while it is being constructed. The compressive strengths of mortar mixed and placed according to these specifications are more excellent, however, the bond strengths are weaker. The maximum bond strength within the mortar's capacity will be provided by mixing the mortar with the most amount of water consistent with workability (Hendry, 2001).

5.5 Failure Criteria

The strengths and strains to be uniform at the materials' contact, the connection between the blocks and the mortar is crucial. Complex stress conditions act on the components because of adhesion and strain equality. A triaxial compressive condition known as confinement is applied to mortar when it is more deformable than the block. Its mechanical characteristics, compressive strength, and elastic modulus make mortar a useful confining material that prevents free expansion. Mortar behaves differently when compressed than when it is simply compressed, for example, is modified therefore, the confining modifies the masonry system performance (Khalaf *et al*., 2015, G. Mohamad *et al*., 2015, Hayen *et al*., 2004). Tensile stress in the block or mortar joint crushing, which happens when mortar hits its confining strength limit, can cause masonry to fail. Therefore, the proportions of the mortar mix and the block be comparable to prevent failure due to tensile stress in the block. The mortar has a significant impact on the behaviour of the masonry when the joint crushing failure occurs, without lowering the failure load (Nalon *et al*., 2022). In prisms built with low-strength mortar, the mortar-block connection had been severed. According to Parsekian *et al*., (2019) and Fonseca *et al*., (2019), because of tension in the block shells, the grouted prisms failed while the grout cores remained intact, and the components acted in a non-homogeneous but uniform manner. High-strength concrete hollow block grouted prisms were compressed, and the hollow prism failed because of vertical cracks and block crushing close to the mortar joint, whereas vertical cracks and debonding of concrete hollow block and grout caused the grouted prism to fail (Thaickavil & Thomas, 2018). Masonry prisms made of cement-stabilized pressed earth bricks and burnt clay bricks were investigated for their behaviour and strength. Because of the outward bursting force caused by Poisson's effect on the composite specimen, they discovered vertical cracks in the middle of the specimens in their experiment. They also discovered that masonry unit strength and the strength of masonry prisms were significantly influenced by mortar strength. In addition, the masonry unit's volume fraction, the bed joint's volume ratio to mortar, and the specimen's height-to-thickness ratio were all calculated, all influenced the masonry prisms' strength. This occurrence has been confirmed by G. Mohamad *et al*., (2007), in the investigation of the tested prism with various block strengths and four types of mortar. Masonry's nonlinear behaviour is primarily due to the mortar, and different types of mortar cause masonry prisms to fail in different ways.

6.0 CONCLUSIONS

Cement concrete hollow blocks are becoming more popular than traditional building materials like bricks and stones because the air space in the block accounts for 25% of the total area. Hollow blocks enable thinner walls, resulting in more floor space; this saves material and lowers construction costs. Additionally, it speeds up the building, conserves steel and cement, and lowers labor expenses on the project site. These blocks help masonry structures lose weight naturally while also improving physical properties, noise reduction, and thermal insulation. They also have areas where electrical conduits, water pipes, and soil pipes can be hidden. Masonry hollow blocks can be used to build load-bearing and non-load-bearing walls, depending on the material's compressive strength. If cost reductions over alternative materials can be accomplished, masonry hollow blocks seem to have a bright future in the construction sector. The appropriate experimental procedures have been done to achieve the objectives of this study. The characteristics of hollow concrete blocks and mortar are known based on the results. The conclusions are listed below:

- The compressive strength for a masonry hollow block is 8.39 MPa at 28 days which does not pass the specifications for it to be a load-bearing unit. The standards state that the compressive strength must exceed 7 MPa for it to be qualified as a load-bearing unit. The compressive strength of mortar is approximately 21.34 MPa at 28day is also in accordance with the specification.
- The masonry hollow concrete blocks are considered dense due to their dry density values that exceed 1500 kg/m^3.
- The water absorption rate of masonry blocks is lower than that of ordinary concrete blocks as the former has low permeability.

7.0 ACKNOWLEDGMENT

The authors would like to thank Universiti Sains Malaysia (USM), School of Civil Engineering which provided financial support. ■

REFERENCES

[1] Giordano, E. M. A. D. L. (2002). Modelling of Historical Masonry Structures: Comparison of Different Approaches Through A Case Study, Eng. Struct. , 24 (8), 1057–1069.

[2] L. Murmu and A. Patel. (2018). Towards Sustainable Bricks Production: An Overview. Construction and Building Materials, 165, 112–125.

[3] Ordun˜ A, P. B. L. (2005). Three-Dimensional Limit Analysis of Rigid Blocks Assemblages. Part II: Load-Path Following Solution Procedure and Validation, Int. J. . . Solids Struct. , 5161–5180.

[4] Abd Manan, T. S. B., Beddu, S., Khan, T., Wan Mohtar, W. H. M., Sarwono, A., Jusoh, H., Mohd Kamal, N. L., Sivapalan, S., and Ghanim, A. A. J. (2019). Step By Step Procedures: Degradation of Polycyclic Aromatic Hydrocarbons in Potable Water Using Photo-Fenton Oxidation Process. Methodsx, 6, 1701–1705. Https://Doi.Org/10.1016/J.Mex.2019.07.011

[5] Abd Manan, T. S. B., Beddu, S., Mohamad, D., Mohd Kamal, N. L., Wan Mohtar, W. H. M., Khan, T., Jusoh, H., Sarwono, A., M. Ali, M., Che Muda, Z., Mohamed Nazri, F., Isa, M. H., Ghanim, A. A. J., Ahmad, A., Wan Rasdi, N., and Basri, N. A. N. (2021). Physicochemical and Leaching Properties of Coal Ashes from Malaysian Coal Power Plant. Chemical Physics Letters, 138420. Https://Doi.Org/10.1016/J.Cplett.2021.138420

[6] Al-Shugaa, M. A., Rahman, M. K., Baluch, M. H., Al-Gadhib, A. H., Sadoon, A. A., and Al-Osta, M. A. (2019). Performance of Hollow Concrete Block Masonry Walls Retrofitted With Steel-Fiber And Microsilica Admixed Plaster. Structural Concrete, 20(1), 236–251. Https://Doi.Org/10.1002/SUCO.201700261

[7] Amalkar, M. S., Renukadevi, M. V., Jagadish, K. S., and Basutkar, S. M. (2020). Effect of Slenderness and Eccentricity on The Strength of Concrete Block Masonry: An Experimental Investigation. SN Applied Sciences, 2(6). Https://Doi.Org/10.1007/S42452-020-2829-6

[8] AS 3700. (2001). Australian Standards for Masonry Structures. In Standards Australia.

[9] ASTM C 27007. (2007). Standard Specification for Mortar for Unit Masonry. United States: American Society for Testing and Material. 2–13.

[10] ASTM C140/C140M-14. (2014). Standard Test Methods for Sampling and Testing Concrete Masonry Units and Related Units,. ASTM International. Https://Www.Academia.Edu/31630062/Standard_Test_Methods_For_Sampling_And_Testing_Concrete_Masonry_Units_And_Related_Units_1

[11] ASTM C476: Standard Specification for Grout for Masonry: American Society for Testing and Materials : Free Download, Borrow, and Streaming : Internet Archive. (N.D.). Retrieved August 23, 2023, From Https://Archive.Org/Details/Gov.Law.Astm.C476.1971

[12] Atamturktur, S., Ross, B. E., Thompson, J., and Biggs, D. (2017). Compressive Strength of Dry-Stacked Concrete Masonry Unit Assemblies. Journal of Materials in Civil Engineering, 29(2), 0601–6020. Https://Doi.Org/10.1061/(Asce)Mt.1943-5533.0001693

[13] Bakhteri, J., Makhtar, A. M., and Sambasivam, S. (2004). Finite Element Modelling of Structural Clay Brick Masonry Subjected To Axial Compression.

[14] Bakhteri, J., Makhtar, A. M., and Sambasivam, S. (2012). Finite Element Modelling of Structural Clay Brick Masonry Subjected to Axial Compression. Jurnal Teknologi. Https://Doi.Org/10.11113/JT.V41.698

[15] Barbosa, C. S., Lourenço, P. B., and Hanai, J. B. (2010). On the Compressive Strength Prediction for Concrete Masonry Prisms. Materials and Structures/Materiaux ET Constructions, 43(3), 331–344. Https://Doi.Org/10.1617/S11527-009-9492-0/METRICS

[16] Beddu, S., Abd Manan, T. S. B., Zainoodin, M. M., Khan, T., Wan Mohtar, W. H. M., Nurika, O., Jusoh, H., Yavari, S., Kamal, N. L. M., Ghanim, A. A., Pati, S., and Abdullah, M. T. (2020). Dataset on Leaching Properties of Coal Ashes from Malaysian Coal Power Plant. Data in Brief, 31, 105843. Https://Doi.Org/10.1016/J.Dib.2020.105843

[17] Bennett, R. M., Boyd, K. A., and Flanagan, R. D. (1997). Compressive Properties of Structural Clay Tile Prisms. Journal of Structural Engineering, 123(7), 920–926. Https://Doi.Org/10.1061/(ASCE)0733-9445(1997)123:7(920)

[18] Bindiganavile, V., Islam, M. T., and Suresh, N. (2016). Evaluation of Water Permeability in Fibre Reinforced Hydraulic Lime Mortar Intended for Conservation. Key Engineering Materials, 711, 630–637. Https://Doi.Org/10.4028/WWW.SCIENTIFIC.NET/KEM.711.630

[19] Bolhassani, M., Hamid, A. A., and Moon, F. L. (2016). Enhancement of Lateral In-Plane Capacity of Partially Grouted Concrete Masonry Shear Walls. Engineering Structures, 108, 59–76. Https://Doi.Org/10.1016/J.Engstruct.2015.11.017

[20] Borcheltl, J. G., and Melande, J. M. (1999). Bond Strength and Water Penetration of High Ira Brick and Mortar. 8th North American Masonry Conference, 12.

[21] British Standards Institution BSI. (1980). Mortars, Screeds and Plasters. British Standards Institution BSI.

[22] BS 1881-122:2011+A1. (2020). Testing Concrete. Method for Determination of Water Absorption. British Standards Institution.

[23] BS EN 12390-7. (2009). Testing Hardened Concrete Part 7: Density of Hardened Concrete. Journal of Chemical Information and Modeling, 53(9), 1689–1699.

[24] BSI 5628: British Standards Institution (BSI). BSI-5628. (1992). Structural Use of Unreinforced Masonry.

[25] Bui, T. T., Limam, A., and Sarhosis, V. (2021). Failure Analysis of Masonry Wall Panels Subjected to In-Plane and Out-Of-Plane Loading Using the Discrete Element Method. European Journal

of Environmental and Civil Engineering, 25(5), 876–892. Https://Doi.Org/10.1080/19648189.2018.1552897

[26] Calderón, S., Vargas, L., Sandoval, C., and Araya-Letelier, G. (2020). Behavior of Partially Grouted Concrete Masonry Walls under Quasi-Static Cyclic Lateral Loading. Materials (Basel, Switzerland), 13(10). Https://Doi.Org/10.3390/MA13102424

[27] Chi, B., Yang, X., Wang, F., Zhang, Z., and Quan, Y. (2019). Experimental Investigation into the Seismic Performance of Fully Grouted Concrete Masonry Walls Using New Prestressing Technology. Applied Sciences (Switzerland), 9(20). Https://Doi.Org/10.3390/APP9204354

[28] Chourasia, A., Parashar, J., and Singhal, S. (2019). Confined Masonry Construction for India: A Techno Economical Solution for Improved Seismic Behaviour. Current Science, 117(7), 1174–1183. Https://Doi.Org/10.18520/Cs/V117/I7/1174-1183

[29] Cintya3, Juliana Machado1, S. C., Alexandre Lima2, O., Sakamoto, Rudiele4, L. R., and Prudêncio Jr. (2012). The Effect of Mortar Bedding Type and Hollow Concrete Block Geometry on the Mechanical Behavior of High-Strength Structural Masonry. 15th International Brick and Block Masonry Conference. Http://Www.Hms.Civil.Uminho.Pt/Ibmac/2012/7A5.Pdf

[30] Costigan, A., Pavía, S., Kinnane, O., and Adriancostigansarapavíaoliverkinnane. (2015). An Experimental Evaluation of Prediction Models for the Mechanical Behavior of Unreinforced, Lime-Mortar Masonry Under Compression. Journal of Building Engineering, 4, 283–294.

[31] Dhanasekar, M. (2010). Review of Modelling of Masonry Shear. International Journal of Advances in Engineering Sciences and Applied Mathematics, 2(3), 106–118. Https://Doi.Org/10.1007/S12572-011-0022-2

[32] Doran, B., Karslioglu, M., Unsal Aslan, Z., and Vatansever, C. (2022). Experimental and Numerical Investigation of Unreinforced Masonry Walls with and Without Opening. International Journal of Architectural Heritage. Https://Doi.Org/10.1080/15583058.2022.2080611

[33] Drysdale, R. G., and Hamid, A. A. (1979). Behavior of Concrete Block Masonry under Axial Compression. J Am Concr Inst, 76(6), 707–721. Https://Doi.Org/10.14359/6965

[34] Edri, I. E., Yankelevsky, D. Z., and Rabinovitch, O. (2020). Blast Response of One-Way Arching Masonry Walls. International Journal of Impact Engineering, 141(3), 1–16. Https://Doi.Org/10.1016/J.Ijimpeng.2020.103568

[35] Eslami, A., Ronagh, H. R., Mahini, S. S., and Morshed, R. (2012). Experimental Investigation and Nonlinear FE Analysis of Historical Masonry Buildings - A Case Study. Construction and Building Materials, 35, 251–260. Https://Doi.Org/10.1016/J.Conbuildmat.2012.04.002

[36] Evaluating the Compressive Strength of Concrete Masonry - 2012 IBC/2011 MSJC - NCMA. (N.D.). Retrieved January 31, 2022, From Https://Ncma.Org/Resource/Evaluating-The-Compressive-Strength-Of-Concrete-Masonry-2012-Ibc/

[37] Fonseca, F. S., Fortes, E. S., Parsekian, G. A., and Camacho, J. S. (2019). Compressive Strength of High-Strength Concrete Masonry Grouted Prisms. Construction and Building Materials, 202, 861–876. Https://Doi.Org/10.1016/J.Conbuildmat.2019.01.037

[38] Fortes, E. S., Parsekian, G. A., and Fonseca, F. S. (2015). Relationship between the Compressive Strength of Concrete Masonry and the Compressive Strength of Concrete Masonry Units. Journal of Materials in Civil Engineering, 27(9), 04014238. Https://Doi.Org/10.1061/(Asce)Mt.1943-5533.0001204

[39] G. Giambanco, S. R. R. S. (2001). Numerical Analysis of Masonry Structures via Interface Models, Comput. Methods. Appl. Mech. Eng., 190 (49–50), 6493–6511.

[40] G. Milani, P. B. L. A. T. (2006). Homogenization Approach for the Limit Analysis of Out-Of-Plane Loaded Masonry Walls, J. Eng Struct., ASCE 132 (10), 1650–1663.

[41] Gabor, A., Ferrier, E., Jacquelin, E., Hamelin, P., Mohamad, G., Lourenço, P. B., Roman, H. R., Sarhat, S. R., Sherwood, E. G., Council, W. C., Singh, S., Consulting, H., Zea-, N., Oña Vera, M. Y., Metelli, G., Barros, J. A. O., Plizzari, G., Can, Ö., Zhou, X. X., … Asad, M. (2019). Mechanics of Hollow Concrete Block Masonry Prisms under Compression: Review and Prospects. Construction and Building Materials, 20(3), 1–10. Https://Doi.Org/10.1016/J.Cemconcomp.2006.11.003

[42] Gauthier, T. D., and Hawley, M. E. (2007). Statistical Methods. In B. L. M. Robert D. Morrison (Ed.), Introduction to Environmental Forensics (Pp. 129–183). Elsevier Academic Press. Https://Doi.Org/10.1016/B978-012369522-2/50006-3

[43] Gheni, A. A., Elgawady, M. A., and Myers, J. J. (2017). Mechanical Characterization of Concrete Masonry Units Manufactured With Crumb Rubber Aggregate. ACI Materials Journal, 114(1), 65–76. Https://Doi.Org/10.14359/51689482

[44] Hamid, A. A., and Drysdale, R. G. (1988). Flexural Tensile Strength of Concrete Block Masonry. Journal of Structural Engineering, 114(1), 50–66. Https://Doi.Org/10.1061/(Asce)0733-9445(1988)114:1(50)

[45] Hasan, M., Saidi, T., Sarana, D., and Bunyamin. (2021). The Strength of Hollow Concrete Block Walls, Reinforced Hollow Concrete Block Beams, and Columns. Journal of King Saud University - Engineering Sciences. Https://Doi.Org/10.1016/J.JKSUES.2021.01.008

[46] Hayen, R., Van Balen, K., and Van Gemert, D. (2004). The Mechanical Behaviour of Mortars in Triaxial Compression. International Congress on Arch Bridges ARCH'04, 1–10.

[47] Hendry, E. A. W. (2001). Masonry Walls: Materials and Construction. Construction and Building Materials, 15(8), 323–330. Https://Doi.Org/10.1016/S0950-0618(01)00019-8

[48] Inst., B. S. (1985). "British Standard Specification for Clay Bricks". BS 3921, London.

[49] Jafari, S., Rots, J. G., Esposito, R., and Messali, F. (2017). Characterizing the Material Properties of Dutch Unreinforced Masonry. Procedia Engineering, 193, 250–257. Https://Doi.Org/10.1016/J.PROENG.2017.06.211

[50] Kaushik, H. B., Rai, D. C., and Jain, S. K. (2007). Stress-Strain Characteristics of Clay Brick Masonry under Uniaxial Compression. Journal of Materials in Civil Engineering, 19(9), 728–739. Https://Doi.Org/10.1061/(ASCE)0899-1561(2007)19:9(728)

[51] Khalaf, F. M. (2015). Factors Influencing Compressive Strength of Concrete Masonry Prisms. Http://Dx.Doi.Org/10.1680/Macr.1996.48.175.95,48(2),95.Https://Doi.Org/10.1680/MACR.1996.48.175.95

[52] Khalaf, F. M., Hendry, A. W., and Fairbairn, D. R. (2015). Mechanical Properties of Materials Used in Concrete Blockwork Construction. Http://Dx.Doi.Org/10.1680/Macr.1992.44.158.1, 44(158), 1–14. Https://Doi.Org/10.1680/MACR.1992.44.158.1

[53] Köksal, H. O., Karakoç, C., and Yildirim, H. (2005). Compression Behavior and Failure Mechanisms of Concrete Masonry Prisms. Journal of Materials in Civil Engineering, 17(1), 107–115. Https://Doi.Org/10.1061/(ASCE)0899-1561(2005)17:1(107)

[54] Kouris, L. A. S., and Kappos, A. J. (2012). Detailed and Simplified Non-Linear Models for Timber-Framed Masonry Structures. Journal of Cultural Heritage, 13(1), 47–58. Https://Doi.Org/10.1016/J.Culher.2011.05.009

[55] Kuddus, M. A., and Fabregat, P. R. (2017). Literature Review of Experimental Study on Load Bearing Masonry Wall. IOSR Journal of Mechanical and Civil Engineering, 14(01), 52–58. Https://Doi.Org/10.9790/1684-1401045258

[56] L. Macorini, B. A. I. (2013). Nonlinear Analysis of Masonry Structures Using Mesoscale Partitioned Modeling. Adv. Eng. Software, 60–61.

[57] Liu, Z., and Crewe, A. (2020). Effects of Size and Position of Openings on In-Plane Capacity of Unreinforced Masonry Walls. Bulletin of Earthquake Engineering, 18(10), 4783–4812. Https://Doi.Org/10.1007/S10518-020-00894-0

[58] Lourenço, P. B. (1994). Analysis of Masonry Structures with Interface Elements. Theory and Applications. TNO Building and Construction Research Computational Mechanics, 03(03), 34.

[59] Ma, G., Huang, L., Yan, L., Kasal, B., Chen, L., and Tao, C. (2016). Experimental Performance of Reinforced Double H-Block Masonry Shear Walls under Cyclic Loading. Materials and Structures 2016 50:1, 50(1), 1–13. Https://Doi.Org/10.1617/S11527-016-0943-0

[60] Maldonado, N. G., Martín, P., Solar, G. G. Del, Domizio, M., Maldonado, N. G., Martín, P., Solar, G. G. Del, and Domizio, M. (2019). Historic Masonry. Heritage. Https://Doi.Org/10.5772/INTECHOPEN.87127

[61] Maroliya, M. M. K., Maroliya, 1. Mr. M K, and Maroliya, M. M. K. (2012). Load Carrying Capacity Of Hollow Concrete Block Masonry Column. IOSR Journal of Engineering, 02(10), 05–08. Https://Doi.Org/10.9790/3021-021010508

[62] Martínez, M., and Atamturktur, S. (2019). Experimental and Numerical Evaluation of Reinforced Dry-Stacked Concrete Masonry Walls. Journal of Building Engineering, 22, 181–191. Https://Doi.Org/10.1016/J.Jobe.2018.12.007

[63] Ömer. C. (2018). Investigation of Seismic Performance of In-Plane Aligned Masonry Panels Strengthened With Carbon Fiber Reinforced Polymer. Elsevier. Retrieved August 22, 2023, from link Https://Www.Sciencedirect.Com/Science/Article/Pii/S0950061818319664?Casa_Token=Ubuqhjn1cxmaaaaa:55gbk9vpfyukhclwatvnsqkukcj9z_Wd7h2tir4ycxhtugd2dnxribpco2v4yczkgwelo_Bg

[64] Mohamad, A. B. A. E., and Chen, Z. (2016). Experimental and Numerical Analysis of the Compressive and Shear Behavior for a New Type of Self-Insulating Concrete Masonry System. Applied Sciences (Switzerland), 6(9). Https://Doi.Org/10.3390/App6090245

[65] Mohamad, G., Fonseca, F. S., Roman, H. R., Vermeltfoort, A. T., and Rizzatti, E. (2015). Behavior of Mortar under Multitaxial Stress. Proceedings of The 12th North American Masonry Conference, Denver, May, 17–20.

[66] Mohamad, G., Lourenço, P. B., and Roman, H. R. (2007). Mechanics of Hollow Concrete Block Masonry Prisms under Compression: Review and Prospects. Cement and Concrete Composites, 29(3), 181–192. Https://Doi.Org/10.1016/J.Cemconcomp.2006.11.003

[67] Mohamad, G., Lourenço, P. B., and Roman, H. R. (2011). Study of the Compressive Strength of Concrete Block Prisms: Stack and Running Bond. Revista IBRACON De Estruturas E Materiais, 4(3), 347–358. Https://Doi.Org/10.1590/S1983-41952011000300002

[68] MS 76. (1972). Specification for Bricks and Blocks Ff Fired Brickearth, Clay or Shale Part 2 : Metric Units. MALAYSIAN Standard.

[69] Muthukumar, G., and Kumar, M. (2015). Influence of Openings on the Structural Response of Shear Wall. Advances in Structural Engineering: Materials, Volume Three, 2014, 2229–2239. Https://Doi.Org/10.1007/978-81-322-2187-6_169

[70] N. Sathiparan, M. K. N. Anusari, and N. N. S. (2014). Effect of Void Area on Hollow Cement Masonry Mechanical Performance. Arabian Journal for Science and Engineering, 39 No 11, 7569–7576.

[71] Nalon, G. H., Ribeiro, J. C. L., Pedroti, L. G., Silva, R. M. Da, Araújo, E. N. D. De, Santos, R. F., and Lima, G. E. S. De. (2022a). Review of Recent Progress on the Compressive Behavior of Masonry Prisms. Construction and Building Materials, 320(January), 327–337. Https://Doi.Org/10.1016/J.Conbuildmat.2021.126181

[72] Nalon, G. H., Ribeiro, J. C. L., Pedroti, L. G., Silva, R. M. Da, Araújo, E. N. D. De, Santos, R. F., and Lima, G. E. S. De. (2022b). Review of Recent Progress on the Compressive Behavior of Masonry Prisms. Construction and Building Materials, 320, 126181. Https://Doi.Org/10.1016/J.CONBUILDMAT.2021.126181

[73] Notes, T. (2020). Technical Notes on Brick Construction 8 Mortars for Brickwork (Issue March, Pp. 1–13).

[74] Oliveira, M. F. De, Filho, S. K., Pacheco, F., Patrício, J. V., and Tutikian, B. F. (2021). Influence of Ceramic Block Geometry and Mortar Coating on the Sound Reduction of Walls. Ambiente Construído, 21(2), 195–207. Https://Doi.Org/10.1590/S1678-86212021000200521

[75] P.B. Lourenc¸O. (1996). Computational Strategies for Masonry Structures. Delft University.

[76] Parajuli, R. R., Furukawa, A., and Gautam, D. (2020). Experimental Characterization of Monumental Brick Masonry in Nepal. Structures, 28(June), 1314–1321. Https://Doi.Org/10.1016/J.Istruc.2020.09.065

[77] Parajuli, R. R., and Kiyono, J. (2015). Ground Motion Characteristics of the 2015 Gorkha Earthquake, Survey of Damage to Stone Masonry Structures and Structural Field Tests. Frontiers in Built Environment, 1, 23.

[78] Parsekian, G. A., Hamid, A. A., and Drysdale, R. G. (2012). Comportamento E Dimensionamento De Alvenaria Estrutural. Edufscar. São Carlos, 625.

[79] Parsekian, G. A., Medeiros, W. A., and Sipp, G. (2018). High-Rise Concrete and Clay Block Masonry Building in Brazil. Mauerwerk, 22(4), 260–272. Https://Doi.Org/10.1002/DAMA.201800010

[80] Parsikian, G., Roman, H. R., Silver, C. O and Faria, M. S. (2019). Concrete Block. In Long Term Performance and Durability of Masonry Structures. Woodhead Pulishing, 21–57.

[81] Popescu, C., Sas, G., Blanksvärd, T., and Täljsten, B. (2015). Concrete Walls Weakened by Openings as Compression Members: A Review. Engineering Structures, 89, 172–190. Https://Doi.Org/10.1016/J.Engstruct.2015.02.006

[82] R.E. Klingner. (2010). Masonry Structural Design. Mcgraw-Hill Professional, 588.

[83] Rai, D. C. (2017). Review of Design Codes for Masonry Buildings By. Earthquake, 10(6) (January), 0–22. Http://Etheses.Dur.Ac.Uk/6122/

[84] Reboul, N., Si Larbi, A., and Ferrier, E. (2018). Two-Way Bending Behaviour of Hollow Concrete Block Masonry Walls Reinforced By Composite Materials. Composites Part B: Engineering, 137, 163–177. Https://Doi.Org/10.1016/J.COMPOSITESB.2017.11.002

[85] S.Y. Chen, F. L. M. T. Y. (2008). A Macroelement for the Nonlinear Analysis of In-Plane Unreinforced Masonry Piers. Eng Struct., 30 (8), 2242–2252.

[86] Sajanthan, K., Balagasan, B., and Sathiparan, N. (2019). Prediction of Compressive Strength of Stabilized Earth Block Masonry. Advances in Civil Engineering, 2019. Https://Doi.Org/10.1155/2019/2072430

[87] Scutaru, M. (2018). Modern Strengthening Techniques for Masonry Structures. In Construcţii. Arhitectură (Vol. 64, Issue 68).

[88] Shrive, N. G., and El-Rahman, M. (1985). Understanding the Cause of Cracking in Concrete: A Diagnostic Aid. Concrete International, 7(5), 39–44.

[89] Sureshchandra, H. S., Sarangapani, G., and Kumar, B. G. N. (2014). Experimental Investigation on the Effect of Replacement Of Sand By Quarry Dust In Hollow Concrete Block For Different Mix Proportions. Citeseerhs Sureshchandra, G Sarangapani, BGN Kumarinternational Journal of Environmental Science and Development, 2014•Citeseer, 5(1), 1–5. Https://Doi.Org/10.7763/IJESD.2014.V5.443

[90] Tennant, A. G., Foster, C. D., and Reddy, B. V. V. (2016). Detailed Experimental Review of Flexural Behavior of Cement Stabilized Soil Block Masonry. Journal of Materials in Civil Engineering, 28(6), 0601–6004. Https://Doi.Org/10.1061/(Asce)Mt.1943-5533.0001548

[91] Thaickavil, N. N., and Thomas, J. (2018). Behaviour and Strength Assessment of Masonry Prisms. Case Studies in Construction Materials, 8, 23–38. Https://Doi.Org/10.1016/J.Cscm.2017.12.007

[92] Thamboo, J. A., and Dhanasekar, M. (2016). Behaviour of Thin Layer Mortared Concrete Masonry under Combined Shear and Compression. Australian Journal of Structural Engineering, 17(1), 39–52. Https://Doi.Org/10.1080/13287982.2015.1116181

[93] Types of Mortar - Masonry Structures Eurocode - Euro Guide. (N.D.). Retrieved August 23, 2023, From Https://Www.Euroguide.Org/Masonry-Structures-Eurocode-6/Types-Of-Mortar.Html

[94] Udi, U. J., et al. (2020). Mechanical Behavior of Brick Masonry Panels under Uniaxial Compression. Journal of Structural Engineering & Applied Mechanics, 3(4), 385–395. Https://Doi.Org/10.31462/Jseam.2020.03153168

[95] Umair, M., Alam, M., and Anas, S. M. (2022). Experimental Studies on Blast Performance of Unreinforced Masonry Walls of Clay Bricks and Concrete Blocks: A State-Of-The-Art Review. International Journal of Masonry Research and Innovation, 1(1), 1. Https://Doi.Org/10.1504/Ijmri.2022.10049719

[96] Varshney, H. (2016). A Review Study on Different Properties of Hollow Concrete Blocks. 4(03), 2015–2017.

[97] Varzaneh, M. S., et al. (2020). Influence of A Window-Type Opening on The Shear Response of Partially-Grouted Masonry Shear Walls. Engineering Structures, 201(1), 109783. Https://Doi.Org/10.1016/J.Engstruct.2019.109783

[98] Venkatarama Reddy, B. V., and Uday Vyas, C. V. (2008). Influence of Shear Bond Strength on Compressive Strength and Stress-Strain Characteristics of Masonry. Materials and Structures/Materiaux Et Constructions, 41(10), 1697–1712. Https://Doi.Org/10.1617/S11527-008-9358-X

[99] Walker, D. (1996). The Effect of Freezing and Thawing on the Flexural Strength of Masonry. In American Society for Testing and Materials. Masonry: Esthetics, Engineering and Economy, ASTM STP 1246 Donald H. Taubert and Tim Conway, Eds.

[100] Wheeler, G. (2005). Interlocking Compressed Earth Blocks Volume II. Manual of Construction. Center for Vocational Building Technology, Thailand, II, 110.

[101] Yang, X., Wu, H., Zhang, J., and Wang, H. (2019). Shear Behavior of Hollow Concrete Block Masonry with Precast Concrete Anti-Shear Blocks. Advances in Materials Science and Engineering, 2019(Cm). Https://Doi.Org/10.1155/2019/9657617

[102] Zahra, T., Thamboo, J., and Asad, M. (2021). Compressive Strength and Deformation Characteristics of Concrete Block Masonry Made With Different Mortars, Blocks and Mortar Beddings Types. Journal of Building Engineering, 38(November 2020), 102213. Https://Doi.Org/10.1016/J.Jobe.2021.102213

PROFILES

KABIRU MUSA AYAGI is currently undergoing PhD in Concreting technology at School of Civil Engineering, Universiti Sains Malaysia(USM). He is the Principal Lecturer at Kano State Polytechnic, School of Technology, Department of Civil Engineering Technology, Nigeria. He previously served as Departmental Examination Officer and Head of the Department of Civil Engineering Technology. He also has experinceed in supervising National and High National Diploma students. He is fully enthisiastic in experimental and numerical analysis related to concrete hollow block wall panels.
Email address: ayagikabirumusa@gmail.com

BADORUL HISHAM BIN ABU BAKAR obtained his PhD from Leeds University, UK in the year 1998. He is currently a full Professor in the School of Engineering, Universiti Sains Malaysia. He has published more than 60 papers in international journals and currently interested in the behaviour of ultra-high strength concrete and the structural properties of rubberised concrete.
Email address: cebad@usm.my

TEH SABARIAH BINTI ABD MANAN is a Senior Lecturer and Research Fellow at The Institute of Tropical Biodiversity and Sustainability Development (IBTPL), Universiti Malaysia Terengganu (UMT). she was an academic fellow at the School of Civil Engineering (PPKA), Universiti Sains Malaysia (USM) from 2022 to 2023. She has experience as a postdoctoral researcher at the Civil Engineering Department, School of Engineering and Built Environment, Universiti Kebangsaan Malaysia (UKM) and IBTPL, UMT from 2019 to 2022. She received her PhD and MSc. from Universiti Teknologi Petronas (UTP) in 2018 and 2010. She has published 56 papers in indexed journals. Her research insterest is in environmental engineering and sustainable material for concrete technology.
Email address: tehsabariah@umt.edu.my

NOISE POLLUTION NEAR TO THE CONSTRUCTION SITE IN AN URBAN AREA (A CASE STUDY IN SHAH ALAM)

(Date received: 12.01.2023/Date accepted: 02.10.2023)

Suhaila Nasim[1], Janmaizatulriah Jani[2*]

[1] Chec Construction (M) Sdn Bhd, Kuala Lumpur, Malaysia

[2] School of Civil Engineering, College of Engineering, Universiti Teknologi MARA. 40450, Selangor, Malaysia

[*]Corresponding author: janmaizatulriah@uitm.edu.my

ABSTRACT

In the contemporary era of Malaysia's rapid modernisation, a multitude of construction and urbanisation projects are underway, particularly in urban areas. As Malaysia strives to achieve its modernisation goals and join the ranks of developed nations, it is imperative to prioritise and mitigate noise emissions stemming from these construction and urban development endeavors. Urban regions characterised by residential, commercial, educational zones, construction activities, and heavy traffic congestion often experience elevated noise levels. These multiple sources of noise have a detrimental impact on the health and well-being of the surrounding communities. The primary objectives of this study are to assess noise levels in areas near construction sites (specifically the Light Rail Transit (LRT) project), as well as away from construction sites, and to gauge the extent of noise disturbance experienced by the community. Additionally, the study seeks to measure the community's awareness of the effects of noise pollution. The chosen study areas encompassed the LRT-3 Shah Alam line construction site (coordinates: 3° 4'2.50 "N, 101°29'22.12 "E) and the non-construction site in Seksyen 9 (coordinates: 3°05'17.80" N, 101°31'24.42" E). Two methods were employed for data collection: first, the measurement of noise levels at the study areas using the Decibel X smartphone application, and second, the distribution of a questionnaire survey to the community residing near the construction site.

The questionnaire aimed to evaluate the impact of noise pollution and the community's acceptance of noise emissions from the construction site. The findings revealed that the Equivalent Continuous Sound Pressure Level (LAeq) at the LRT-3 Shah Alam line construction site exceeded the permissible equivalent noise level (65 dB (A), registering at 83.44 dB (A) during weekdays and 74.82 dB (A) during weekends. In contrast, at the non-construction site in Seksyen 9, the LAeq remained below the permissible limit, with values of 54.13 dB (A) during weekdays and 49.42 dB (A) during weekends. The questionnaire survey indicated that a majority of the community living near the LRT-3 construction site were significantly disturbed by the construction activities and the additional noise stemming from vehicular traffic, given the site's proximity to a university. Respondents reported suffering from various effects of noise pollution, including headaches, stress, insomnia, diminished focus, and increased stress levels. The community expressed a consensus that raising awareness about the impacts of noise pollution from construction and urbanisation areas is essential, and they called upon the government to play a pivotal role in regulating noise emissions.

Keywords: Community Awareness, Noise Level, Noise Pollution

1.0 INTRODUCTION

In the new era of development, the demand for modern vehicles, buildings, highways, and many more facilities has risen. Therefore, many development activities are being done worldwide including Malaysia. One of unexpected effect of development is pollutions. Noise is one of the types of pollution people have to deal when living in urban areas. The source of noise pollution in urbanise areas may come from vehicles and also from construction projects for new development areas. Noise emission from construction and urbanisation projects also trigger as one of the causes of noise pollution (Feng *et al*., 2020). The usage of bulldozers, trucks, piling machines, and other equipment in construction produces an elevated level of noise. As stated by the National Institute of Deafness and Other Communication Disorder, "long or repeated exposure to sound at or above 80 decibels can cause hearing loss" (Daniel, 2017). The human auditory system lies in the frequency range of 20Hz to 20 kHz (Gorai & Pal, 2006).

Noise pollution can cause direct or indirect results on physical health such as directly caused hearing impairment. For example, humans will experience abnormal loudness perception and tinnitus (Millar, 2020). The quality of sleep will also be affected when someone is exposed to noise pollution. They will have difficulty falling asleep or are inability to stay asleep. Each task in construction uses a different type of machinery. The sources of noise pollution are motorised vehicles, crowds, concerts, fireworks, etc. A construction project is also one of the

sources of noise pollution. Construction activities such as filling, cutting, site clearance and excavation produce a high level of noise because it is linked to the machinery used (Haron *et al*., 2012). Therefore, the noise production is different in accordance with equipment use. Since Malaysia is a developing country, there are a lot of construction projects in this country especially urban areas. Noise pollution level should be compared with the Guidelines for Environmental Noise Limits and Control (as shown in Table 1) to measure whether exceed permissible limit or not.

Table 1: Recommended Permissible Sound Level (LAeq) Receiving Land Use for Existing Built-up Areas (DOE, 2019)

Receiving Land Use Category	LAeq Day (7.00 am – 10.00 am)	LAeq Night (10.00 pm – 7.00 am)
Low Density Residential, Noise Sensitive Receptors, Institutional (School, Hospital, Worship)	60 dBA	55 dBA
Suburban and Urban Residential, Mixed Development	65 dBA	60 dBA
Commercial Business Zones	70 dBA	65 dBA
Industrial Zones	75 dBA	75 dBA

However, pollution must be controlled for the safety of human and ecosystem well-being. For this study, the project of Light Rail Transit 3 (Shah Alam – Klang) was chosen as study area because the project is located close to residential area, educational and commercial area. This study will measure whether noise emission from construction projects contributes a huge amount of noise to the environment or not. The objectives of this study are to evaluate the noise level for area near to the construction site and away from construction site and to measure awareness of the community on the effect of noise pollution.

2.0 METHODS

Essentially, two research methods were selected: 1. Utilising the Decibel X smartphone application to measure noise levels, and 2. Employing a questionnaire as a tool to gauge both the extent of noise disturbance experienced by the community and the community's awareness of the consequences of noise pollution.

2.1 Decibal X Application

The noise level in these two locations was measured by using Decibel X application on smartphone. This application was rated 3.9 stars by the users. It has day and night features where it is safe to use the application during nighttime or when the user wants to experience dark mode. The application is already calibrated, and the data collected will be save in the history. Decibel X offers frequency weighing filters such as A, B, C, ITU-R 468, and Z. Moreover, the application is also compliant with NIOSH and OSHA standards. The data collected for noise levels in both study areas, namely the LRT-3 construction site in Section 7 and the non-construction site in Section 9, Shah Alam were compared to the Guidelines for Environmental Noise Limits and Control. The selection of these study areas was based on their proximity to commercial, residential, and educational zones. The data sampling occurred during the months of March and April 2022, coinciding with ongoing piling works at LRT-3 construction site. Data collection for the LRT-3 project encompassed areas near both roadways and machinery zones. In contrast, data collection near the roadside was confined to Section 9, Shah Alam, Selangor.

It is crucial to acknowledge that this study may be subject to potential human error, primarily due to the need to measure the distance from the noise source to the collection point. For the evaluation of noise pollution levels and identifying contributing factors, three daily sessions were conducted on both weekdays and weekends in the selected study areas. Data samplings were consistently obtained from the same locations during each session. These sessions took place at specific times: from 7:30 a.m. to 8:30 a.m., coinciding with the morning rush as people commute to work and construction activities commence; from 11:30 a.m. to 12:00 p.m., during peak traffic hours; and from 4:00 p.m. to 4:30 p.m., as people return home from work. The Equivalent Continuous Sound Pressure Level (LAeq) in the study areas was calculated using the equation:

$$L_{Aeq} = 10log \sum_{(i=t)}^{(i=n)} (10)^{L_i/10} (t_i) \quad (1)$$

Where, n is the total number of samples take, L_i is the noise level in dB(A) of i^{th} sample and t_i is the fraction of total sample time.

2.2 Questionnaire Survey

A set of questionnaires was established to evaluate the awareness of community on the effect of noise pollution. Table 2 shows the summary of the questionnaire. The questionnaire consists of two sections which are A and B. The questionnaire was distributed to the community in the study area through both offline and online methods. Online distribution was primarily conducted through WhatsApp and social media.

Table 2: Summary of the Questionnaire for the Community

Section	Related Question
A	Section A consists of the respondent's background information which includes gender, age group and ethnicity.
B	Section B consists of the respondents' knowledge on the definition of noise pollution, its sources, whether the respondents are disturbed by the noise, and at what time usually they experience noise pollution. Therefore, the aim of this section is to create awareness of the sources of noise pollution. By conducting this survey, it strengthens the evidence of noise emission from construction projects can be harmful to humans and the environment. This section also consists of the respondent's perception towards the noise pollution issues particularly the noise emission produced from the construction site and urbanisation area.

2.3 Data Analysis Using SPSS

Statistical Package for the Social Sciences (SPSS 2019) version 26 was used for analysis of the questionnaires. Descriptive analysis was used to analyse the demographic of respondents in Section A, whereas reliability test or Cronbach's alpha was used to test the questions that contain Likert Scale in the questionnaire in Section B.

3.0 RESULTS

This section shows the analyses obtained from the recorded noise level and questionnaires survey. The noise reading from both study areas was compared to the Guideline for Environmental Noise Limit and Control and from questionnaires were analysed using SPPS software.

3.1 Noise Level

The noise level was measured during weekdays and weekend at LRT-3 construction site at Seksyen 7 and non-construction site at Seksyen 9 is located at Sekolah Menengah Kebangsaan Seksyen 9. Table 3 shows the comparison between L_{Aeq} at the study areas and permissible L_{Aeq} by Department of Environment.

Table 3: Comparison between L_{aeq} at the Study Areas and Permissible L_{aeq} by Department of Environment

Suburban and Urban Residential Mixed Development, L_{Aeq} 65 dB (A)	Seksyen 7		Seksyen 9	
	Weekday	Weekend	Weekday	Weekend
	83.44 dB (A)	74.82 dB (A)	54.13 dB (A)	49.42 dB (A)

The Department of Environment sets the allowable LAeq (Equivalent Continuous Sound Pressure Level) for suburban and urban residential mixed development at 65 dB (A). Any noise exceeding this permissible equivalent noise level is deemed detrimental to nearby communities, as it can harm the human auditory system, elevate blood pressure, and disrupt sleep patterns. The data in Table 3 shows that at the LRT-3 Shah Alam line construction site, the LAeq exceeds the acceptable equivalent noise level, reaching 83.44 dB (A) on weekdays and 74.82 dB (A). This clearly indicates that the primary contributors to noise pollution in the study area are heavy traffic (Mohd Isa *et al.*, 2018) and construction activities, as noted by Kantová in 2017. In contrast, the study conducted at the non-construction site in Section 9 recorded LAeq values below the permissible limit, measuring at 54.13 dB (A) during weekdays and 49.42 dB (A) during weekends. Therefore, the measurements indisputably highlight that construction activities are a significant source of noise pollution in the study area.

3.2 Sources of Noise Pollution and Awareness of the Community on the Effect of Noise Pollution

A total of 172 individuals, comprising local community members such as UiTM and UNISEL students, workers from commercial areas and residents living near the LRT-3 construction site, participated in the questionnaire survey. Based on SPSS analysis, the highest frequency of respondents responded to the questionnaire were female at 51.7% more than male respondents. Highest age of the respondents was between 20–30 years old (64%). The mode of race of respondents was Malay, 79.7% compared to China and India, which are 12.2% and 5.8% respectively. Section 7 is situated near to the educational, commercial as well as residential areas. Based on the questionnaires analysis as shown in Figure 1(a), 133 respondents have chosen noise pollution is coming from vehicles. Based on Figure 1(b), 55% of respondents agreed noise from LRT-3 construction is definitely disturbing the community. As been mentioned by Geetha & Ambika, (2015) noises from construction sites are from diesel power generators, cutting and wielding procedures, heavy machinery, material transit, and equipment condition. Based on the reliability test (Cronbach's alpha), the value of Cronbach's Alpha is 0.657, indicating that the survey data is acceptable and reliable.

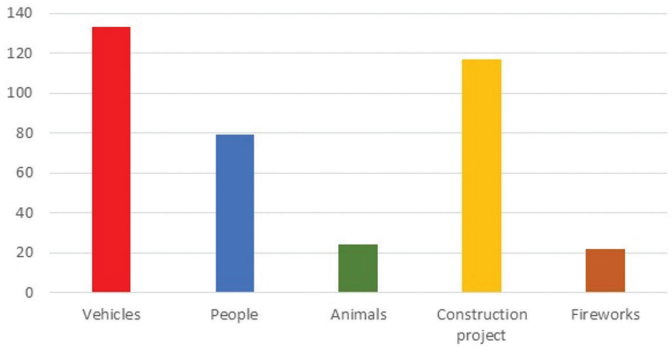

Figure 1(a): Major Sources of Noise Pollution in Seksyen 7, Shah Alam

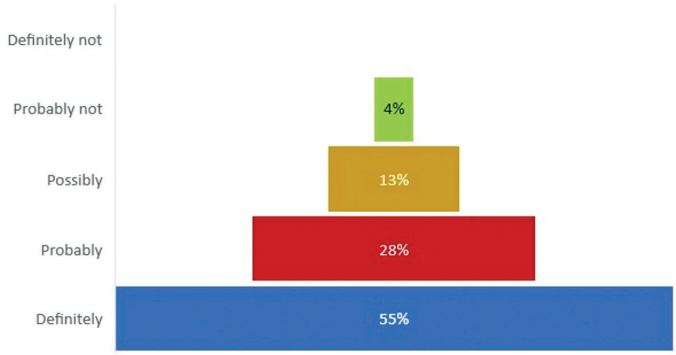

Figure 1(b): Noise Disturbance from LRT-3 Construction Site

Based on Figure 1(b), 55% of respondents agreed noise from LRT-3 construction is definitely disturbing the community. Section 7 is known as a commercial area as well as residential area where the shophouse is rented by most of the students from UiTM (Universiti Teknologi MARA) Shah Alam and other universities. 28% of respondents agreed that noise from LRT-3 construction is probably disturbing, while 13% agreed that noise is possibly disturbing the community. However, only 4% of the respondents agreed that noise from LRT-3 construction is probably not disturbing to the community because the respondents are not live nearby to the active construction site.

Table 4 shows 109 respondents out of 172 respondents were from age range 20-30 years old. 68 respondents from age range 20-30 years old agreed that noise pollution have caused headache and 74 respondents cannot focus on what they are doing due to

the loud noise. On the other hand, 4 respondents from age range 20-30 years old claimed there is no disturbance even when they are facing the noise pollution. 9 out of 109 respondents from this age range suffered from hypertension even they are still young. The risk of developing hypertension in younger adults is enhanced by the rising incidence of classis risk factors in the young such as obesity, diabetes mellitus and renal illness (Mammoser, 2017). For respondents at age range between 31-40 years old, 5 out of 34 respondents claimed that they suffered from insomnia due to the loud noise occurs near to their residential area. Most of the respondents agreed that they feel stressed and suffered from headache whenever noise pollution occur. For the age range 51-60 years old, 4 out of 5 respondents agreed that they suffered from hypertension. It shows that the older the age, the more they can resist with the noise pollution.

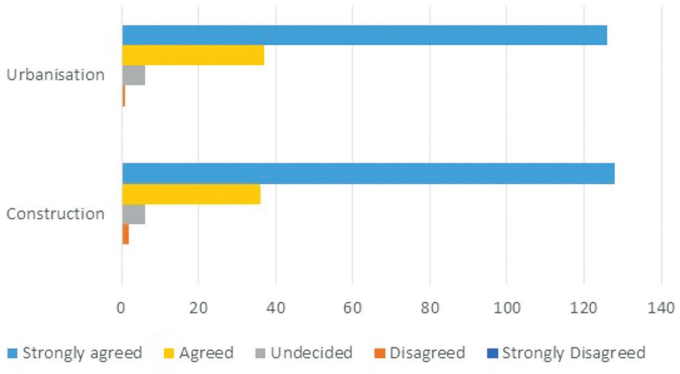

Figure 2: Respondent's Awareness on the Impact of Noise Pollution in Construction Sites and Urbanisation Area

As shown in Figure 2, most of the respondents strongly agreed that Malaysia government should improve the awareness among community on the impact of noise pollution from construction and urbanisation area to their life. The construction site located near to the commercial, residential and educational areas should have a noise control plan such as installation of a noise barrier in order to preserve the health condition of the community, especially in the urban area.

4.0 CONCLUSIONS

The results of this study clearly demonstrate that the LAeq (Equivalent Continuous Sound Pressure Level) exceeds permissible Environmental Noise Limits and Control standards at the construction site area compared to non-construction sites, both on weekends and weekdays. The primary sources contributing to noise pollution in the study area are heavy traffic and construction activities. The findings from the questionnaire survey also indicate that a majority of respondents attribute the main source of noise to vehicles and construction activities. It can be inferred that the community has experienced various adverse effects of noise pollution, including headaches, stress, insomnia, and hypertension. Additionally, the community expressed agreement that the Malaysian construction industry should take measures to reduce noise emissions stemming from their construction and urbanisation activities. Reducing noise emissions is expected to enhance the quality of life for the community. Furthermore, the government is encouraged to enforce legal actions against construction projects that fail to implement noise control measures, such as noise barriers at their construction sites.

Table 4: The Age of Respondent Vs the Effect of Noise Pollution

			Age and effect Crosstabulation The effect of noise pollution						Total
			No Disturbance	Headache	Stress	Insomnia	Hypertension	Cannot focus	
Age (years old)	20-30	Count	4	68	65	21	9	74	109
	31-40	Count	2	26	29	5	9	14	34
	41-50	Count	1	20	19	5	9	10	23
	51-60	Count	0	4	3	2	4	2	5
	61 and above	Count	0	0	0	1	1	1	1
Total		Count	7	118	116	34	32	101	172
Percentages and totals are based on respondents									
a. Dichotomy group tabulated at value 1.									

5.0 ACKNOWLEDGEMENTS

Authors wishing to acknowledge School of Civil Engineering, College of Engineering, Universiti Teknologi MARA for the support. The authors also gratefully acknowledge the respondents and community of Seksyen 7, Shah Alam for the remarkable supports throughout this research. ■

REFERENCES

[1] Daniel, J. F. (2017) What Is a Safe Noise Level for the Public? Am J Public Health. 107(1): 44–45.

[2] Department of Environment DOE (2019). Guidelines for Environmental Noise Limit and Control. Third Edition. ISBN 978-967-9795-38-7

[3] Feng, C. Y., Md Noh, N. I., and Al Mansob, R. (2020). Study on the Factors and Effects of Noise Pollution at Construction Site in Klang Valley. Journal of Advanced Research in Applied Sciences And Engineering Technology, Volume 20, Issue 1 (2020) 18-26.

[4] Geetha, M., and Ambika, D. (2015). Study on Impact of Noise Pollution at Construction Job Site. International Journal of Latest Trends in Engineering and Technology (IJLTET), 5(1), 46–49.

[5] Gorai, A. K., and Pal, A. K. (2006). Noise and Its Effect on Human Being - A Review. Journal of Environmental Science and Engineering, 48(4), 253–260.

[6] Haron, Z., Noh, H. M., Yahya, K., and Majid, Z. A. (2012). Assessing Noise Emission Levels from Earthwork Construction Equipment. Malaysian Journal of Civil Engineering (MJCE), 24(1), 13–28. Https://Doi.Org/10.11113/Mjce.V24n1.272

[7] Kantová, R. (2017). Construction Machines as a Source of Construction Noise. Procedia Engineering, 190, 92–99. Https://Doi.Org/10.1016/J.Proeng.2017.05.312

[8] Mammoser, G. (2017, June 8). High Blood Pressure in Young Adults, Teens. Healthline. Retrieved June 15, 2022, From Https://Www.Healthline.Com/Healthnews/High-Blood-Pressure-Ignore

[9] Millar, H. (2020). December 21. Noise Pollution Health Effects: Impact on Mental and Physical Health. Medical News Today. Retrieved January 7, 2022, From Https://Www.Medicalnewstoday.Com/Articles/Noise-Pollution-Health-Effects

[10] Mohd Isa, I. I. M., Zaki, Z. Z. M., and Kassim, J. (2018). Traffic Noise Pollution at Residential Area. International Journal of Engineering and Technology (UAE), 7(3), 250–253. Https://Doi.Org/10.14419/Ijet.V7i3.11.1601

PROFILES

SUHAILA BINTI NASIM, a dedicated 25-year-old civil engineer, achieved academic excellence by graduating with honors in Civil Engineering from UiTM Shah Alam in September 2022. She has demonstrated her commitment and expertise during her employment at CHEC Construction (M) Sdn Bhd, where she has been actively engaged for over a year. Suhaila's profound interest lies in conducting research related to Water Resources and Environmental Systems, with a current emphasis on exploring greenhouse gas emissions and air temperature dynamics in the context of global warming. Her unwavering dedication is driven by a strong belief in fostering a sustainable future.
Email address: suhailansim@gmail.com

TS DR JANMAIZATULRIAH JANI, a distinguished senior lecturer hailing from the School of Civil Engineering, College of Engineering, Universiti Teknologi MARA. She has been contributing to the field of education since December 1999. Her academic journey includes a master's thesis focused on rainfall modelling and a doctoral thesis centered on GIS-based groundwater modelling. Her research pursuits encompass a diverse range of interests, including flood and erosion modelling, the utilisation of GIS in groundwater and hydrological modelling, as well as investigations into environmental assessment and monitoring.
Email address: janmaizatulriah@uitm.edu.my

COMPARISON OF ARTIFICIAL INTELLIGENCE (AI) BASED MODELS FOR SEDIMENT TRANSPORT PREDICTION USING SWOT AND STATISTICAL ANALYSES

(Date received: 15.08.2023/Date accepted: 12.10.2023)

Chin Ren Jie[1*], Lee Foo Wei[2], Kwong Kok Zee[3], Lai Sai Hin[4]

[1,2,3] Department of Civil Engineering, Lee Kong Chian Faculty of Engineering and Science, Universiti Tunku Abdul Rahman, 43000 Kajang, Malaysia

[4]Department of Civil Engineering, Faculty of Engineering, Universiti Malaysia Sarawak, 94300 Kota Samarahan, Sarawak, Malaysia

[*]Corresponding author: chinrj@utar.edu.my

ABSTRACT

The dynamics involved in sediment scour are complicated. Hence, it is a challenging task to create a general empirical optimisation algorithm for reliable sediment load estimation. This study aims to analyse the architectures of assorted artificial intelligence (AI) based model to predict suspended sediment load in fluvial system. An in-depth study on Artificial Neural Network (ANN), Adaptive NeuroFuzzy Inference System (ANFIS), and Support Vector Machine (SVM) was carried out. The goal of this study is to evaluate the performance of AI-based models from various research using statistical as well as Strengths, Weaknesses, Opportunities, and Threats (SWOT) analyses. Three statistical measures of model prediction accuracy including coefficient of correlation (R), root mean square error (RMSE), and mean absolute error (MAE) were used. The results revealed that the SVM and ANFIS models outperformed the other soft computing and conventional models. It is concluded that the SVM and ANFIS models are preferred and may be successfully used to estimate the suspended sediment concentration for the research area.

Keywords: Artificial Intelligence, Sediment Transport, Statistical Analyses, SWOT

1.0 INTRODUCTION

Sediment is usually defined as tiny particulate in the form of fine silt and clay in nature. Sediment can exist as soil-based, mineral substance, decomposing organic substances, and inorganic biogenic matter in the aquatic environment. Sediment transport is the movement of particles along with the flow of water (Pu *et al*., 2021; Samantaray & Ghose, 2019).

Sediment transport is a complex issue in nature as the sediments travel unpredictable stream wise corresponding to the associated fluid forces. There is no fixed rule or rule of thumb in the sediment transport prediction. Approximate all current sediment transport formulae are based on the premise that sediment transport can be completely represented by stream wise parameters such as velocity or boundary shear stress, while the parameters representing vertical motion of flow such as water depth (pressure) variance over time and space, vertical velocity, as well as seepage are not involved (Vittori *et al*., 2020; Yang *et al*., 2009). In the previous research, it was found that the aforementioned parameters could affect the sediment's flow behaviour in terms of mobility and stability. The analysis showed the speed of the flow can provoke upward flow or vice versa, which may cause the erosion. In general, the combination of joint driving forces and resistance forces are the factors to drive sediment transport (Pektas & Dogan, 2015; Yuan *et al*., 2021).

Since the introduction of AI approaches in hydro-climatology, there has been a significant increase in research effort in the areas of modelling, analysing, forecasting, and prediction of water quantity and quality (Cui *et al*., 2021; Khozani *et al*., 2020; Mohammadi *et al*., 2021; Nourani *et al*., 2014). There are plenty of models related to the sediment transport prediction, however the study comparing the performance of different models is still limited. Therefore, this study aims to investigate the performance of the AI-based models for sediment transport prediction using statistical and Strengths, Weaknesses, Opportunities, and Threats (SWOT) analysis.

2.0 MATERIALS AND METHODS

2.1 Information Collection and Preparation

A comprehensive review study on the application of the AI-based models in sediment transport was conducted to obtain more information on the architecture framework of different AI-based models, as well as their performance. After extracting all the relevant information from the published journal articles, the SWOT and statistical analyses were performed.

For this stage, the systematic review strategy was implemented. The procedure started with framing questions for

a review, followed by identifying the relevant work. The main research question for this study is "what are the available AI-based models in sediment transport prediction and their respective performance". Hence, the keywords for information searching were narrowed down to "AI-based models in hydrological application", "sediment transport prediction model", "SWOT analysis in prediction model", etc. After having the keywords, the relevant studies were searched, identified and reviewed. Nevertheless, only the studies matching with certain criteria was selected for further analysis, i.e. it matches with the minimum acceptable level of prediction accuracy, it is specifically for the sediment transport prediction study, etc. The last step in this stage is the findings interpretation using the SWOT and statistical analyses (Huai *et al*., 2021; Wallwork *et al*., 2022).

2.2 SWOT Analysis

SWOT analysis is a kind of assessment to examine the performance of the AI-based model in this study. A SWOT analysis is a tool that is widely used to aid in the identification of strategic strategies for an entity or activity. It is recommended for this study because it provides valuable knowledge about the potential feasibility of the method under consideration. SWOT analysis is very useful at the model's front end for assessing environmental factors in performance analyses and gauging the level of expertise, talents, attitudes, abilities, and environmental support in cause analyses (Stolovitch & Keeps, 2006). SWOT analysis contains internal environment and external factor. The internal environment decides a system's strengths and weaknesses, while external factors dictate opportunities and threats. Figure 1 shows the overview of the SWOT analysis.

Strength can be defined as any accessible resource that can be used to boost the efficiency of overall performance (Panigrahi & Mohanty, 2012). Strength can be classified as an internal factor like the structural component of an AI-based model including the parameters and algorithms. Strength defines the resources and capabilities of system, which can provoke the further development (Panigrahi & Mohanty, 2012). The strength of the AI- based model is also based on the presence of regulatory authorities to ensure that the law is followed throughout the related field.

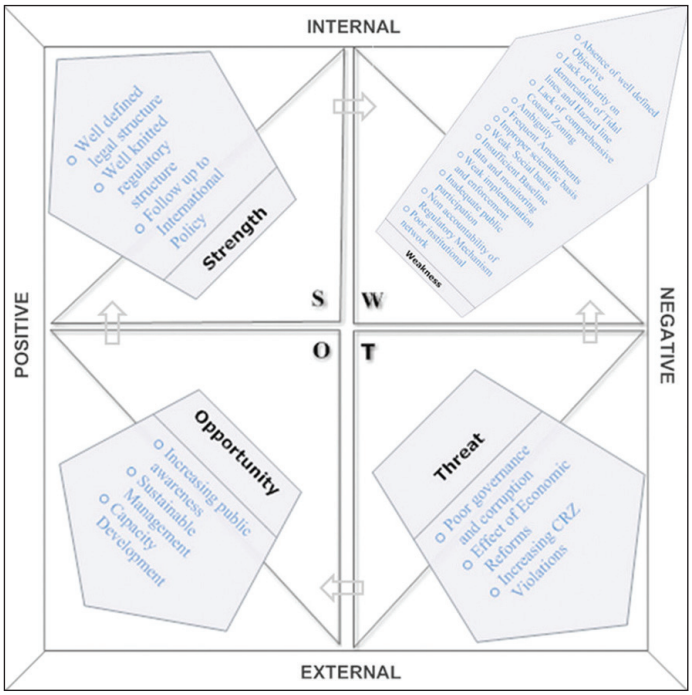

Figure 1: SWOT Analyses Chart (Panigrahi & Mohanty, 2012)

Weaknesses are defects or deficiencies in any structure that can result in a loss of competitive advantage, productivity, or financial capital (Panigrahi & Mohanty, 2012). Therefore, the approaches aiming for improvement should be proposed to minimise the effect of the weakness. This can be achieved by reviewing more journal articles with critical observation.

The relationship between calculated parameters and algorithm stems from the model's strengths and limitations in the field of sediment transport prediction, which may present opportunities and threats. Opportunities are a confluence of various conditions at a given time that have a favorable outcome (Stolovitch & Keeps, 2006). It is external factors that contribute to the development and brings a good impact to the overall system. Some parties may take benefits at a certain time and situation but cannot be "made" on-demand. Identification of opportunity is worth for the improvement on the model performance.

Threats are described as something that could harm your business, venture, or product (Stolovitch & Keeps, 2006). The threats are detrimental and similar to opportunities because there is no way to prevent or control them from occurring. However, an appropriate analysis could handle and interact with them with ease. Unpredictable threats may affect the performance of the AI-based model and show important effects when anticipation is prepared.

2.3 Statistical Analysis

On the other hand, the model evaluation is an essential step to test the accuracy or reliability of a model in performing the prediction. In this study, three statistical indicators were chosen for the analyses purposes and comparison, which are correlation coefficient (R), root mean square error (RMSE), and mean absolute error (MAE). The equations for R, RMSE, and MAE are as shown:

$$R = \frac{n\sum xy - \sum x_i \sum y_i}{\sqrt{n\sum x_i^2 - (\sum x_i)^2}\sqrt{n\sum y_i^2 - (\sum y_i)^2}} \quad (1)$$

$$RMSE = \sqrt{\frac{1}{n}\sum (y_i - x_i)^2} \quad (2)$$

$$MAE = \frac{\sum |y_i - x_i|}{n} \quad (3)$$

where n is the number of data pairs, x is the observed variable, y is the predicted variable.

3.0 RESULTS AND DISCUSSION

3.1 Statistical Analyses

Table 1 displayed the statistical performance of the 5 selected models related to sediment transport. The effectiveness of the studied AI-based models is investigated statistically by evaluating and comparing selected statistical parameters, which are R, RMSE and MAE. These statistical parameters were chosen because they are widely utilised to analyse the errors associated

in model as goodness of fit between the measured and estimated values. R is a statistical term used to measure the strength in anticipated values that follow the correct trends in the past. In short, it is a measurement of predicted values matching with the observed data from a forecast model. Meanwhile, RMSE can determine the sample variance of errors independently. The model performs better with a smaller RMSE. MAE shows the average of the individual prediction errors. Basically, the greater value of R that is closer to 1 represents better performance of the model. In contrary, a smaller RMSE and MAE indicates a better model performance.

In general, all the models have R value greater than 0.90. SVM-RBF model has highest R value of 0.994 among the others. It is then followed by the ANFIS models with values of 0.9879 (ANFIS-PSO) and 0.9824 (ANFIS-BLM) respectively. In terms of RMSE, it is ranged between 0.0010 to 0.26, where the smallest value is recorded by SVM-RBF model. A similar trend can be observed from the perspective of MAE, where the smallest number of 0.0010 is exhibited by the SVM-RBF model.

3.2 SWOT Analysis

Support vector machine (SVM), adaptive-neuro fuzzy inference system (ANFIS) and artificial neural network (ANN) are the three basic models in sediment transport. Their strength, weakness, opportunity and threat are presented in Table 2.

3.3 Summary

In short, SVM is attractive as it features a optimization parameter to address the issue of computational burden that is typical in ANN and ANFIS modelling. Second, SVM is characterised by a quadratic optimisation method that employs effective ways to avoid the difficulty of having local minima. SVM gives good out-of-sample generalisation when a suitable Gaussian kernel is used. This implies that by selecting proper generalisation evaluation values, SVM is stable even the sample data was bias during the training phase. Meanwhile, ANFIS was proved to adequately manage the inconsistencies and ambiguity of sediment concentration properly. As a conclusion, SVM and ANFIS models has outperformed the ANN model based on the statistical and SWOT analyses.

4.0 CONCLUSION

An assessment of several AI-based models in sediment transport prediction, especially suspended material, was undertaken in this study. AI-based models have yielded promising results in estimating the phenomenon of sediment transport in rivers. According to the statistical analyses and SWOT analyses, SVM and ANFIS performed better than the ANN.

There are some recommendations for future works. Data pre-processing is an important step before estimation model can established after collecting the discharge data. The goal of pre-processing is to eliminate undesired variation. It was noted that the discharge is very important parameter to observe the sediment transport properties. The dynamic behaviour of sediment discharge changes with the flowing velocity, it is advisable to build one more extra model based on discharge parameters. Prediction accuracy will be improved if the categorized data values are closed to another. Furthermore, employment of evolutionary algorithms is better to have good global minima and maxima prediction.

Table 1: Performance Assessment of Different AI Models in Sediment Transport

Models	Sources	R	RMSE	MAE
Adaptive Neuro-Fuzzy Inference System with Backpropagation and Levenberg- Marquardt (ANFIS-BLM)	Bui, *et al.* 2017	0.9824	0.0056	0.0037
Adaptive Neuro-Fuzzy Inference System with Particle Swarm Optimisation (ANFIS-PSO)	Qasem *et al.,* 2017	0.9879	0.2600	0.0570
Artificial Neural Network with Genetic Algorithm and Multi-Objective Optimisation (ANN-GA-MOO)	Yadav *et al.,* 2021	0.9650	0.0090	0.0050
Support Vector Machine with Radial Basis Function (SVM-RBF)	Bababali and Dehghani, 2020	0.9940	0.0010	0.0010
Support Vector Machine with Genetic Algorithm (SVM-GA)	Yadav *et al.,* 2018	0.9813	0.0027	0.0125

Table 2: SWOT Analysis for Conventional AI Model in Sediment Transport Studies

AI Models	SWOT Analysis			
	Strength	**Weakness**	**Opportunity**	**Threat**
SVM	• Effectively solve regression analysis (Samantaray, 2019) • Allow the use of non-linear function in the input space through kernel function (Khozani, 2020)	• Heavily dependent on the correct parameters selection (Yadav, 2018; Yadav, 2021) • Adopt trial and error method to select kernel functions and hyperparameters (Nourani, 2014)	• Require proper and multiple combination of input variables to generate strong correlation between input and output data (Khozani, 2020) • Have a good estimation on maximum value while integrating with gene expression programming (Samantaray, 2019) • Show a good ability to predict minimum and middle values while implementing it with radial basis function (Khozani, 2020)	• Consume more time during testing phase due to complicated combined models (Pektas, 2015)
ANFIS	• Employ neural network to tune membership function automatically (Bui, 2017; Qasem, 2017) • Enhance non-linearity between input and output hydrological parameters through the fuzzy logic concept with neural network training algorithms (Cui, 2021)	• Inconsistent during convergence process (Cui, 2021) • Require configurable parameters to achieve trial and error method (Yadav, 2018; Yadav, 2021) • Hard to employ optimisation methods (Cui, 2021) • Require large amount of data to increase prediction accuracy (Qasem, 2017)	• Apply different training algorithms (Yadav, 2018; Yadav, 2021) • Has high tolerance against data sample errors (Bui, 2017)	• Yield a black-box representation through the network training (Qasem, 2017; (Yadav, 2018; Yadav, 2021)
ANN	• Achieve 90% of prediction accuracy (Yang, 2009) • Synthesise machine learning techniques using modelling approach (Qasem, 2017) • Not necessary to have relevant mathematical expression (Nourani, 2014)	• Implement trial-and-error method to alter the weights (Yang, 2009) • Require a vast amount of data during training process (Qasem, 2017)	• Employ antecedent discharge data (Mohammadi, 2021) • Observe the peak value using daily scale (Qasem, 2017)	• Sensitive to the initial weight values (Yang, 2009) • Occasionally stuck by local error minima to reach global minimum (Nourani, 2014)

5.0 ACKNOWLEDGMENT

This research was supported by the KURITA Overseas Research Grant 2022 (8128/0002), and Universiti Tunku Abdul Rahman Research Fund (IPSR/RMC/UTARRF/2022-C2/C04). ■

REFERENCES

[1] Bababali, H., and Dehghani, R. (2020). Comparison and Evaluation of Support Vector Machine and Gene Programming in River Suspended Sediment Estimation (Case Study: Kashkan River). International Journal of Horticulture, Agriculture and Food Science (IJHAF), 4 (2), 53-61. https://dx.doi.org/10.22161/ijhaf.4.2.5.

[2] Bui, M. D., Kaveh, K., and Rutschmann, P. (2017). Performance Analysis of Different Model Architectures Utilized in an Adaptive Neuro Fuzzy Inference System for Contraction Scour Prediction. IOSR Journal of Mechanical and Civil Engineering (IOSR-JMCE), 14(3), 18-32. https://doi.org/10.9790/1684-1403051832.

[3] Cui, X., Yang, F., Wang, X., Ai, B., Luo, Y., and Ma, D. (2021). Deep Learning Model for Seabed Sediment Classification Based on Fuzzy Ranking Feature Optimization. Marine Geology, 432, 106390. https://doi.org/10.1016/j.margeo.2020.106390.

[4] Huai, W., Li, S., Katul, G. G., Liu, M., and Yang, Z. (2021). Flow Dynamics and Sediment Transport in Vegetated Rivers: A Review. Journal of Hydrodynamics, 33, 400-420. https://doi.org/10.1007/s42241-021-0043-7.

[5] Khozani, Z. S., Safari, M. J. S., Mehr, A. D., and Mohtar, W. H. M. W. (2020). An Ensemble Genetic Programming Approach to Develop Incipient Sediment Motion Models in Rectangular Channels. Journal of Hydrology, 584, 124753. https://doi.org/10.1016/j.jhydrol.2020.124753.

[6] Mohammadi, B., Guan, Y., Moazenzadeh, R., and Safari, M. J. S. (2021). Implementation of Hybrid Particle Swarm Optimization-Differential Evolution Algorithms Coupled with Multi-Layer Perceptron for Suspended Sediment Load Estimation. Catena, 198, 105024. https://doi.org/10.1016/j.catena.2020.105024.

[7] Nourani, V., Baghanam, A. H., Adamowski, J., and Kisi, O. (2014). Applications of Hybrid Wavelet–Artificial Intelligence Models in Hydrology: A Review. Journal of Hydrology, 514, 358-377. https://doi.org/10.1016/j.jhydrol.2014.03.057.

[8] Panigrahi, J. K., and Mohanty, P. K. (2012). Effectiveness of the Indian Coastal Regulation Zones Provisions for Coastal Zone Management and Its Evaluation Using SWOT Analysis. Ocean & Coastal Management, 65, 34-50. https://doi.org/10.1016/j.ocecoaman.2012.04.023.

[9] Pektas, A. O., and Dogan, E. (2015). Prediction of Bed Load via Suspended Sediment Load Using Soft Computing Methods. Geofizika, 32(1), 27-46. https://doi.org/10.15233/gfz.2015.32.2.

[10] Pu, J. H., Wallwork, J. I., Khan, Md. A., Pandey, M., Pourshahbaz, H., Satyanaga, A., Hanmaiahgari, P. R., and Gough, T. (2021). Flood Suspended Sediment Transport: Combined Modelling from Dilute to Hyper-Concentrated Flow. Water, 13(3), 379. https://doi.org/10.3390/w13030379.

[11] Qasem, S. N., Ebtehaj, I., and Riahi Madavar, H. (2017). Optimizing ANFIS for Sediment Transport in Open Channels using Different Evolutionary Algorithms. Journal of Applied Research in Water and Wastewater, 4(1), 290-298. https://doi.org/10.22126/arww.2017.773.

[12] Samantaray, S., and Ghose, D. K. (2019). Sediment Assessment for A Watershed in Arid Region via Neural Networks. Sadhana, 44(10), 1-11. https://doi.org/10.1007/s12046-019-1199-5.

[13] Stolovitch, H. D., and Keeps, E. J. (2006). Handbook of Human Performance Technology: Principles, Practices, and Potential. John Wiley & Sons Hoboken, New Jersey, United States.

[14] Vittori, G., Blondeaux, P., Mazzuoli, M., Simeonov, J., and Calantoni, J. (2020). Sediment Transport Under Oscillatory Flows. International Journal of Multiphase Flow, 133, 103454. https://doi.org/10.1016/j.ijmultiphaseflow.2020.103454.

[15] Wallwork, J. T., Pu, J. H., Kundu, S., Hanmaiahgari, P. R., Pandey, M., Satyanaga, A., Khan, Md. A., and Wood, A. (2022). Fluids, 7(1), 23. https://doi.org/10.3390/fluids7010023.

[16] Yadav, A., Chatterjee, S., and Equeenuddin, S. M. (2018). Suspended Sediment Yield Estimation Using Genetic Algorithm-Based Artificial Intelligence Models: Case Study of Mahanadi River, India. Hydrological Sciences Journal, 63(8), 1162-1182. https://doi.org/10.1080/02626667.2018.1483581.

[17] Yadav, A., Chatterjee, S., and Equeenuddin, S. M. (2021). Suspended Sediment Yield Modeling in Mahanadi River, India by Multi-Objective Optimization Hybridizing Artificial Intelligence Algorithms. International Journal of Sediment Research, 36(1), 76-91. https://doi.org/10.1016/j.ijsrc.2020.03.018.

[18] Yang, C. T., Marsooli, R., and Aalami, M. T. (2009). Evaluation of Total Load Sediment Transport Formulas Using ANN. International Journal of Sediment Research, 24(3), 274-286. https://doi.org/10.1016/S1001-6279(10)60003-0.

[19] Yuan, S., Tang, H., Li, K., Xu, L., Xiao, Y., Gualtieri, C., Rennie, C., and Melville, B. (2021). Hydrodynamics, Sediment Transport and Morphological Features at the Confluence Between the Yangtze River and the Poyang Lake. Water Resources Research, 57(3), e2020WR028284. https://doi.org/10.1029/2020WR028284.

PROFILES

TS. DR CHIN REN JIE received his BEng and Ph.D. degrees in Environmental Engineering from University of Malaya, Malaysia, in 2015 and 2019, respectively. He is currently an assistant professor in the Department of Civil Engineering, Lee Kong Chian Faculty of Engineering and Science, Universiti Tunku Abdul Rahman, Malaysia. He is a registered Professional Technologist (Malaysia Board of Technologists). He has been the leader or been part of the team for about several national and international research projects. His research direction focused on flood, drought, and water resources management in the context of climate change, which involved computational simulation, development of decision support system, artificial intelligent, and optimisation models. He has published a total number of 24 research papers in reputed ISI journals and conference proceedings.
Email address: chinrj@utar.edu.my

TS. DR LEE FOO WEI received his BEng. (Civil) and MSc. (Construction Management) from Universiti Teknologi Malaysia in year 2008 and 2009 respectively. In year 2017, he received his Ph.D. (Structural and Materials) from University of Malaya. He is currently an assistant professor in the Department of Civil Engineering, Lee Kong Chian Faculty of Engineering and Science, Universiti Tunku Abdul Rahman, Malaysia. He is a registered Professional Technologist (Malaysia Board of Technologists). He has been the leader or been part of the team for about several national and international research projects. His research direction focused on structural engineering (NDT structural assessment and health monitoring), concrete technology (high performance concrete, sustainable green construction and crumb rubberised concrete) and soil stabilising agent. He has published a total number of 27 research papers in reputed ISI journals and conference proceedings.
Email address: leefw@utar.edu.my

Ir. DR KWONG KOK ZEE received his BEng. (Civil and Construction Engineering) from Curtin University of Technology, Malaysia. He received his Ph.D. (Civil Engineering) from Universiti Malaysia Sabah. He is currently an assistant professor in the Department of Civil Engineering, Lee Kong Chian Faculty of Engineering and Science, Universiti Tunku Abdul Rahman, Malaysia. He is a registered Professional Engineer (PEng, Malaysia). He has been the leader or been part of the team for about several national and international research projects. His research direction focused on structural engineering (NDT structural assessment and health monitoring as well as piezoelectric smart material). He has published a total number of 16 research papers in reputed ISI journals and conference proceedings.
Email address: kwongkz@utar.edu.my

ASSOC. PROF. DR LAI SAI HIN is currently with the Department of Civil Engineering, Faculty of Engineering (No 38 in QS World Ranking – Faculty of Engineering), University of Malaya (No 59 in QS World Ranking - University). He is a registered Professional Engineer (PEng, Malaysia), and Chartered Engineer (CEng, UK). He serves as a Fellow of Asean Academy of Engineering; Technology (FAAET) and Institution of Engineering and Technology (FIET). He has been the leader or been part of the team for about 40 national and international research projects. His research is focused on flood, drought, and water resources management in the context of climate change, which involved computational simulation, development of decision support system, artificial intelligent, and optimisation models. He has published more than 80 research papers in reputed SCI journals.
Email address: shlai@unimas.my

MANUSCRIPT PREPARATION GUIDELINES FOR IEM JOURNAL AUTHORS

The aim of publishing the Journal of the Institution of Engineers Malaysia (or IEM Journal) is to promote the advancement of science, engineering, and technology; disseminate new and current knowledge; share novel findings among practising engineers, researchers and other interested colleagues. Hence, the IEM Journal covers a wide range of practical and diversified engineering disciplines, including publishing papers on any subjects relevant to the engineering and technology of today. As in other journals, all paper submissions to the IEM journal will be peer-reviewed by professionals.

Submission of a contribution is taken to manifest the fact that the submission has not been submitted, accepted, published, or copyrighted elsewhere. To avoid publication delays, please send all manuscripts to the Editor (via the Online Journal Submission) and observe the following guidelines. Each paper is independently peer-reviewed.

Types of Papers

IEM Journal will accept any submissions that fall within the three types of papers shown below:

- **Research Paper**

Significant research and development or applications in any field of engineering and/or technology. Submissions should be about 8-14 pages.

- **Review Paper**

Articles which summarises the state-of-the-art of a specific area of research. Submissions should be about 10-20 pages.

- **Brief Paper**

A concise description of new technical concepts or applications within the scope of the journal. Submission should be about 4 pages

Together with the paper submission, at least four (4) reviewers complete with their contact details (official postal and email address, and telephone number) are to be proposed by authors. Reviewers should be the experts in their research areas.

Plagiarism Policy

IEM Journal strictly prohibits any form of Plagiarism.

If the manuscript has been presented, published, or submitted for publication elsewhere, please inform the Editor. Our primary objective is to publish technical materials not available elsewhere.

Format and Elements of Submitted Texts

a) Initial Submission

For initial submission and reviewing, ALL papers are accepted regardless of the formatting used.

b) Final Submission

Upon final submission of paper, authors are required to follow the manuscript instruction guidelines and paper template as presented below.

Please prepare your main text document in Microsoft Word and PDF format, text should be single line spaced, line numbered and pages should be numbered. You can download the paper template here.

Please note that the style that you submit your paper in (e.g. any additional italics or bold fonts, bullet points, etc.) may be changed on publication to accommodate our publication style.

Manuscript Style

Language:

- The language of the IEM Journal is in English. However, a paper in Bahasa Melayu is also accepted. For accepted papers, an abstract in English and Bahasa Melayu must be included.
- The manuscript should be able to be readily understood by an engineer and researchers alike and should avoid any colloquialisms.
- The terms, including nomenclature and abbreviations, and style should be consistent throughout your journal paper. If you collaborate with other writers, please communicate clearly with them.
- Avoid referring directly to the names of individuals, organisations, products, or services unless essential to the comprehension of the manuscript. Gratuitous flattery or derogatory remarks about a person or organisation should not be included.
- Symbols and Units: SI and derived units should be used, if possible.
- Abbreviations: the use of internationally recognised abbreviations is allowed in the text. The abbreviations should be defined on first use. Abbreviations should not be used in the title.

Manuscript Guide

The following is a detailed manuscript preparation guide for articles submitted to IEM Journal; however, they can, in the most part, be used as a basis for other article types amending to concur with the page limit and premise of the formats, as appropriate.

The manuscript should be typewritten using single-spacing, font of 12 Times Roman; on one side of sheet only and in a single column format.

Title

Titles are limited to 150 characters, including spaces. Please avoid the use of any abbreviations, acronyms, or formulae. Titles should clearly reflect the content of the manuscript and any search terms that readers may use should be considered and incorporated.

List of Authors Name

List down all the names of authors (who has contributed to the paper) and the respective affiliations. From the list of authors, place an asterisk (*) next to the corresponding author's name. Provide an official email address of the corresponding author. **Please DO NOT include your personal telephone number on the title page.**

Abstract

Provide an informative 100 to 250 words abstract at the head of the manuscript. This should be a concise reflection of the aims, findings, conclusions and any interesting or important results. Carefully incorporate any terms that may be used by potential interested readers to improve the article's discoverability online (search engine optimisation). The abstract should contain no reference. Abbreviations that are not commonly used should be defined (for the benefit of the non-specialist reader) at first use.

Keywords

These are used for indexing. Please include between 3-5 keywords.

List of Notations

Please provide a list of symbols and definitions used in the text. This will ease our readers.

Introduction

A concise summary of current background knowledge, with reference to relevant previous works in the field should be presented. Please also describe the objectives of and justification for the work contained in the submitted manuscript.

Main Text

The methods and processes applied to investigate and achieve the objectives should be communicated in sufficient detail that readers could repeat the work successfully. The results should be reported clearly and interpreted accurately and analysed thoroughly. Figures/tables can be used to support these results.

It is important that all research articles include a section at the end of the main text that highlights the novelty of the results to the engineering field and any potential applications.

All sections should be numbered in Arabic such as 1, 2, etc. with the title in capitals. Sub-sections should be numbered such as 1.1, 2.3, etc. Numbered all equations in round brackets ( ) flush to the right. The equation should be in the centre.

Style for Illustrations (Tables and Figures)

Try to include the illustrations in between the text. Each illustration must be numbered such as "Figure 1, Figures 2-3, etc." and have a meaningful caption at the bottom. For tables, the caption must be at the top.
On graphs, show only the coordinate axes, or at most the major grid lines, to avoid a dense hard-thread result.

All lettering should be large enough to permit legible reduction of the figure to column width. Typing on figures is not acceptable. Photographs should be glossy prints, of good contrast and gradation and any reasonable size.

Conclusions

A concise summary of the results of case studies or research project papers and the lessons learned should be discussed. If necessary, please elaborate the applicability / relevance of your article to readers in other countries.

Research journals must discuss the practical relevance and potential applications of the engineering work described. This is important to readers working in engineering related practice.

Please also include relevant references to demonstrate how previous engineering research work has been used. These references could be standards, codes or relevant past journal papers.

Appendices

Additional information, such as tables or mathematical derivations can be included. These will be included in the article.

Acknowledgements

Please provide acknowledgement details to those persons or organization that contributed to the paper. Additional details required by funding bodies can be included.

References

The references to other literature that you have cited in your main text should be based on the APA style of referencing (Author, Date) as described below. Please refer https://apastyle.apa.org/ for a detailed guide on the referencing style.

- Single author: (Author, Year) or Author (Year)
- Two authors: (Author 1 & Author 2, Year) or Author 1 and Author 2 (Year)
- Three and more authors: (Author 1 et al., Year) or Author 1 et al. (Year)

In the text, the author and year of the reference should be put in parentheses immediately after the work referred to, for example 'Controlled tests on the Millennium Bridge (Chapman et al., 2005; Murray & Geddes, 1987; Wilby et al., 2011) during which.....' or 'as mentioned by Lim et al. (2018), the NCA derived from the agricultural wastes...'

All references must be listed, in full, at the end of the paper in alphabetical order, irrespective of where they are cited in the text.

In the reference section, the references should be written in full, as follows:

Books: Author 1 surname, author 1 initials, & Author 2 surname, author 2 initials. (Year of publication). Book title. Publisher, City, Country. doi reference. For example:

Kobayashi, K., Khairuddin, A. R., Ofori, G. & Ogunlana, S. (Eds.). (2009). *Joint ventures in construction*. Thomas Telford, London, UK.

Owen, G. & Totterdill, B. (2008). *The dispute board hearing. In Dispute Boards: Procedures and Practice*. Thomas Telford, London, UK.

Journal, magazine and newspaper articles: Author 1 surname, author 1 initials, & Author 2 surname, author 2 initials. (Year of publication). Paper title. Journal title, Volume (Issue number), First page-Last page. doi reference. Unpublished papers and theses should not be cited as they are not readily available.

Lim, J. L. G., Raman, S. N., Lai, F. C., Zain, M. F. M., & Hamid, R. (2018). Synthesis of nano cementitious additives from agricultural wastes for the production of sustainable concrete. *Journal of Cleaner Production*, 171, 1150-1160. https://doi.org/10.1016/j.jclepro.2017.09.143.

Soon, F. C., Khaw, H. Y., Chuah, J. H., & Kanesan, J. (2018). Hyper-parameters optimisation of deep CNN architecture for vehicle logo recognition. *IET Intelligent Transport System*, 12(8), 939-946. https://doi.org/10.1049/iet-its.2018.5127.

Conference proceedings: Author 1 surname, author 1 initials, & Author 2 surname, author 2 initials. (Year of publication). Paper title. Proceedings title, Volume (Issue number), First page-Last page. doi reference. Unpublished conference proceedings (i.e. that were only given to delegates) should not be cited as they are not generally available.

Chuah, J. H., Khaw, H. Y., Soon, F. C., & Chow, C. (2017). Detection of Gaussian noise and its level using deep convolutional neural network. *Proceedings of the TENCON 2017 - 2017 IEEE Region 10 Conference*, 2447-2450. https://doi.org/10.1109/TENCON.2017.8228272.

Unpublished material should not be included in the Reference list.

Please refer to https://apastyle.apa.org/ for a detailed guide on the referencing style. Authors should strictly adhere to the referencing style specified herein.

Mathematical Equations

Only relevant equations should be included in the main text and should be numbered. An equation editor program can be used to type in a formula.

Figures and tables caption list: Please supply a figure caption list at the end of your journal paper. Figures and tables must be put in the text in consecutive order. All figures must have a brief title accompanied with a short description.

Brief Profile

At the end of the manuscript, each author should provide a brief profile (less than 150 words), together with recent photographs (preferable less than 3 MB).

Corresponding Authors

We only permit one corresponding author per submission.

Conflict of Interest

Conflict of interest occurs when an author (or the author's institution) has personal or financial relationships that inappropriately influence the statements in the publication. Authors should ensure that publications will be written in an unbiased, ethical and responsible manner. The authors working on any sponsored engineering work or publications should declare such work under Conflict of Interest during submission.

Submission of Paper

Authors are required to submit via the IEM Online Journal Submission (OJS) through the following link:

https://iemjournal.com.my/index.php/iem/about/submissions.

Together with the manuscript, the corresponding author should enclose a cover letter containing the significance of the paper, the postal and email address, and telephone number for correspondence. In the cover letter, kindly provide four (4) names as reviewers. The selected reviewers must have the relevant knowledge and research experience. Provide the reviewers postal and email addresses and telephone numbers (if possible).

Further Enquiries

For further enquires, please contact Secretariat at the address shown below:

The Institution of Engineers, Malaysia
Bangunan Ingenieur, Lots 60 & 62, Jalan 52/4
Peti Surat 223 (Jalan Sultan), 46720 Petaling Jaya, Selangor Darul Ehsan
Tel: 03–79684001/2 Fax: 03–79577678
E-mail: pub@iem.org.my or iemjournal@gmail.com

ADVERTISING
To advertise in Journal of IEM, please contact Dimension Publishing Sdn. Bhd. Advertisements that appear in Journal of IEM implies neither endorsement nor recommendation by The Institution of Engineers, Malaysia.

SUBSCRIPTIONS
To subscribe Journal of IEM please contact Dimension Publishing Sdn. Bhd.

DIMENSION PUBLISHING SDN. BHD.
Level 18-01, PJX-HM Shah Tower,
No. 16A, Persiaran Barat,
46050 Petaling Jaya,
Selangor Darul Ehsan, Malaysia.
Tel : (603) 7493 1049
Fax: (603) 7493 1047
Email: info@dimensionpublishing.com

The Institution of Engineers, Malaysia

Bangunan Ingenieur, Lots 60/62, Jalan 52/4, Peti Surat 223 (Jalan Sultan), 46720 Petaling Jaya, Selangor Darul Ehsan
Tel : 03-79684001/2 Fax : 03-79577678 E-mail : sec@iem.org.my IEM Homepage: http://www.iem.org.my

REFEREES FOR VETTING OF IEM PUBLICATIONS

Dear IEM Members/Readers,

The Standing Committee on Information and Publications is revising the list of referees to assist in the vetting of articles received from members and non-members. The referees should preferably be at least Corporate Members of The Institution or graduates with higher degrees.

The aim of appointing the referee is to ensure and maintain a standard in the IEM Publications namely the bulletin and the Journal.

Members who are interested to be placed in the database of referees are to return the registration form to the IEM Secretariat, providing details of their degrees and particular expertise and experience in the engineering fields.

We need your services to look into the vetting of articles received for Publications and due acknowledgement would be announced yearly in the Bulletin. Referees must be committed to return the papers within a month from date of appointment.

Chairman
Standing Committee on Information and Publications

All correspondences are to be addressed to: -

The Chief Editor
Standing Committee on Information and Publications
The Institution of Engineers, Malaysia
Bangunan Ingenieur, Lots 60 & 62, Jalan 52/4
P.O. Box 223 (Jalan Sultan)
46720 Petaling Jaya
Selangor Darul Ehsan

AREAS OF INTEREST FOR VETTING OF PAPERS

Please tick (√) the appropriate area of interest that you are able to vet the papers.

□ Acoustics
□ Engineering Education
□ Military Vehicles
□ Room Temperature
□ Aerodynamics
□ Environmental Engineering
□ Mini Pressure Meters
□ Safety Engineering
□ Air Conditioning
□ Fine Chemical
□ Mining Engineering
□ Scaffolding Works
□ Air Pollution Control
□ Finite Element
□ Naval Architecture
□ Seepage
□ Aircraft
□ Fire Detection
□ Navigation
□ Sewerage
□ Airport Engineering
□ Fire Engineering
□ Oil & Gas Engineering
□ Shipbuilding
□ Aluminium Design
□ Floods
□ Operation Research
□ Signal Processing
□ Arbitration
□ Food Processing
□ Palm Oil Industries
□ Solar Energy Technology
□ Automation
□ Foundation Engineering
□ Petrochemicals
□ Steelworks Design
□ Automotive Engineering
□ Fuzzy Logic
□ Petroleum Engineering
□ Stream Turbine Power Plant
□ Biochemical Engineering
□ Gas Engineering
□ Pharmaceuticals
□ Sructural Analysis
□ Biotechnology
□ Geotechnical
□ Piling
□ Structural Rehabilitation
□ Boiler Engineering
□ Heat Exchanger
□ Plumbing Engineering
□ Survey Engineering
□ Bridge Engineering
□ Highway
□ Pollution Control
□ Taligates
□ Building Services
□ Hydraulics
□ Ports & Harbour Engineering
□ Telecommunication
□ Coastal Engineering
□ H.V. Electrical Distribution
□ Power Electronics
□ Thermal Engineering
□ Co-Generation
□ Industrial Engineering
□ Power Generation
□ Timber Design
□ Computer Engineering
□ Industrial Transport
□ Pressure Vessels
□ Tool Engineering
□ Concrete Design
□ Industrial Ventilation
□ Prestressed Concrete
□ Transfer Tunnels
□ Concrete Technology
□ Information Technology
□ Project Management
□ Transportation Engineering
□ Construction Management
□ Instrumentation
□ Public Administration
□ Urban Planning
□ Control Engineering
□ Lighting System
□ Public Health Engineering
□ Vehicles
□ Drainage Engineering
□ L.V. Electrical Distribution
□ Quarry Engineering
□ Vertical Transportation
□ Dynamics Design
□ Manufacturing
□ Railways
□ Waste Treatment
□ Earthworks
□ Mass Transit
□ Reclamation Works
□ Waste Water
□ Edible Oil Refining
□ Mechanical Handling Equipment
□ Refrigeration
□ Water Resources Engineering
□ Electrical Transmission
□ Management
□ Reinforced Concrete Beams
□ Water Pollution Control
□ Electrochemical
□ Metal Fabrication
□ Road Transport
□ Wind Engineering
□ Electrotechnology
□ Metallurgy
□ Robotics
□ Others (please specify)
□ Energy Technology
□ Micro Electronics
□ Roof Structures

DISCIPLINES / SUB-DISCIPLINES OF VETTER

Please tick (√) the appropriate boxes.

□ Aerospace
□ Electrical
□ Marine
□ Petroleum
□ Aeronautical
□ Electronics
□ Mechanical
□ Production
□ Agricultural
□ Environmental
□ Mining
□ Structural
□ Chemical
□ Industrial
□ Naval Architecture
□ Others (Please specify)

VETTER'S DETAILS

Name : _____
Membership No. : _____ *(if applicable)*
Grade : ☐ Graduate ☐ Member ☐ Fellow ☐ Affiliate ☐ Others
(please specify) _____
Qualifications : _____
Addresses : *(Office)* _____
_____
(Residence) _____
_____
Contact No. : _____ *(Handphone)* _____ *(Office)* _____ *(Residence)*
E-mail Address : _____

Please mail all correspondences to the below. Please tick (√) the appropriate boxes.
Mail to : ☐ Office ☐ Residence

Brief Biodata (not longer than 50 words) (to be appended with this Reply Slip).
_____
_____
_____
_____
_____

Have you ever reviewed submissions for publication in any Journal(s) before? ☐ Yes ☐ No
If YES, name the Journal(s) _____

Do you have papers published in any Journal(s)? ☐ Yes ☐ No
If YES, name the Journal(s) _____

Date: _____ Signature : _____

INTERNATIONAL ADVISORY PANEL FOR IEM JOURNAL

IEM BRANCHES

HEADQUARTERS	**THE INSTITUTION OF ENGINEERS, MALAYSIA** Bangunan Ingenieur, Lots 60/62, Jalan 52/4, P.O.Box 223, (Jalan Sultan), 46720 Petaling Jaya, Selangor	Tel : 03-7968 4001 / 4002 Fax : 03-7957 7678 sec@iem.org.my www.myiem.org.my
PENANG	**IEM PENANG BRANCH SECRETARIAT** 1-04-02 E-Gate, Lebuh Tunku Kudin 2, 11700 Gelugor, Pulau Pinang	Tel : 04-606 599 iempenangbranch@gmail.com http://iempenang.org
SOUTHERN	**IEM SOUTHERN BRANCH SECRETARIAT** 24-B, Jalan Abiad, Taman Tebrau Jaya, 80400 Johor Bahru, Johor Darul Takzim	Tel : 07-331 9705 Fax : 07-331 9710 iemsouthern@gmail.com www.iemsb.org.my
PERAK	**IEM PERAK BRANCH SECRETARIAT** No. 60B, Jalan Lapangan Siber 1, Bandar Cyber (Business Centre), 31350 Ipoh, Perak Darul Ridzuan	Tel : 05-313 8459 iemperakbranch@gmail.com
EASTERN	**IEM PAHANG BRANCH SECRETARIAT** Ketua Penolong Pengarah Kanan Elektrik, JKR Cawangan Elektrik, Jalan Kamunting 2, Seri Kemunting, 25100 Kuantan, Pahang	Tel : 09-513 3533 Fax : 09-514 1594 mazman@jkr.gov.my
TERENGGANU	**IEM TERENGGANU BRANCH SECRETARIAT** 23-05, KT Business Centre, Padang Hiliran, Jalan Sultan Mohamad, 21100 Kuala Terengganu	Tel : 09-620 4500 Fax : 09-620 4502 iemterengganu@gmail.com
NEGERI SEMBILAN	**IEM NEGERI SEMBILAN BRANCH SECRETARIAT** No. 77-A-1, Lorong Haruan 5/3, Oakland Commerce Square, 70300 Seremban, Negeri Sembilan	Tel : 06-631 1011 Fax : 06-631 4619 iemnsembilan@gmail.com www.iemns.org.my
MELAKA	**IEM MELAKA BRANCH SECRETARIAT** C/O Sri Perunding Consulting Engineers, No. 2, Jalan Malinja 2, Taman Malinja Bukit Baru, 75150 Melaka	Tel : 06-284 8028 Fax : 06-283 8919 spcesb@gmail.com
SARAWAK	**IEM SARAWAK BRANCH SECRETARIAT** International Engineering Centre (IntEC), A2-G-19 & A2-1-19, Isthmus Raintree Square, Lot 3249, MTLD Block 7, Jalan Keruing, 93450 Kuching, Sarawak	Tel : 082-288 856 Fax : 082-288 856 iemsarawak@gmail.com
SABAH	**IEM SABAH BRANCH SECRETARIAT** Lot 25, 3rd Floor, Block C, Damai Point Commercial Centre, Lorong Damai Point, Off Jalan Damai, 88100 Kota Kinabalu, Sabah	Tel : 088-259 122 Fax : 088-236 749 iemsabah@gmail.com www.iemsabah.org.my
MIRI	**IEM MIRI BRANCH SECRETARIAT** 2nd Floor, Unit 14 (906-3-14), Soon Hup Tower Complex, (Mega Hotel), Jalan Merbau, 98000 Miri Sarawak	Tel : 085-423 718 Fax : 085-424 718 iem.miri@gmail.com www.iem-miri.org.my
KEDAH / PERLIS	**IEM KEDAH/PERLIS BRANCH SECRETARIAT** No. 164, Tingkat 2, Kompleks Alor Setar, Lebuhraya Darul Aman 05100 Alor Setar, Kedah Darul Aman	Tel : 04-734 3420 Fax : 04-733 3962 iemckps@gmail.com
PAHANG	**IEM PAHANG BRANCH SECRETARIAT** No. 114, Block F, Lorong Seri Teruntum, Medan Warisan, 25100 Kuantan, Pahang Darul Makmur	Tel : 019-855 6509 Fax : 09-514 6493 iempahang@gmail.com
KELANTAN	**IEM KELANTAN BRANCH SECRETARIAT** Lot 5139, Kompleks Niaga INOtrus Kawasan Perindustrian Pengkalan Chepa II, 6100 Kota Bharu, Kelantan	Tel : 09-773 0899 Fax : 04-733 3962 iemckps@gmail.com

THE INSTITUTION OF ENGINEERS, MALAYSIA
Bangunan Ingenieur, Lots 60 & 62, Jalan 52/4,
P.O. Box 223 (Jalan Sultan),
46720 Petaling Jaya, Selangor Darul Ehsan.

Tel: 03-7968 4001/4002
Fax: 03-7957 7678
E-mail: sec@iem.org.my
Homepage: http://www.myiem.org.my